



**Fisheries New Zealand**

Tini a Tangaroa

## The 2018 Chatham Islands (CRA 6) rock lobster (*Jasus edwardsii*) stock assessment

New Zealand Fisheries Assessment Report 2019/47

M.B. Rudd  
V. Haist  
K. Large  
D.N. Webber  
P.J. Starr

ISSN 1179-5352 (online)  
ISBN 978-1-99-000838-2 (online)

September 2019



Requests for further copies should be directed to:

Publications Logistics Officer  
Ministry for Primary Industries  
PO Box 2526  
WELLINGTON 6140

Email: [brand@mpi.govt.nz](mailto:brand@mpi.govt.nz)  
Telephone: 0800 00 83 33  
Facsimile: 04-894 0300

This publication is also available on the Ministry for Primary Industries websites at:  
<http://www.mpi.govt.nz/news-and-resources/publications>

<http://fs.fish.govt.nz> go to Document library/Research reports

© Crown Copyright – Fisheries New Zealand

**TABLE OF CONTENTS**

- EXECUTIVE SUMMARY ..... 1**
  
- 1. INTRODUCTION ..... 2**
  
- 2. STOCK ASSESSMENT ..... 3**
  - 2.1 Data ..... 3**
  - 2.2 Model..... 3**
  - 2.3 Parameters and priors..... 5**
  - 2.4 Assessment indicators..... 5**
  - 2.5 Maximum *a posteriori* (MAP) inference..... 6**
    - 2.5.1 MAP base case ..... 6
    - 2.5.2 MAP sensitivity trials..... 7
  - 2.6 Bayesian inference using Markov chain Monte Carlo (MCMC)..... 8**
    - 2.6.1 MCMC base case..... 8
    - 2.6.2 MCMC sensitivity trials ..... 9
  - 2.7 Projections ..... 10**
  - 2.8 Model averaging..... 10**
  
- 3. DISCUSSION ..... 11**
  - 3.1 Future research ..... 11**
  
- 4. ACKNOWLEDGEMENTS ..... 11**
  
- 5. REFERENCES..... 12**



## EXECUTIVE SUMMARY

Rudd, M.B.; Haist, V.; Large, K.; Webber, D.N.; Starr, P.J. (2019). The 2018 Chatham Island (CRA 6) rock lobsters (*Jasus edwardsii*) stock assessment.

*New Zealand Fisheries Assessment Report 2019/47. 90 p.*

This document describes a new stock assessment of red rock lobsters (*Jasus edwardsii*) in CRA 6, the Chatham Islands. The length-structured stock assessment used the lobster stock dynamics (LSD) model. Data manipulation and technical decisions were discussed by the Rock Lobster Fishery Assessment Working Group who oversaw the stock assessment.

The model was fitted to standardised catch per unit effort (CPUE) indices, size frequency data, sex ratio data, and tag-recapture data. This document describes the procedures used to find an acceptable base case and shows the model fits. We conducted several sensitivity trials to test assumptions in the base case model. The three most plausible model runs were averaged.

Model inference for this assessment was based on maximum *a posteriori* (MAP) fits and Markov chain Monte Carlo (MCMC) simulations. This document describes the diagnostics for each and shows the results of MAP and MCMC sensitivity trials.

The stock assessment revealed a stock that was initially fished heavily resulting in a rapid decline of the stock size between 1965 and 1975, followed by a steady decline until 1995 when the stock approached the soft limit (20%  $SSB_0$ ). Since then the stock has steadily grown and is projected to increase over the next 5 years assuming current catches and recent recruitment patterns.

## 1. INTRODUCTION

This work addresses Objective 4 of Fisheries New Zealand contract CRA2015-01C. This contract is the third in a three-year contract which began in April 2016. This contract was awarded to the New Zealand Rock Lobster Industry Council Ltd. (NZ RLIC) who sub-contracted Objective 4 to the authors of this report.

*Objective 4 - Stock assessment: To estimate biomass and sustainable yields for rock lobster stocks.*

Fisheries New Zealand and the National Rock Lobster Management Group (NRLMG) decided that the Chatham Islands stock (CRA 6, Figure 1) should be assessed in 2018. This work was done by a team sub-contracted to the NZ RLIC: Vivian Haist (Haist Consultancy), Merrill Rudd (Scaleability LLC), Paul Starr (Starrfish), D'Arcy Webber (Quantifish), and Kath Large (NIWA). Decisions on data and modelling choices were discussed and approved by the Rock Lobster Fishery Assessment Working Group (RLFAWG).

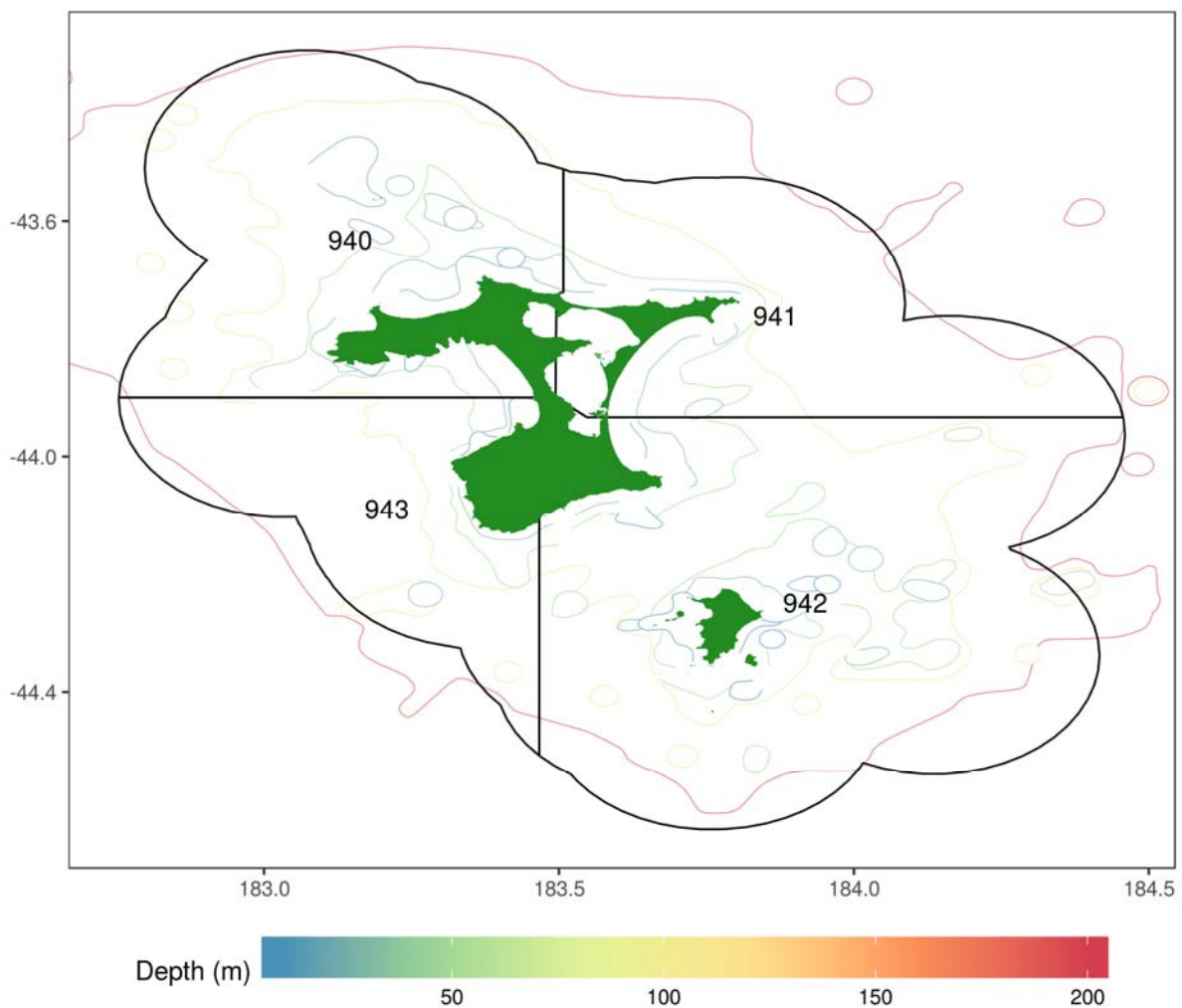


**Figure 1: Map of the Chatham Islands showing the four statistical areas that make up CRA 6 and depth contour lines.**

This document describes a new stock assessment for CRA 6. Data used in this stock assessment are documented in Starr et al. (2019). CRA 6 was assessed assuming a single homogeneous stock across the four statistical areas (940, 941, 942, and 943), using the lobster stock dynamics (LSD) model (Webber et al. 2018b).

The CRA 6 commercial fishery is primarily a trap or pot fishery, fished by small boats on day trips in relatively shallow waters. However, a few fishers still collect rock lobsters by hand around the Chatham Islands. A fixed annual total allowable commercial catch (TACC) is set for CRA 6. Allowances are added by the Minister for the non-commercial fisheries to produce a total allowable catch (TAC). Other management measures include protection of ovigerous (berried) females, a different minimum legal size (MLS) for each sex, escape gaps in pots, and the closure of the commercial fishery during April. The MLS is 54 mm tail width (TW) for males and 60 mm TW for females for both the commercial and recreational fisheries.

The number of vessels operating in CRA 6 has remained relatively constant (32–42 vessels) since the late 1990s, with 36 vessels counted in 2016–17 and 40 in 2017–18 (Starr 2018). The current 370 tonne TAC for the fishery was set in 1998–99. In addition to the 360 tonne TACC, the TAC comprises 10 tonnes for illegal removals with no allowance provided for customary or recreational catches.

The stock assessment was completed in a workshop held in Wellington during September/October 2018 and was presented to the Fisheries New Zealand Mid-year Plenary in November 2018.

## 2. STOCK ASSESSMENT

This is the first CRA 6 stock assessment using a length-structured model. A surplus production model was used by Breen & Kendrick (1998) in 1996 which concluded that the unfished equilibrium stock size was about 20 000 t and that the maximum sustainable yield (MSY) was 344 t. For this assessment, the lobster stock dynamics model (LSD) of Webber et al. (2018b) was used. This model is coded in Stan (Stan Development Team 2016, 2017). The transition from the multi-stock length-based model (MSLM) of Haist et al. (2009) to the new lobster stock dynamics (LSD) model is considered complete, having been tested alongside the MSLM model for the CRA 4 stock assessment in 2016, and used as the main assessment model for CRA 2 in 2017 after ascertaining that the two models (LSD and MSLM) in that year provided equivalent results.

Maximum *a posteriori* (MAP) estimation and Markov chain Monte Carlo (MCMC) were used to make inferences about the CRA 6 stock. A series of MAP sensitivity trials were explored and several of these were extended to a full Bayesian implementation using MCMC. Results from the three most plausible model runs were averaged.

### 2.1 Data

Data used in this stock assessment are documented fully in Starr et al. (2019) and the extent of these data is illustrated in Figure 2. Following the example of the 2017 CRA 2 stock assessment (Webber et al 2018a), a vessel explanatory variable was included in the CPUE standardisation procedure (see Starr et al. 2019) and CPUE was split into two series: one derived from the 1979–1988 data stored in the Fisheries Statistics Unit (FSU) database and the other derived from the post-1989 Catch Effort Landing Return (CELR) data stored in the Warehouse database. Only the latter series included a vessel explanatory variable.

Due to the limited number of tag-recaptures, this assessment combined tag data from CRA 6 and three statistical areas from the Fiordland region of CRA 8 (926, 927 and 928). Initial model exploration suggested that individuals that were re-captured multiple times tended to have slower growth rates, resulting in a decision to only fit to the first tag recapture event.

### 2.2 Model

This stock assessment treats CRA 6 as a single homogeneous area with a single population. Despite some differences in the size composition of sampled individuals among the four statistical areas (see the observer catch sampling and logbook length frequency, Appendix C in Starr et al. 2019), a multi-area assessment was not possible due to the limited amount of data in most of the areas.

The first fishing year in the model was set to 1965<sup>1</sup> because this was the year that the commercial fishery began. The last year is 2017, because this was the last full year with data. The model recognises two six-month seasons within a fishing year: autumn-winter (AW, April through September) and spring-summer (SS, October through March). The model tracks the numbers of immature females, mature females, and males in 46 2-mm TW bins (i.e. {[30, 32), [32, 34), ..., [120, ∞)}). The maximum bin size was extended from 90 to 120 mm to accommodate the prevalence of large lobsters when the fishery commenced.

In summary, the model dimensions are:

- Fishing years: 1965–2017 (i.e. ending with the 2017–18 fishing year)
  - Explored starting the model in 1979 (see sensitivity analyses below)
- Two seasons: AW and SS during each fishing year
- Three sexes: immature females, mature females, males
- Tail width bins: 46 2-mm wide bins from 30 mm to 122 mm tail width (last bin is a “plus” or accumulator bin)

In recent rock lobster stock assessment models, fishing mortality (F) has been calculated iteratively using the Newton-Raphson (NR) algorithm (Press et al. 2007). However, preliminary MCMC runs using this procedure were very slow. Therefore, runs that estimated F parameters were tested because MAP results showed negligible differences between the two options and MCMC iterations were faster during runs which estimated F. However, these preliminary MCMC runs showed evidence of non-convergence. Consequently, all reported model runs (both MCMC and MAP, except one which showed that the two procedures give the same MAP result) used the Newton-Raphson procedure to calculate fishing mortality. This assessment assumed a double-normal selectivity curve with an estimated right-hand limb and used length-weight parameters specific to the Chatham Islands (see Table 2).

In summary, major model options and choices included:

- recruitment: mean 32 mm with standard deviation 2 mm
- mature females: allowed to be caught in SS but not in AW
- likelihoods:
  - lognormal for three CPUE series (CR, FSU, and CELR)
  - robust normal for tags
  - multinomial for LFs, fitted to proportions for males, immature females and mature females, with each sex category normalised separately
  - multinomial for sex ratio
- data weighting: determined iteratively. No re-weighting of tag data because they are self-weighting through estimation of an observation error parameter
- fishing mortality dynamics: instantaneous using Newton-Raphson
- growth model: Schnute-Francis
- recruitment deviations (*Rdevs*) estimated: 1965–2015 (final two years are set to the 2015 estimate given no real information in data for these recruitments and lack of puerulus settlement data)
- selectivity: “double-normal” with right-hand limb parameter estimated
  - Explored logistic selectivity, and two selectivity periods from 1979–1992 and 1993–2017 (see sensitivity analyses below)
- handling mortality: two periods 1965–1989 and 1990–2017
- stock-recruitment relationship: off
- density-dependent growth: off
- three CPUE series:

---

<sup>1</sup> Fishing years extend from 1 April to 31 March and are designated with the first year of the pair.

- o The catch rate (CR) series is a seasonal unstandardised daily catch rate from 1966 to 1972, derived from the Annala & King data (1980) (1965 SS data point was dropped due to the very small amount of recorded catch). Catchability ( $q$ ) is assumed constant over this period
- o The Fisheries Statistics Unit (FSU) series is a seasonal standardised index from 1979 to 1988. The standardisation model includes year, month and statistical area explanatory variables but no vessel effect. Catchability ( $q$ ) is assumed constant over this period
- o The Catch Effort Landing Return (CELR) series is a seasonal standardised series from 1989 to 2017 with a vessel explanatory variable (vessels required to have fished CRA 6 for least 5 years). Catchability ( $q$ ) is assumed constant over this period

### 2.3 Parameters and priors

Estimated model parameters are listed in Table 1. Priors and parameter bounds for these parameters are provided in Table 3. Wide uniform priors were specified for average recruitment ( $R_0$ ) and the catchability coefficients ( $q$ ) for each CPUE series. Uniform priors between 0.001 and 0.7 were assumed for the growth parameter  $Gdiff$  and 0.01 and 1 for the vulnerability parameters, all of which are constrained to be between 0 and 1. An informative lognormal prior was specified for natural mortality and an informative prior based on an unpublished meta-analysis was specified for  $GCV$ . Uninformative normal prior distributions were specified for all other model parameters. These uninformative normal priors do not influence the outcome of the stock assessment, but do help with MCMC mixing.

The vulnerability of immature females and mature females during the SS was assumed to be the same. The four vulnerability parameters were estimated relative to the vulnerability of males during the AW (which is fixed to 1) because males during AW have the highest fishing mortality among the six available sexes/seasons (Table 2).

### 2.4 Assessment indicators

Stock assessment indicators requested by Fisheries New Zealand and the RLFAWG are summarised in Table 3. These included several based on vulnerable biomass such as current biomass ( $B_{2018}$ ) and the minimum of the vulnerable biomass trajectory ( $B_{MIN}$ ). Vulnerable biomass is defined as start-of-season AW biomass, which does not include mature females. Vulnerable biomass takes MLS, selectivity, and sex/seasonal vulnerability into account and is the biomass available to the fishery. Vulnerable reference biomass was calculated by applying the MLS and selectivity from the final model year to all previous years, including those years where alternative regulations applied.

There is no agreed  $B_{REF}$  indicator for CRA 6. Estimated  $B_{MSY}$  is sensitive to growth and mortality estimates and the assumptions under which it is estimated. The RLFAWG and the 2017 Plenary concluded that more work was needed to evaluate how this quantity should be calculated for rock lobsters. Consequently MSY-related quantities are not reported here.

Spawning stock biomass (SSB) was the biomass of all mature females at the start of AW.  $SSB_0$  was the spawning stock biomass at unfished equilibrium with  $R_0$ . The soft and hard limits are set at the default 20%  $SSB_0$  and 10%  $SSB_0$ , respectively.

Handling mortality was assumed to be 5% for all lobsters returned to the sea from 1990 and 10% before 1990. This mortality was applied to undersized lobsters of both sexes taken in either season by the size limited (SL) fishery as well as to mature females taken in the AW SL fishery. It was assumed that there were no discards in the non-size limited (NSL) fishery.  $H_{2017}$  is the model estimate of the amount (in tonnes) of handling mortality in the final (2017) fishing year.

In addition to the reference point indicators, the RLFAWG requested the posterior distributions of several ratios (e.g., the ratio of current biomass to  $B_0$  and  $B_{MIN}$ ), as well as the probability of each ratio being below specific levels important for management. These indicators were calculated from the MCMC posterior samples.

## 2.5 Maximum *a posteriori* (MAP) inference

Maximum *a posteriori* inference was used for exploring potential model options without committing the computing time required for Bayesian inference. A base case was developed and sensitivity runs were used to test the base case assumptions.

### 2.5.1 MAP base case

Searching for a base case involved:

- determining LF bins for fitting
- checking the season and sex used to set the vulnerability to 1 to ensure that no estimated sex- and seasonal-specific vulnerability was on the upper bound of 1
- adjusting dataset weights iteratively until the SDNRs were close to 1 and/or the MARs were close to 0.67 (except for tagging data which are self-weighting and length-frequencies which are weighted using Francis iterative reweighting; Francis 2011)

The following assumptions were made in the base case run:

- assume unfished population before 1965
- separate  $q$ 's for CR (1966 – 1978), FSU CPUE (1979–1988), and CELR CPUE (1989–2017)
- $q$  is constant for each CPUE series (no drift parameter)
- length-weight relationship based on CRA 6 data (see Starr et al. 2019)
- sex-specific double-normal selectivity with an estimated right-hand limb that allows for dome-shaped selectivity
- selectivity is constant through time

Diagnostic plots for the base case are presented in Figure 3 to Figure 16, consisting of model predictions relative to observed data or the standardised residuals of the model fits to the data. These include:

- the fit to the three AW and SS CPUE series (Figure 3)
- the standardised residuals of the fits to the three CPUE series (Figure 4)
- fits to the observer and logbook LF data by sex (Figure 5, Figure 6, Figure 7, Figure 8)
- residuals to the LF fits by sex, size, and data source (observer or logbook) (Figure 9)
- residuals to the LF fits by sex, year, and data source (observer or logbook) (Figure 10)
- residuals to the fit to the tag-recovery data by sex, and statistical area of release (Figure 11)
- estimated and observed sex ratios, by sex, year, and data source (Figure 12)
- unfished size distribution by sex (Figure 13)
- predicted growth increments, with standard deviation, at length, and sex (Figure 14)
- selectivity curve by selectivity period and sex (Figure 15)
- estimated female maturity function (Figure 16)

Annual plots of important generated quantities for the base case can be found in Figure 17 (recruitment), Figure 18 (fishing mortality), Figure 19 (recruited biomass by season), and Figure 20 (vulnerable biomass by season).

Parameter estimates, likelihoods, and indicators for the base case can be found in the table which also reports the sensitivity runs (Table 4). Parameter estimates were checked against the estimates from other rock lobster stock assessments. This comparison highlighted that natural mortality ( $M$ ) in CRA 6 was estimated to be the lowest of any stock.

## 2.5.2 MAP sensitivity trials

Seventeen sensitivity trials (Table 5) were run as single variants relative to the base case. These included sensitivity runs relating to the catch data, selectivity, tag data, length-weight relationship, and data set weighting. While the results of the sensitivity runs span a range of relative spawning stock biomass and recruitment, most of these runs did not have a large impact on the stock trajectories. A comparison of the vulnerable biomass for all 18 runs is made in Figure 21 (upper panel) and as relative spawning biomass (lower panel, Figure 21). Figure 22 compares the values of  $SSB_{2018}/SSB_0$  for all 17 sensitivity runs with the equivalent base case value. Figure 23 compares the recruitment trends for all 17 sensitivity runs with the base case recruitment trend. Figure 24 compares the male and female selectivity curves for all 17 sensitivity runs with the base case selectivity curve.

Summary of sensitivity tests:

- Three Newton-Raphson iterations compared to estimating fishing mortality parameters (*base* and *estimate F*) (Figure 25, Figure 26 and Figure 27)
  - Effectively no difference between the two runs
- Catch +/- 30% (*catch\_hi* and *catch\_lo*) (Figure 28, Figure 29 and Figure 30)
  - Relative spawning biomass proportionally higher or lower across the time series
  - *catch\_hi*: vulnerable reference biomass higher in initial years but *M* lower; nearly equivalent to base case throughout the time series
  - *catch\_lo*: vulnerable reference biomass lower in initial years but *M* higher; nearly equivalent to base case throughout the time series
- Start 1979 (*start\_1979*) (Figure 28, Figure 29 and Figure 30)
  - Relative vulnerable reference biomass spawning biomass is consistently higher than the base case
  - Relative spawning biomass similar to 30% less catch scenario
  - Higher recruitment than in the base case
- Drop early CR series (*drop\_CR*) (Figure 28, Figure 29 and Figure 30)
  - Similar to the base case run
- Use South Island length-weight relationships (*lw\_SI*) (Figure 31, Figure 32 and Figure 33)
  - Similar to the base case run
- Use alternative tag data sets (*tag\_CRA6*, *tag\_CRA8*) (Figure 34, Figure 35 and Figure 36)
  - CRA 6 tag data give a more pessimistic assessment but similar biomass trajectory
  - CRA 8 tag data similar to base case but slightly more optimistic
  - Tag residuals for Statistical Areas 922–925 show departure from the CRA 6 data while the tag residuals for areas 926, 927 and 928 are consistent with the residuals from the CRA 6 tagging data (Figure 37)
- Upweighting CPUE (*wgup\_CPUE*) (Figure 38, Figure 39 and Figure 40)
  - Lower vulnerable reference biomass
  - Lower relative spawning biomass with increase in last few years
  - More variable recruitment
- Downweighting CPUE (*wtdown\_CPUE*) (Figure 38, Figure 39 and Figure 40)
  - Similar to base case up to about 2000, followed by lower vulnerable reference biomass and relative spawning biomass
- Upweighting LF and sex ratio (*wgup\_LFSexRatio*) (Figure 38, Figure 39 and Figure 40)
  - Much higher vulnerable reference biomass across time series
  - Strong increase in relative spawning biomass in recent years
  - Higher recruitment in some periods
- Drop CELR *sndr* to 1 (*base\_cpue3\_sdnr1*) (Figure 38, Figure 39 and Figure 40)
  - Similar to base case
- Increase weight on 1966 LF (*wgup\_LF1996*) (Figure 38, Figure 39 and Figure 40)
  - Similar to base case: improves fit to the early LF series but has little impact on the overall stock assessment (Figure 41)
- Fixing right-hand limb selectivity to have a strong dome-shaped curve selectivity (*sel\_rh\_lo*) (Figure 42, Figure 43 and Figure 44)
  - Negligible differences in relative spawning biomass

- o Negligible differences in vulnerable reference biomass for the majority of the time series.
- Logistic selectivity (*sel\_logistic*) (Figure 42, Figure 43 and Figure 44)
  - o Similar to base case
- Estimating two selectivity epochs (*sel\_1993*) (Figure 42, Figure 43 and Figure 44)
  - o More optimistic than the base case; minimal LF data available for this sensitivity run
  - o Right shift of first selectivity period curve and strong dome for second selectivity period, which seems counter-intuitive (Figure 45)
- Estimating q-drift parameter (improvement in catchability over time) (*qdrift*) (Figure 46, Figure 47 and Figure 48)
  - o Initial biomass similar to base case
  - o Improvement in catchability is approximately 2% per year or an overall increase of about 60% (Figure 49)
  - o Current vulnerable stock status relative to  $B_0$  reduced by about 40% relative to base case
  - o Current spawning biomass stock status relative to  $SSB_0$  reduced by 23% relative to the base case

## 2.6 Bayesian inference using Markov chain Monte Carlo (MCMC)

Bayesian inference was used to estimate parameter uncertainty in this stock assessment. LSD uses Stan to run MCMC simulations using the Hamiltonian Monte Carlo (HMC) algorithm, starting with the MAP values in Table 4. For the base case and each selected sensitivity run (Table 6), we explored the posterior distributions with a total of approximately 1000 samples across eight chains, each with a warm-up phase of 500 iterations and length of 286 samples, retaining every second sample. The number of samples achieved was variable across the runs because some of the chains did not complete, stalling during the warm-up phase. This occurred because the observed biomass decline from 1966 to 1970 occasionally led to a conflict between the large initial catches and the requirement to have a sufficient vulnerable biomass from which to remove the catches. Despite these setbacks enough samples from the posterior were obtained for the base case and all sensitivity runs.

### 2.6.1 MCMC base case

MCMC was used to obtain samples from the posterior distribution for the base case model described in Section 2.5.1. Diagnostic traces are shown for estimated parameters in Figure 50, Figure 51 and Figure 52; density plots of the posterior distributions of estimated parameters and important derived quantities are shown in Figure 53, Figure 54 and Figure 55; cumulative density diagnostic plots are shown in Figure 56, Figure 57 and Figure 58. Posterior distributions of parameter estimates and derived quantities are summarised in Table 7.

Traces for important estimated parameters such as  $M$  and  $R_0$  show reasonable stability. MCMC chains for most parameters stayed away from parameter bounds. Trace and cumulative density plots indicate that MCMC chains are well-mixed.

A set of base case MCMC diagnostic plots consisting of posterior distributions of the model predictions relative to the observed data, or the standardised residuals of model fits to the data, can be found in Figure 59 through to Figure 71. These are comparable to those provided for the base case MAP results:

- the fit to the two AW and SS CPUE series, along with standardised residuals (Figure 59 and Figure 60)
- fits to the observer and logbook LF data by sex (Figure 61, Figure 62, Figure 63 and Figure 64)
- residuals to the LF fits by sex, size, and data source (observer or logbook) (Figure 65)
- residuals to the LF fits by sex, year, and data source (observer or logbook) (Figure 66)
- residuals to the fit to the tag-recovery data by sex, and statistical area of release (Figure 67)
- estimated and observed sex ratios, by sex, year, and data source (Figure 68)

- predicted growth increments, with standard deviation, at length, and sex (Figure 69)
- selectivity curve by selectivity period and sex (Figure 70)
- estimated female maturity function (Figure 71)

The model fits the CPUE time series reasonably well, with acceptable residual patterns (Figure 59 and Figure 60). These CPUE fits were similar to the equivalent MAP fits (Figure 3 and Figure 4). Model fits to the LF data are acceptable, with good agreement with the logbook (LB) data, particularly in the tails of the recent observed distributions (Figure 61 to Figure 64). The fit to the proportions-at-sex showed agreement with the observations (Figure 68). Maturation was estimated to be below the female MLS (Figure 71) with 50% of females maturing at 55 mm TW.

This stock assessment estimated a descending limb for the selectivity curve; in other assessments the descending limb is fixed. This approach was considered justified given the preponderance of large individuals in this population, especially at the beginning of the fishery. Model estimates of the descending limb are credible (Figure 70 and Table 7), encompassing the value of the fixed parameters used in other CRA stock assessments (e.g., a value of 200 was used in the 2017 CRA 2 stock assessment – see Webber et al 2018a).

Three strong recruitment events are estimated, one in the mid-1990s, the second in the early 2000s, and the most recent (and largest) in the early 2010s (Figure 72). Recent mean (2006–2015) recruitment is estimated to be above  $R_0$ , as indicated by the derived parameters  $B_{0now}$  and  $SSB_{0now}$  being larger than the equivalent parameters  $B_0$  and  $SSB_0$  which are based on the mean recruitment (i.e.  $R_0$ ) from 1965–2015 (Table 7).

Fishing mortality was high in the initial years of this fishery, followed by substantial reductions as the catches moved to a more sustainable level (Figure 73). Vulnerable biomass decreased rapidly in the initial years of the fishery, dropping to low levels in the mid-1990s (Figure 74). Vulnerable biomass has since slowly increased and is projected to continue to increase over the next five years, assuming that recent recruitment and annual catches continue at estimated levels. A similar trajectory is seen for the spawning stock biomass (Figure 75), with the lowest levels near the soft limit and a gradually increasing trend since then. Current (2018) spawning stock biomass is estimated to be at 36% of  $SSB_0$  ( $SSB_{2018}/SSB_0 = 0.36$  [90% credible interval (CI) = 0.35-0.38]; Table 7) and is projected to increase to 40% of  $SSB_0$  ( $SSB_{2022}/SSB_0 = 0.40$  [90% CI = 0.38-0.44]; Table 7). This assessment indicates zero probability of the base run being below the soft limit (20%  $SSB_0$ ) and 100% probability of being above  $B_{MIN}$  (Table 7).

## 2.6.2 MCMC sensitivity trials

A reduced number of sensitivity trials (see Table 6) was chosen to be simulated using MCMC. These runs represented plausible alternative hypotheses as well as ones that differed in the parameter space (biomass trajectories) investigated. All sensitivity runs had acceptable MCMC diagnostics for the completed chains (Table 6).

The two catch sensitivity runs (*catch\_hi* and *catch\_lo*) differed predictably from the base case. Stock size for the *catch\_hi* run was larger than the base case ([top panel], Figure 76) and stock status was lower at 31% of  $SSB_0$  ( $SSB_{2018}/SSB_0 = 0.31$  [90% CI = 0.30-0.33]; Table 7). Both  $B_0$  and  $SSB_0$  are larger for this run, but  $M$  is lower at 0.042 and the reduced productivity results in lower stock status. Similarly, the *catch\_lo* biomass was smaller than the base case ([top panel], Figure 76) but stock status was higher at 44% of  $SSB_0$  ( $SSB_{2018}/SSB_0 = 0.44$  [90% CI = 0.42-0.46]; Table 7).  $B_0$  and  $SSB_0$  are smaller for this run, but  $M$  is higher at 0.055 and the increased productivity results in better stock status. Both of these catch runs show the same recruitment pattern (Figure 77) and have very similar selectivity patterns (Figure 78).

The *q-drift* sensitivity run estimates this parameter to be a 1.8% increase per year (0.018 [90% CI = 0.009-0.028]; Table 7). This converts to an increase in the CELR  $q$  of about 60% over the 29-year

period of the CELR series (1989–2017; Figure 79). The credibility of this increase is unknown but the impact of the vessel explanatory variable is much less marked in the CRA 6 standardised CPUE analysis compared to the equivalent analysis performed on CRA 2 in 2017. Adding the *q-drift* parameter to the base case run results in a similar sized stock but a lower stock status (27% of  $SSB_0$  ( $SSB_{2018}/SSB_0 = 0.27$  [90% CI = 0.24-0.31]; Table 7).  $M$  is also estimated to be lower than in the base case ( $M = 0.043$  [90% CI = 0.037-0.050]; Table 7). However, the pattern of low abundance in the 1990s followed by an increasing trend into the projection period is similar to the other three runs (Figure 76). This sensitivity run also shows the same three recruitment peaks (Figure 80) with a similar estimated selectivity curve (Figure 81).

The base run and the three sensitivity runs evaluated in Table 6 have zero probability of being below the soft limit (20%  $SSB_0$ ) and 100% probability of being above  $B_{MIN}$  (Table 7).

## 2.7 Projections

Projections extend from 2018–2021 with simulated recruitment from 2016–2022 (i.e. the final two years recruitment deviations that were fixed at the 2015 recruitment deviation estimate during MAP estimation were overwritten). Recruitment deviations were simulated from a normal distribution with mean and standard deviation calculated from the last 10 years of estimated recruitment deviations (2006–2015). Recruitment autocorrelation was calculated from the 1965–2015 recruitment deviations.

Projections assumed 2017 catch levels (359.07 t commercial, 6.02 t recreational, 4 t customary, 10 t illegal). The proportion of the catch taken during the AW was simulated from a logit regression of AW CPUE (with normally distributed error in logit-space) with parameters estimated from the relationship between the observed proportion of catch taken during AW and the AW CPUE from 1993–2017 (Figure 82). Unlike most other CRA QMAs, there is very little signal in this relationship, indicating that the AW CPUE is a poor predictor of the AW/SS seasonal split.

Projections indicate that, at current levels of removals, the CRA 6 population is expected to increase as a result of recent good recruitment.

## 2.8 Model averaging

The first four model runs listed in Table 6 were reviewed in November 2018 by the Fisheries New Zealand Stock Assessment Plenary (Chapter 14: Fisheries New Zealand 2018). The *base*, *q-drift* and *catch\_hi* runs were considered by the Plenary to be credible alternative scenarios, while the fourth run (*catch\_lo*), which explored the possibility that the early catch history was 30% lower than the *base* run, was not accepted because it was unlikely that catches had been overestimated during the early years of the fishery. The Plenary concluded that none of the three accepted runs captured the full range of uncertainty associated with this stock assessment and requested that a combined model consisting of the combined posterior distributions of the three accepted runs be used to provide CRA 6 management advice (each contributing run was given equal weight by having the same number of samples). Results from the *combined* run are presented in Table 7 and the discussion below applies to the *combined* model.

Model estimates of the descending right-hand limb are credible (Figure 83, Table 7), encompassing the value of the fixed parameters used in other CRA stock assessments (e.g., a value of 200 was used in the 2017 CRA 2 stock assessment, Webber et al. 2018a). There is a slow increasing trend in the CELR CPUE  $q$  for the combined run because it includes the *q-drift* sensitivity run (Figure 84).

Three strong recruitment events are estimated, one in the mid-1990s, the second in the early 2000s and the most recent (and largest) in the early 2010s (Figure 85). This recruitment pattern is unlike that seen in any of the other assessed CRA QMAs and suggests that this population may be independent of rock lobster populations on either the North or the South Islands. Recent mean (2006–2015) recruitment is estimated to be above  $R_0$ , as indicated by the derived parameters  $B_{now}$  and  $SSB_{now}$  being larger than the equivalent parameters  $B_0$  and  $SSB_0$ , which are based on the mean recruitment (i.e.  $R_0$ ) from 1965–2015 (Table 7).

Fishing mortality was high in the initial years of this fishery, followed by substantial reductions as catches moved to a more sustainable level (Figure 86). Vulnerable biomass decreased rapidly in the initial years of the fishery, dropping to low levels in the mid-1990s (Figure 87). Vulnerable biomass has since slowly increased and is projected to continue to increase over the next five years, given recent recruitment. A similar trajectory is seen for the spawning biomass (Figure 88), with the lowest levels near the soft limit and a gradually increasing trend since then. Current (2018) spawning biomass is estimated to be at 32% of  $SSB_0$  ( $SSB_{2018}/SSB_0 = 0.32$  [90% credible interval (CI) = 0.24–0.39]; Table 7) and is projected to increase to 35% of  $SSB_0$  ( $SSB_{2022}/SSB_0 = 0.35$  [90% CI = 0.25–0.44]; Table 7). There is zero probability of the *combined* model being below the soft limit (20%  $SSB_0$ ) and 100% probability of being above  $B_{MIN}$  (Table 7). All three accepted model runs and the *combined* model average run show similar increases in spawning biomass relative to  $SSB_0$  over the projection period (Figure 89).

### 3. DISCUSSION

This stock assessment shows a stock that was initially fished heavily resulting in a rapid decline of the stock size between 1965 and 1975, followed by a steady decline until 1995 where the stock approached the soft limit (20%  $SSB_0$ ). Since then the stock has steadily grown and is projected to increase over the next 5 years assuming current catches and recent recruitment patterns.

The LSD model fitted the CRA 6 data reasonably well with acceptable fits to the CPUE, LF, sex ratio, and tag-recapture data. Estimates of growth, maturity, and selectivity were credible with tight posterior distributions. Three strong historical recruitment events are estimated to have occurred in CRA 6 (one in the mid-1990s, the second in the early 2000s, and the most recent in the early 2010s). This recruitment pattern is unlike that seen in any of the other assessed CRA QMAs and suggests that this population may be independent of rock lobster populations on either the North or the South Islands.

This assessment relies on tag-recapture data borrowed from the three Fiordland statistical areas in CRA 8. These statistical areas were chosen because residuals from fits to the CRA 6 and selected CRA 8 tags were similar.

This stock assessment estimated a natural mortality ( $M$ ) in CRA 6 of about 0.05, the lowest of any stock. This was surprising but is considered credible, given the preponderance of large lobsters in CRA 6, both historically and more recently.

#### 3.1 Future research

Future research to help inform CRA 6 stock assessments should include the deployment of more tags so that future assessment do not need to rely on tag-recapture data outside of CRA 6. Additional morphometric data (length and weight) would also help confirm the length-weight relationship used in this model.

Acceptable reference points and management targets are required for CRA 6. A study is currently underway that is intended to provide a method for calculating  $B_{MSY}$  for all rock lobster stocks, which is expected to be available later in 2019.

### 4. ACKNOWLEDGEMENTS

We thank Fisheries New Zealand who awarded the contract for this work to the New Zealand Rock Lobster Industry Council Ltd under Objectives 3 and 4 of CRA2015-01C. We thank Mark Edwards and Daryl Sykes for encouragement, Helen Regan for support, and members of the Rock Lobster Fishery Assessment Working Group for advice.

## 5. REFERENCES

- Annala, J.H.; King, M.R. (1983). The 1963–73 New Zealand rock lobster landings by statistical area. Fisheries Research Division Occasional Publication, Data Series 11. 20 p.
- Breen, P.A.; Kendrick, T.H. (1998). The 1996 assessment for the New Zealand red rock lobster (*Jasus edwardsii*) fishery. New Zealand Fisheries Assessment Research Document 98/13. 42 p.
- Fisheries New Zealand (2018). Fisheries Assessment Plenary, November 2018: stock assessments and stock status. Compiled by the Fisheries Science and Information Group, Fisheries New Zealand, Wellington, New Zealand. 526 p.
- Francis, R.I.C.C. (2011). Data weighting in statistical fisheries stock assessment models. *Canadian Journal of Fisheries and Aquatic Sciences* 68(6): 1124–1138.
- Haist, V.; Breen, P.A.; Starr, P.J. (2009). A new multi-stock length-based assessment model for New Zealand rock lobsters (*Jasus edwardsii*). *New Zealand Journal of Marine and Freshwater Research* 43(1): 355–371.
- Press, W.H.; Teukolsky, S.A.; Saul, A.; Vetterling, W.T.; Flannery, B.P. (2007). Numerical Recipes 3<sup>rd</sup> Edition: The Art of Scientific Computing. Cambridge University Press, NY.
- Stan Development Team (2016). *CmdStan: User's Guide*. Version 2.16.0.
- Stan Development Team (2017). *Stan Modelling Language: User's Guide and Reference Manual*. Version 2.16.0.
- Starr, P.J. (2018). Rock lobster catch and effort data: summaries and CPUE standardisations, 1979–80 to 2016–17. *New Zealand Fisheries Assessment Report 2018/27*. 141 p.
- Starr, P.J.; Webber, D.N.; Rudd, M.; Large, K.; Haist, V. (2019). Data for the 2018 stock assessment of red rock lobsters (*Jasus edwardsii*) in CRA 6. *New Zealand Fisheries Assessment Report 2019/16*. 36 p.
- Webber, D.N.; Haist, V.; Starr, P.J.; Edwards, C.T.T. (2018b). A new model for the assessment of New Zealand rock lobster (*Jasus edwardsii*) stocks and an exploratory multi-area CRA 4 assessment. *New Zealand Fisheries Assessment Report 2018/53*. 111 p.
- Webber, D.N.; Starr, P.J.; Haist, V.; Rudd, M.; Edwards, C.T.T. (2018a). The 2017 stock assessment and management procedure evaluation for rock lobsters (*Jasus edwardsii*) in CRA 2. *New Zealand Fisheries Assessment Report 2018/17*. 87 p.

**Table 1: Definitions of parameters and derived quantities discussed in the text.**

Parameter	Definition
$R_0$	initial numbers recruiting
$U_0$	initial exploitation rate (first year is in equilibrium using this estimate)
$M$	instantaneous rate of natural mortality
$Rdevs$	annual recruitment deviations
$\sigma R$	standard deviation of $Rdevs$
$qCR$	catchability coefficient (relationship between $Bvuln$ and CR series)
$qFSU$	catchability coefficient (relationship between $Bvuln$ and FSU CPUE series)
$qCELR$	catchability coefficient (relationship between $Bvuln$ and CELR CPUE series)
$Mat50$	size where 50% of immature females become mature
$Mat95$	difference between $Mat50$ and $Mat95$
$Galpha$	annual growth increment at 50 mm TW
$Gdiff$	the ratio of $Gbeta$ to $Galpha$
$Gshape$	parameter for shape of growth curve: 1 implies vonB straight line; >1 implies concave upwards
$GCV$	standard deviation of growth-at-size divided by growth-at-size
$Gobs$	standard deviation of observation error for tag-recaptures
$SelLH$	shape of the LH of selectivity curve (as if it were a standard deviation)
$SelMax$	size at maximum selectivity
$SelRH$	shape of the RH of selectivity curve (as if it were a standard deviation)
$vuln$	relative vulnerability by sex and season
$Gbeta$	annual growth increment at 80 mm TW
$Bvuln$	start-of-season AW biomass available to be caught legally
$B_{2018}$	vulnerable biomass at start of AW 2018

**Table 2: Fixed quantities used in the CRA 6 models.**

Quantity	Value	Quantity	Value
<b>data set weights</b>		<b>fixed parameters</b>	
tags	1	$\sigma R$	0.4
CELR CPUE	0.86	male length-weight $a$	6.6302e-7
FSU CPUE	0.28	male length-weight $b$	3.3629
CR CPUE	0.945	female length-weight $a$	1.0495e-5
sex ratio	22.83	female length-weight $b$	2.6025
LFs	5.70	<b>recruitment</b>	
<b>catch and handling</b>		last year of estimated $Rdevs$	2015
handling mortality, 1965–1989	0.10	years for estimating $Rdev$ 's for projections	2006–2015
handling mortality, 1990–2017	0.05	years for estimating autocorrelation	1965–2015
projected SL commercial catch	359.07 t	recruitment size mean	32 mm
projected SL recreational catch	6.02 t	recruitment size SD	2 mm
Projected NSL illegal catch	10.0 t	<b>other</b>	
Projected NSL customary catch	4.0 t	Newton-Raphson iterations	3
		Tail compression: male bins	4 to 40
		Tail compression: female immature bins	4 to 20
		Tail compression: female mature bins	6 to 40

**Table 3: Specifications for estimated parameters in the CRA 6 models including the upper and lower bounds, prior type, prior mean and standard deviation (SD), and the initial values.**

Season	Sex	Parameter	lower bound	upper bound	prior type	prior mean	prior std/CV
		$R_0$	exp(1)	exp(25)	uniform		
		$M$	0.01	0.35	lognormal	0.12	0.4
		$Rdevs$	-2.3	2.3	normal	0	$\sigma R$
		$qCR$	exp(-25)	exp(0)	uniform		
		$qFSU$	exp(-25)	exp(0)	uniform		
		$qCELR$	exp(-25)	exp(0)	uniform		
		$Mat50$	10	80	normal	50	15
		$Mat95$	1	60	normal	10	10
	male	$Galpha$	1	15	normal	5	30
	male	$Gdiff$	0.001	0.7	uniform		
	male	$Gshape$	0.1	12	normal	4.81	5
	male	$GCV$	0.1	2	normal	0.59	1
	female	$Galpha$	1	15	normal	5	30
	female	$Gdiff$	0.001	0.7	uniform		
	female	$Gshape$	0.1	12	normal	4.51	5
	female	$GCV$	0.1	2	normal	0.82	1
		$Gobs$	0.00001	10	normal	1.48	1
	male	$SelLH$	1	50	normal	20	10
	female	$SelLH$	1	50	normal	20	10
	male	$SelMax$	10	100	normal	50	25
	female	$SelMax$	10	100	normal	50	25
	male	$SelRH$	1	2000	normal	30	500
	female	$SelRH$	1	2000	normal	30	500
SS	male	$vuln1$	0.01	1	uniform		
AW	immafem	$vuln2$	0.01	1	uniform		
SS	imma & matfem	$vuln3$	0.01	1	uniform		
AW	matfem	$vuln4$	0.01	1	uniform		

**Table 2: CRA 6 base case: map of vulnerability ( $vuln$ ) parameters. Note that the vulnerability for males in AW is fixed at 1 and all other  $vuln$  parameters are estimated relative to the vulnerability of males during AW.**

Sex	Season	$vuln$
male	AW	1
male	SS	$vuln1$
immature female	AW	$vuln2$
immature female	SS	$vuln3$
mature female	AW	$vuln4$
mature female	SS	$vuln3$

**Table 3: Reference points, performance indicators, and stock status probabilities for the CRA 6 stock assessment.**

<i>Type</i>	<i>Description</i>
<b>Reference Points</b>	
$B_0$	beginning of season AW vulnerable biomass before fishing (1965)
$SSB_0$	female AW spawning stock biomass before fishing began (1965)
$B_{0now}$	equilibrium vulnerable biomass using mean 2006–2015 recruitment
$SSB_{0now}$	equilibrium female spawning biomass using mean 2006–2015 recruitment
$B_{TOT}$	equilibrium total biomass
$B_{MIN}$	the lowest beginning AW vulnerable biomass in the series
$B_{2018}$	beginning of season AW vulnerable biomass for 2018
$B_{2022}$	beginning of season AW vulnerable biomass for 2022
$SSB_{2018}$	female spawning stock biomass at beginning of 2018 AW season
$SSB_{2022}$	female spawning stock biomass at beginning of 2022 AW season
$B_{2018TOT}$	beginning of season AW total biomass for 2018
$CPUE_{2018}$	AW CPUE at beginning of 2018 (in kg/potlift)
$CPUE_{2022}$	AW CPUE at beginning of 2022 (in kg/potlift)
$H_{2017}$	total handling mortality for 2017 (tonnes)
$H_{2021}$	total handling mortality for 2021 (tonnes)
<b>Performance indicators</b>	
$B_{2018} / B_0$	ratio of $B_{2018}$ to $B_0$
$B_{2022} / B_0$	ratio of $B_{2022}$ to $B_0$
$B_{2022} / B_{2018}$	ratio of $B_{2022}$ to $B_{2018}$
$SSB_{2018} / SSB_0$	ratio of $SSB_{2018}$ to $SSB_0$
$SSB_{2022} / SSB_0$	ratio of $SSB_{2022}$ to $SSB_0$
$SSB_{2022} / SSB_{2018}$	ratio of $SSB_{2022}$ to $SSB_{2018}$
$B_{2018TOT} / B_{TOT}$	ratio of $B_{2018TOT}$ to $B_{TOT}$
$B_{2022TOT} / B_{TOT}$	ratio of $B_{2022TOT}$ to $B_{TOT}$
$B_{2022TOT} / B_{2018TOT}$	ratio of $B_{2022TOT}$ to $B_{2018TOT}$
<b>Probabilities</b>	
$P(B_{2018} > B_{MIN})$	probability $B_{2018}$ is greater than $B_{MIN}$
$P(SSB_{2018} < 20\%SSB_0)$	probability $SSB_{2018}$ is less than 20% $SSB_0$
$P(SSB_{2018} < 10\%SSB_0)$	probability $SSB_{2018}$ is less than 10% $SSB_0$

**Table 4: CRA 6 stock assessment: MAP base case and sensitivity run results. Grey indicates quantities not fitted. Growth increment values in mm TW, biomass values in tonnes and  $R_0$  in numbers. Note table continued on next page. Fixed values are indicated in bold.**

	Base		Catch				Selectivity			Tags		length-weight	q-drift	Weighting				
	Newton-Raphson	estimate F	catch_hi	catch_lo	start_1979	drop_CR	sel_logistic	sel_1993	sel_rh_low	tag_CRA6	tag_CRA8	lw_SI	qdrift	cpue3_snr1	wtdown_CPUE	wtup_CPUE	wtup_LF1996	wtup_LFsexratio
<i>Likelihoods</i>																		
LFs-sdnr	0.47	0.47	0.47	0.47	0.47	0.47	0.47	0.46	0.46	0.41	0.46	0.46	0.46	0.47	0.46	4.64	0.46	1.43
LFs-MAR	0.07	0.07	0.07	0.07	0.07	0.07	0.07	0.07	0.07	0.07	0.07	0.07	0.07	0.07	0.07	0.05	0.07	0.21
LFs-LL	3 295	3 318	3 318	3 319	3 278	3 318	3 318	3 311	3 318	3 315	3 323	3 294	3 311	3 401	3 306	3 643	3 651	33 013
Tags-sdnr	2.08	2.08	2.08	2.08	2.09	2.08	2.08	2.08	2.08	3.88	2.29	2.08	2.09	2.08	2.08	1.92	2.08	2.07
Tags-MAR	0.73	0.73	0.73	0.73	0.74	0.73	0.73	0.73	0.73	0.85	0.73	0.73	0.73	0.73	0.73	0.82	0.73	0.74
Tags-LL	5 853	5 853	5 853	5 854	5 554	5 853	5 853	5 853	5 853	153	8 144	5 853	5 853	5 853	5 853	5 987	5 853	5 864
CPUE-sdnr	1.50	1.50	1.51	1.49	1.51	1.51	1.50	1.50	1.50	1.39	1.48	1.50	1.52	1.02	0.37	10.81	1.51	1.79
CPUE-MAR	0.85	0.85	0.85	0.83	0.88	0.81	0.86	0.88	0.86	0.85	0.91	0.87	0.98	0.64	0.25	6.83	0.89	1.16
CPUE-LL	- 98	- 98	- 97	- 98	- 97	- 97	- 98	- 98	- 98	- 107	- 100	- 98	- 96	- 105	- 33	3 036	- 97	- 70
FSU-sdnr	0.96	0.96	0.98	0.94	1.05	0.93	0.96	1.00	1.01	0.91	0.96	0.99	0.94	0.99	0.38	5.18	1.04	1.28
FSU-MAR	0.50	0.48	0.54	0.45	0.64	0.42	0.49	0.59	0.59	0.55	0.47	0.58	0.43	0.55	0.19	4.67	0.67	0.95
FSU-LL	- 28	- 29	- 28	- 29	- 27	- 29	- 28	- 28	- 28	- 29	- 28	- 28	- 29	- 28	- 15	172	- 27	- 22
CR-sdnr	1.06	1.07	0.92	1.33			1.05	1.10	1.16	0.88	1.00	1.02	1.10	1.05	0.12	4.87	1.24	1.94
CR-MAR	0.89	0.91	0.70	1.05			0.87	0.91	0.81	0.54	0.75	0.82	0.91	0.88	0.39	3.57	0.82	1.55
CR-LL	- 10	- 10	- 12	- 5.1			- 10	- 9.3	- 8.3	- 13	- 11	- 11	- 9.3	- 9.5	19	122	- 6.9	10
Sex-sdnr	1.05	1.05	1.03	1.07	0.99	1.04	1.05	1.03	1.04	1.05	1.03	1.03	1.03	1.05	1.03	1.14	1.19	3.08
Sex-MAR	0.63	0.62	0.61	0.63	0.62	0.60	0.63	0.60	0.61	0.63	0.64	0.60	0.60	0.64	0.57	0.65	0.62	1.83
Sex-LL	1 082	1 078	1 077	1 080	1 064	1 078	1 079	1 077	1 078	1 078	1 078	1 080	1 077	1 075	1 077	1 085	1 184	10 739
Priors	-2.93	-3.06	-2.29	-3.26	10.25	-2.90	-9.29	15.09	-8.29	-3.41	-2.17	-2.42	-2.08	-6.28	-7.68	122.55	-1.12	12.62
Function value	10 091	10 111	10 109	10 116	9 782	10 120	10 104	10 121	10 107	4 394	12 403	10 089	10 104	10 179	10 198	14 168	10 556	49 546
<i>Parameters</i>																		
$R_0$	348 337	348 102	334 013	366 544	329 425	338 044	349 011	375 158	353 332	310 147	375 569	361 998	302 229	353 599	320 559	428 046	378 809	997 901
M	0.047	0.047	0.041	0.054	0.048	0.046	0.048	0.049	0.046	0.053	0.049	0.046	0.042	0.048	0.043	0.082	0.047	0.066
qdrift	-	-	-	-	-	-	-	-	-	-	-	-	0.021	-	-	-	-	-
qCPUE	5.016E-04	4.977E-04	5.232E-04	4.605E-04	4.813E-04	4.817E-04	5.020E-04	4.387E-04	5.056E-04	8.852E-04	5.785E-04	5.390E-04	4.650E-04	4.609E-04	5.792E-04	1.612E-03	4.497E-04	1.344E-04
qFSU	5.357E-04	5.291E-04	5.645E-04	4.863E-04	5.206E-04	5.061E-04	5.345E-04	4.849E-04	5.582E-04	8.604E-04	6.117E-04	5.838E-04	5.165E-04	5.061E-04	5.178E-04	1.452E-03	5.069E-04	1.691E-04
qCR	4.402E-02	4.333E-02	4.500E-02	4.299E-02	-	-	-4.328E-02	4.233E-02	5.577E-02	5.927E-02	4.767E-02	5.005E-02	4.235E-02	4.271E-02	9.856E-01	1.156E-01	5.715E-02	3.340E-02
init expl rate	-	-	-	-	0.060	-	-	-	-	-	-	-	-	-	-	-	-	-
mat50	53.9	53.8	53.8	53.7	53.4	54.0	53.9	53.8	53.8	48.1	54.8	54.0	53.8	53.9	53.9	50.9	54.0	53.5
mat95Add	15.6	15.8	15.9	15.7	15.8	15.7	15.6	15.7	15.7	12.2	16.1	15.7	16.0	15.8	15.9	11.8	15.4	18.4
GalphaM	5.26	5.26	5.27	5.25	5.30	5.27	5.26	5.28	5.27	7.65	4.39	5.27	5.28	5.28	5.32	5.37	5.31	5.48
GbetaM	2.53	2.52	2.50	2.52	2.48	2.50	2.53	2.48	2.47	3.93	2.97	2.52	2.51	2.48	2.40	3.73	2.39	2.17
GshapeM	1.90	1.91	1.93	1.87	2.05	1.94	1.90	1.97	1.86	1.46	0.16	1.93	1.90	1.99	2.11	2.46	2.03	2.70
GCVM	0.46	0.46	0.46	0.46	0.46	0.46	0.46	0.46	0.46	0.31	0.48	0.46	0.46	0.46	0.46	0.38	0.46	0.45
GalphaF	4.05	4.04	4.03	4.04	4.20	4.04	4.04	4.03	4.04	5.90	3.66	4.04	4.04	4.02	4.01	4.86	4.04	4.19
GbetaF	1.53	1.53	1.52	1.55	1.52	1.53	1.53	1.55	1.52	1.64	1.60	1.53	1.51	1.54	1.53	1.74	1.53	1.55
GshapeF	3.22	3.19	3.16	3.21	3.51	3.18	3.21	3.22	3.14	4.24	2.63	3.20	3.20	3.17	3.13	5.11	3.13	3.45
GCVF	0.52	0.52	0.52	0.52	0.52	0.52	0.52	0.52	0.52	0.59	0.50	0.52	0.52	0.52	0.52	0.43	0.52	0.52
StdObs	0.33	0.33	0.33	0.33	0.34	0.33	0.33	0.33	0.33	0.47	0.28	0.33	0.33	0.33	0.33	0.49	0.33	0.33

	Base		Catch				Selectivity		Tags		length-weight	q-drift	Weighting						
	Newton-Raphson estimate	F	catch_hi	catch_lo	start_1979	drop_CR	sel_logistic	sel_1993	sel_rh_low	tag_CRA6	tag_CRA8	lw_SI	qdrift	cpue3_sndr1	wtdown_CPUE	wtup_CPUE	wtup_LF1996	wtup_LFsexratio	
vuln1	0.87	0.87	0.85	0.89	0.86	0.87	0.87	0.84	0.87	0.86	0.86	0.77	0.84	0.87	0.80	0.75	0.87	0.82	
vuln2	0.63	0.66	0.68	0.70	0.67	0.64	0.63	0.73	0.66	0.61	0.61	0.63	0.63	0.69	0.79	0.22	0.75	0.99	
vuln3	0.64	0.65	0.65	0.68	0.67	0.68	0.64	0.72	0.64	0.48	0.59	0.61	0.62	0.68	0.70	0.50	0.75	0.97	
vuln4	0.37	0.38	0.37	0.39	0.37	0.38	0.37	0.40	0.37	0.27	0.33	0.38	0.34	0.39	0.40	0.22	0.50	0.51	
SelLH1M	–	–	–	–	–	–	–	10.4	–	–	–	–	–	–	–	–	–	–	
SelMax1M	–	–	–	–	–	–	–	66.9	–	–	–	–	–	–	–	–	–	–	
SelLH1F	–	–	–	–	–	–	–	18.3	–	–	–	–	–	–	–	–	–	–	
SelMax1F	–	–	–	–	–	–	–	85.8	–	–	–	–	–	–	–	–	–	–	
SelRH1	–	–	–	–	–	–	–	297.1	–	–	–	–	–	–	–	–	–	–	
SelLH2M	7.9	7.9	7.8	7.9	7.7	7.6	7.9	7.5	8.2	7.9	8.3	7.8	8.1	7.5	7.3	5.6	8.1	6.9	
SelMax2M	61.0	60.9	60.8	61.1	60.5	60.5	61.0	60.1	61.7	61.2	63.2	60.8	61.7	60.0	59.6	59.0	61.2	58.4	
SelLH2F	9.5	9.6	9.6	9.7	9.8	9.7	9.6	9.8	9.7	10.5	9.6	9.7	9.6	9.7	9.8	5.8	10.5	10.0	
SelMax2F	65.6	66.0	65.9	66.2	66.0	65.9	65.8	66.4	66.1	65.2	66.8	66.1	66.1	66.1	66.6	61.0	68.1	67.2	
SelRH2	220.3	218.3	102.3	302.9	190.3	208.6	–	46.9	<b>50</b>	213.0	241.0	222.6	224.5	227.2	167.6	108.9	43.7	31.0	
<i>Reference points</i>																			
B <sub>0</sub>	17 665	17 714	19 064	14 975	16 285	18 088	18 010	11 186	12 671	16 643	17 411	16 038	18 066	17 740	17 806	11 044	11 531	12 604	
SSB <sub>0</sub>	6 783	6 829	7 968	5 832	6 435	6 983	6 758	7 028	7 254	6 068	6 747	8 364	6 888	6 881	7 120	4 399	7 406	12 078	
B <sub>MIN</sub>	1 614	1 629	1 549	1 765	1 679	1 687	1 614	1 736	1 600	893	1 400	1 497	1 410	1 831	1 939	497	1 816	6 256	
B <sub>2018</sub>	2 817	2 838	2 713	3 037	2 933	2 916	2 819	3 207	2 781	1 756	2 475	2 657	1 647	3 031	2 322	1 014	3 102	11 586	
B <sub>2022</sub>	4 355	4 393	4 236	4 652	4 424	4 517	4 359	4 769	4 266	2 984	3 896	4 048	2 495	4 625	3 322	1 791	4 850	19 460	
SSB <sub>2018</sub>	2 439	2 425	2 419	2 463	2 454	2 427	2 427	2 769	2 650	1 896	2 434	2 818	1 781	2 471	1 967	1 479	2 661	9 203	
SSB <sub>2022</sub>	2 629	2 617	2 637	2 624	2 610	2 620	2 618	2 956	2 854	2 141	2 607	3 059	1 875	2 653	2 093	1 698	2 896	10 729	
B <sub>2018</sub> /B <sub>0</sub>	0.159	0.160	0.142	0.203	0.180	0.161	0.157	0.287	0.219	0.106	0.142	0.166	0.091	0.171	0.130	0.092	0.269	0.919	
B <sub>2022</sub> /B <sub>0</sub>	0.247	0.248	0.222	0.311	0.272	0.250	0.242	0.426	0.337	0.179	0.224	0.252	0.138	0.261	0.187	0.162	0.421	1.544	
B <sub>2022</sub> /B <sub>2018</sub>	1.546	1.548	1.561	1.532	1.509	1.549	1.546	1.487	1.534	1.699	1.574	1.524	1.516	1.526	1.431	1.765	1.564	1.680	
SSB <sub>2018</sub> /SSB <sub>0</sub>	0.360	0.355	0.304	0.422	0.381	0.348	0.359	0.394	0.365	0.312	0.361	0.337	0.259	0.359	0.276	0.336	0.359	0.762	
SSB <sub>2022</sub> /SSB <sub>0</sub>	0.388	0.383	0.331	0.450	0.406	0.375	0.387	0.421	0.393	0.353	0.386	0.366	0.272	0.386	0.294	0.386	0.391	0.888	

**Table 5: List of CRA 6 Maximum *a posteriori* (MAP) sensitivity runs.**

Type	Model name	Model description
Base	<i>base</i>	Estimate catches iteratively using Newton-Raphson procedure and estimate the right-hand limb for selectivity
Catch	<i>catch_hi</i>	Catch from 1965-1970 was 30% higher than the base case
	<i>catch_lo</i>	Catch from 1965-1970 was 30% lower than the base case
	<i>start_1979</i>	Start the model in 1979
Selectivity	<i>drop_CR</i>	Drop the CR series (1 <sup>st</sup> CPUE series)
	<i>sel_logistic</i>	Logistic selectivity curve
	<i>sel_1993</i>	Two selectivity epochs, from 1965-1992 and 1993-2017
Tags	<i>sel_rh_lo</i>	Fix the right-hand limb selectivity parameter for stronger dome
	<i>tag_CRA6</i>	CRA 6 tags only
Length-weight	<i>tag_CRA8</i>	All CRA 8 tag data plus CRA 6 tag data
	<i>lw_SI</i>	Use South Island specific length-weight parameters
Catchability	<i>qdrift</i>	estimate q-drift parameter with uniform prior
Weighting	<i>base_cpue3_sdnr1</i>	Downweight CELR series (3 <sup>rd</sup> CPUE series) such that SDNR=1.0
	<i>wtdown_CPUE</i>	Downweight all CPUE series, dropping the weights to 0.1 each
	<i>wtup_CPUE</i>	Upweight all CPUE series by multiplying the weights by 10
	<i>wtup_LFSexRatio</i>	Upweight length frequency data and sex ratio information by multiplying the weights by 10
	<i>wtup_LF1996</i>	Upweight the initial LF in 1966 to weight=10

**Table 6: List of CRA 6 Markov chain Monte Carlo (MCMC) models. Accepted runs are marked with an asterisk (\*).**

Model name	Model description	Number of usable chains	Number of MCMC samples
<i>base</i>	as defined in Section 2.5.1*	7	1 001
<i>catch_hi</i>	Catch from 1965–1970 was 30% higher than the base case*	7	1 001
<i>catch_lo</i>	Catch from 1965–1970 was 30% lower than the base case	5	715
<i>q-drift</i>	Estimate q-drift parameter with uniform prior*	8	1 144
<i>combined</i>	Posterior distribution stack of the three accepted runs	21	3 003

**Table 7: CRA 6 base case sensitivity runs and combined model (see Table 6 for run descriptions) MCMC outputs, reporting the 5<sup>th</sup>, 50<sup>th</sup> (median), and 95<sup>th</sup> quantiles of the posterior distributions. Growth increment values in mm TW, biomass values in tonnes and  $R_0$  in numbers. Handling mortality ( $H$ ) in tonnes and CPUE in kg/potlift. ‘-’: not applicable.**

	<i>base</i>			<i>catch hi</i>			<i>catch lo</i>			<i>q-drift</i>			<i>combined</i>		
	5%	50%	95%	5%	50%	95%	5%	50%	95%	5%	50%	95%	5%	50%	95%
<i>Likelihood components</i>															
<i>LFs-sdnr</i>	0.412	0.475	0.706	0.413	0.477	0.689	0.415	0.476	0.689	0.410	0.468	0.654	0.411	0.473	0.680
<i>LFs-MAR</i>	0.064	0.072	0.080	0.064	0.071	0.080	0.064	0.072	0.081	0.063	0.071	0.080	0.064	0.071	0.080
<i>LFs-LL</i>	3 295.8	3 301.0	3 307.4	3 319.4	3 324.9	3 331.1	3 318.6	3 324.6	3 332.0	3 312.1	3 317.9	3 324.7	3 297.3	3 317.8	3 328.8
<i>Tags-sdnr</i>	1.991	2.071	2.160	1.984	2.073	2.162	1.983	2.072	2.159	1.998	2.079	2.171	1.992	2.074	2.166
<i>Tags-MAR</i>	0.714	0.729	0.746	0.713	0.730	0.745	0.713	0.729	0.746	0.715	0.731	0.747	0.714	0.730	0.746
<i>Tags-LL</i>	5 854.1	5 856.4	5 860.5	5 853.8	5 856.2	5 860.5	5 854.4	5 856.9	5 861.2	5 853.8	5 856.2	5 860.2	5 853.9	5 856.3	5 860.5
<i>CELR sdnr</i>	1.473	1.536	1.608	1.483	1.543	1.613	1.465	1.526	1.596	1.484	1.552	1.629	1.479	1.544	1.620
<i>CELR MAR</i>	0.825	0.946	1.079	0.836	0.953	1.078	0.821	0.936	1.082	0.843	0.986	1.133	0.835	0.960	1.107
<i>CELR LL</i>	- 99.9	- 94.3	- 87.7	- 99.1	- 93.8	- 87.3	- 100.6	- 95.3	- 89.0	- 99.1	- 93.0	- 85.9	- 99.3	- 93.7	- 86.6
<i>FSU-sdnr</i>	0.886	0.993	1.133	0.895	0.995	1.141	0.868	0.975	1.117	0.875	0.964	1.084	0.883	0.982	1.124
<i>FSU-MAR</i>	0.466	0.606	0.886	0.481	0.628	0.896	0.439	0.587	0.873	0.435	0.563	0.843	0.454	0.596	0.877
<i>FSU-LL</i>	- 29.5	- 27.5	- 24.3	- 29.4	- 27.4	- 24.3	- 29.8	- 27.8	- 24.8	- 29.7	- 28.0	- 25.3	- 29.6	- 27.7	- 24.5
<i>CR-sdnr</i>	0.923	1.038	1.150	0.810	0.890	0.980	1.148	1.292	1.409	0.949	1.071	1.191	0.840	1.009	1.163
<i>CR-MAR</i>	0.651	0.825	0.941	0.491	0.659	0.816	0.870	1.036	1.183	0.698	0.855	1.006	0.539	0.792	0.959
<i>CR-LL</i>	- 11.7	- 9.8	- 7.6	- 13.3	- 12.0	- 10.1	- 8.2	- 5.4	- 2.7	- 11.3	- 9.3	- 6.9	- 12.8	- 10.3	- 7.4
<i>Sex-sdnr</i>	1.022	1.065	1.123	1.013	1.051	1.112	1.034	1.085	1.154	1.017	1.051	1.106	1.016	1.055	1.116
<i>Sex-MAR</i>	0.651	0.825	0.941	0.491	0.659	0.816	0.870	1.036	1.183	0.698	0.855	1.006	0.539	0.792	0.959
<i>Sex-LL</i>	1 080.5	1 082.8	1 086.5	1 076.6	1 078.7	1 081.9	1 077.9	1 080.8	1 085.3	1 076.6	1 078.5	1 081.6	1 076.8	1 079.5	1 084.9
<i>Prior</i>	10.8	18.2	27.4	11.0	18.5	28.5	10.2	18.7	27.4	11.3	18.7	28.0	11.0	18.5	28.0
<i>Function value</i>	10 139.2	10 127.7	10 118.9	10 157.6	10 146.5	10 137.0	10 164.8	10 153.5	10 144.4	10 153.5	10 142.2	10 133.5	10 154.4	10 140.5	10 122.2
<i>Parameters</i>															
$R_0$	285 484	337 830	407 218	270 557	320 682	378 933	304 808	360 388	432 135	249 420	296 374	357 186	261 501	317 884	384 401
$M$	0.0416	0.0475	0.0542	0.0361	0.0416	0.0474	0.0486	0.0551	0.0634	0.0369	0.0428	0.0495	0.0370	0.0437	0.0516
<i>q-drift</i>	4.19E-04	4.83E-04	5.60E-04	4.42E-04	5.15E-04	5.89E-04	3.84E-04	4.51E-04	5.26E-04	4.05E-04	4.62E-04	5.34E-04	4.16E-04	4.86E-04	5.70E-04
<i>qCPUE</i>	4.55E-04	5.27E-04	6.08E-04	4.90E-04	5.61E-04	6.44E-04	4.22E-04	4.87E-04	5.62E-04	4.57E-04	5.22E-04	5.98E-04	4.64E-04	5.35E-04	6.24E-04
<i>qFSU</i>	3.75E-02	4.55E-02	5.49E-02	3.65E-02	4.44E-02	5.42E-02	3.80E-02	4.58E-02	5.57E-02	3.65E-02	4.38E-02	5.31E-02	3.67E-02	4.46E-02	5.42E-02
<i>qCR</i>	-	-	-	-	-	-	-	-	-	0.0088	0.0184	0.0274	-	-	-
<i>mat50</i>	51.9	54.1	56.8	52.0	54.1	56.5	52.1	54.1	56.7	52.0	54.1	56.9	51.9	54.1	56.7
<i>mat95Add</i>	10.1	18.3	30.2	10.5	18.8	30.1	10.3	18.6	29.8	10.4	19.0	30.2	10.3	18.7	30.1
<i>GalphaM</i>	5.1	5.3	5.4	5.1	5.3	5.4	5.1	5.3	5.4	5.2	5.3	5.4	5.2	5.3	5.4
<i>GbetaM</i>	2.4	2.5	2.7	2.4	2.5	2.7	2.4	2.5	2.7	2.4	2.5	2.7	2.4	2.5	2.6
<i>GshapeM</i>	1.6	2.0	2.3	1.6	2.0	2.4	1.6	1.9	2.3	1.6	2.0	2.3	1.6	2.0	2.3
<i>GCVM</i>	0.444	0.458	0.473	0.443	0.458	0.473	0.444	0.458	0.473	0.442	0.457	0.472	0.443	0.458	0.473
<i>GalphaF</i>	3.9	4.0	4.2	3.9	4.0	4.2	3.9	4.0	4.2	3.9	4.0	4.2	3.9	4.0	4.2
<i>GbetaF</i>	1.5	1.5	1.6	1.5	1.5	1.6	1.5	1.6	1.6	1.5	1.5	1.6	1.5	1.6	2.6
<i>GshapeF</i>	2.9	3.2	3.6	2.9	3.2	3.6	2.9	3.3	3.6	2.9	3.2	3.5	2.9	3.2	3.6
<i>GCVF</i>	0.500	0.520	0.540	0.501	0.521	0.540	0.500	0.521	0.541	0.500	0.520	0.540	0.500	0.520	0.540
<i>StdObs</i>	0.283	0.330	0.384	0.283	0.330	0.387	0.281	0.328	0.380	0.283	0.330	0.385	0.283	0.330	0.385
<i>vuln1</i>	0.840	0.870	0.899	0.822	0.852	0.885	0.858	0.890	0.924	0.816	0.846	0.881	0.822	0.856	0.892
<i>vuln2</i>	0.413	0.686	0.963	0.419	0.683	0.951	0.418	0.711	0.969	0.387	0.669	0.944	0.409	0.678	0.951

	<i>base</i>			<i>catch_hi</i>			<i>catch_lo</i>			<i>q-drift</i>			<i>combined</i>		
	5%	50%	95%	5%	50%	95%	5%	50%	95%	5%	50%	95%	5%	50%	95%
<i>vuln3</i>	0.569	0.673	0.792	0.550	0.656	0.781	0.591	0.698	0.839	0.529	0.642	0.757	0.544	0.656	0.781
<i>vuln4</i>	0.317	0.388	0.469	0.302	0.372	0.447	0.332	0.405	0.492	0.283	0.353	0.435	0.293	0.369	0.453
<i>SelLH1M</i>	6.1	7.9	10.1	6.2	7.9	9.9	6.3	8.0	10.1	6.6	8.3	10.7	6.3	8.0	10.3
<i>SelMax1M</i>	58.0	61.0	64.1	58.0	60.8	63.9	58.4	61.1	64.4	59.0	61.7	65.6	58.3	61.2	64.7
<i>SelLH1F</i>	8.3	10.0	12.2	8.2	9.9	12.0	8.3	10.0	12.5	8.3	9.9	12.1	8.3	9.9	12.1
<i>SelMax1F</i>	63.7	66.4	69.6	63.5	66.2	69.2	64.2	66.8	70.4	63.9	66.4	69.7	63.7	66.3	69.5
<i>SelRH1</i>	109	416	1 014	88	372	943	117	430	1 036	125	420	1 038	107	401	995
<i>Reference points</i>															
$B_0$	16 057	17 472	18 550	18 117	20 645	21 786	13 273	14 565	15 587	16 584	17 923	18 994	16 392	18 129	21 348
$B_{onow}$	17 785	21 058	24 859	19 967	24 079	28 555	15 331	18 124	21 422	17 050	20 215	23 932	17 636	21 559	26 834
$SSB_0$	6 282	6 695	7 111	7 191	7 741	8 265	5 302	5 700	6 078	6 263	6 762	7 211	6 337	6 886	8 049
$SSB_{onow}$	6 927	8 046	9 418	7 764	9 099	10 745	6 094	7 074	8 369	6 533	7 609	9 009	6 801	8 187	10 095
$B_{tot}$	23 802	24 974	26 125	28 008	29 282	30 368	19 683	20 986	22 189	24 133	25 368	26 561	24 048	25 654	29 983
$B_{MIN}$	1 438	1 680	1 953	1 360	1 575	1 842	1 534	1 805	2 128	1 201	1 473	1 762	1 279	1 572	1 883
$B_{2018}$	2 502	2 912	3 403	2 374	2 762	3 236	2 662	3 111	3 738	1 369	1 769	2 397	1 482	2 635	3 261
$B_{2022}$	3 786	4 663	5 729	3 567	4 424	5 457	3 982	4 933	6 217	1 997	2 773	3 845	2 206	4 136	5 460
$SSB_{2018}$	2 195	2 442	2 733	2 156	2 403	2 696	2 218	2 491	2 794	1 518	1 836	2 223	1 618	2 310	2 669
$SSB_{2022}$	2 356	2 685	3 106	2 328	2 659	3 082	2 362	2 721	3 169	1 561	1 966	2 462	1 695	2 519	3 035
$B_{2018}^{tot}$	10 660	11 933	13 613	10 241	11 484	13 066	11 064	12 469	14 373	6 776	8 274	10 238	7 195	11 084	13 102
$B_{2022}^{tot}$	11 422	13 314	15 874	10 926	12 817	15 188	11 570	13 747	16 577	6 735	8 799	11 376	7 337	12 121	15 083
$CPUE_{2018}$	1.27	1.42	1.57	1.28	1.42	1.60	1.25	1.40	1.58	0.65	0.85	1.15	0.71	1.35	1.57
$CPUE_{2022}$	1.45	1.71	2.06	1.47	1.75	2.10	1.41	1.67	1.98	0.67	0.97	1.39	0.75	1.60	2.02
$H_{2017}$	2.3	2.6	3.0	2.3	2.6	3.0	2.3	2.6	2.9	2.6	3.0	3.5	2.3	2.8	3.3
$H_{2021}$	1.5	1.9	2.5	1.5	1.9	2.4	1.5	1.9	2.4	1.8	2.4	3.2	1.5	2.0	2.9
$B_{2018} / B_0$	0.140	0.167	0.201	0.113	0.135	0.165	0.180	0.214	0.263	0.075	0.099	0.136	0.082	0.13	0.187
$B_{2022} / B_0$	0.215	0.268	0.331	0.172	0.216	0.277	0.273	0.339	0.434	0.110	0.155	0.222	0.122	0.21	0.309
$B_{2022} / B_{2018}$	1.456	1.596	1.783	1.448	1.589	1.784	1.430	1.580	1.781	1.364	1.558	1.800	1.409	1.58	1.791
$SSB_{2018} / SSB_0$	0.327	0.364	0.409	0.276	0.312	0.351	0.387	0.438	0.492	0.220	0.272	0.335	0.24	0.31	0.39
$SSB_{2022} / SSB_0$	0.352	0.402	0.465	0.297	0.345	0.401	0.410	0.478	0.554	0.229	0.292	0.370	0.25	0.35	0.44
$SSB_{2022} / SSB_{2018}$	1.036	1.101	1.187	1.041	1.104	1.185	1.020	1.089	1.177	0.987	1.072	1.171	1.009	1.09	1.181
$B_{2018}^{tot} / B_0^{tot}$	0.425	0.478	0.548	0.348	0.393	0.448	0.523	0.595	0.702	0.264	0.327	0.406	0.281	0.39	0.518
$B_{2022}^{tot} / B_0^{tot}$	0.452	0.531	0.636	0.372	0.438	0.526	0.553	0.655	0.803	0.260	0.347	0.457	0.287	0.44	0.592
$B_{2022}^{tot} / B_{2018}^{tot}$	1.040	1.111	1.196	1.049	1.114	1.198	1.027	1.099	1.185	0.969	1.064	1.166	0.996	1.10	1.189
<i>Probabilities</i>															
$P(B_{2018} > B_{MIN})$	1.0	1.0	1.0	1.0	1.0	1.0	1.0	1.0	1.0	1.0	1.0	1.0	1.0	1.0	1.0
$P(SSB_{2018} < 20\% SSB_0)$	0.0	0.0	0.0	0.0	0.0	0.0	0.0	0.0	0.0	0.0	0.0	0.0	0.0	0.0	0.0
$P(SSB_{2018} < 10\% SSB_0)$	0.0	0.0	0.0	0.0	0.0	0.0	0.0	0.0	0.0	0.0	0.0	0.0	0.0	0.0	0.0

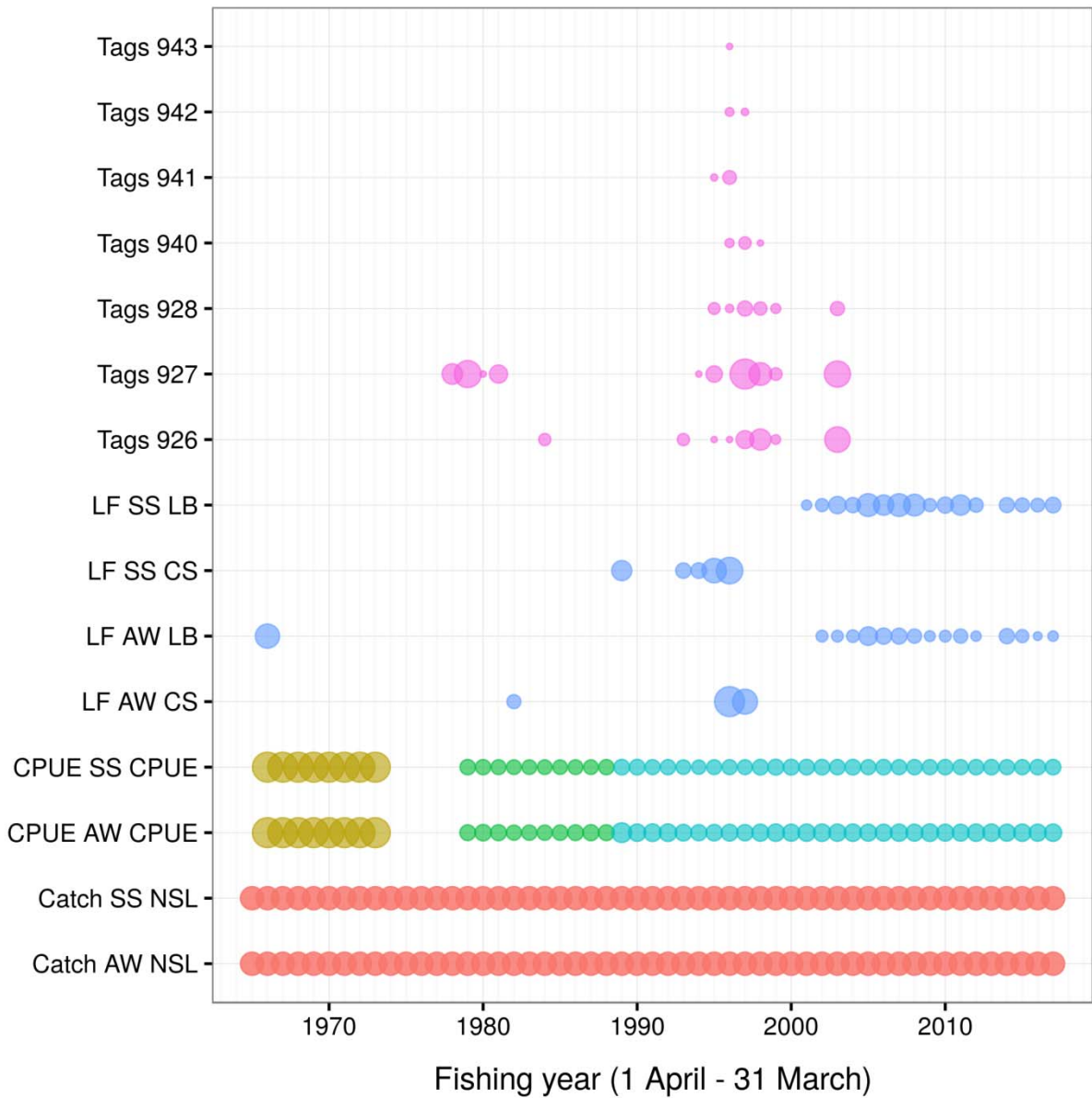


**Figure 2:** Extent of data for each fishing year used in the CRA 6 stock assessment. The size of the bubbles respectively represent the relative number of recaptured tags, the effective sample size for length frequency distributions, the standard deviation for CPUE, and a fixed size for catch. The different bubble colours represent different datasets (e.g. for CPUE the CR, FSU and CELR series).

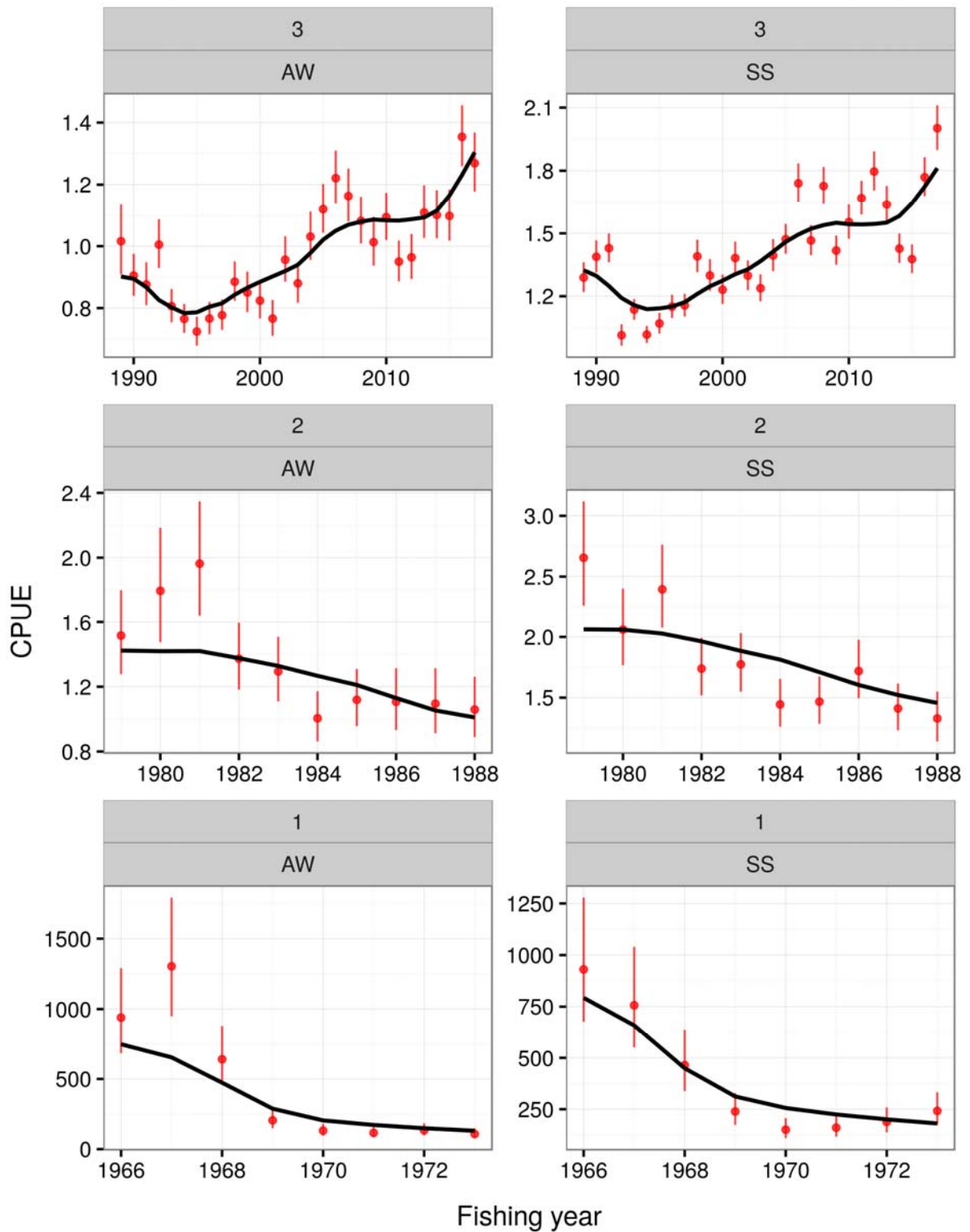
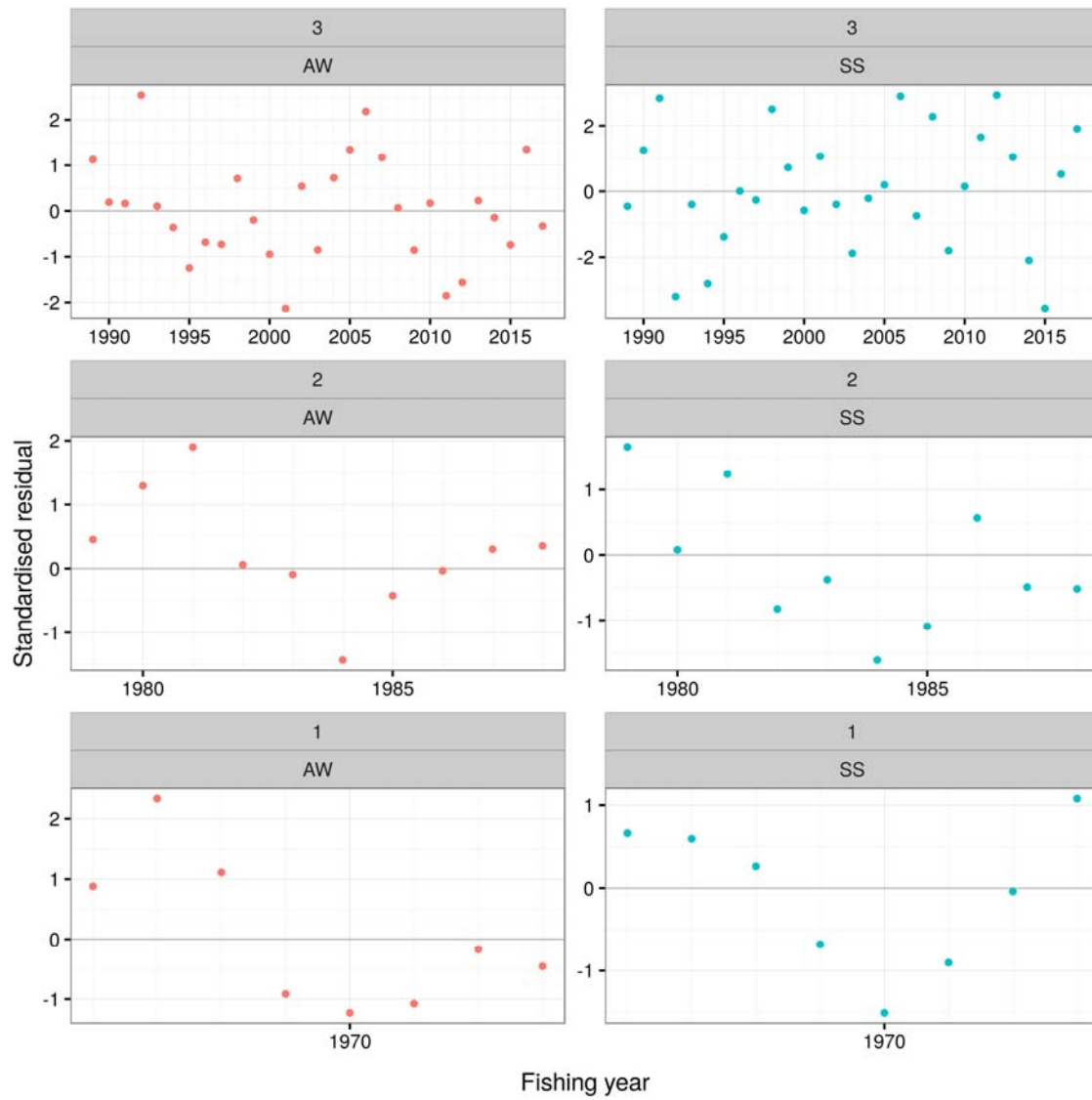


Figure 3: CRA 6 base case: MAP model fit to CPUE. Upper panels=CELR fit; middle panels=FSU fit; lower panels=CR fit.



**Figure 4: CRA 6 base case: MAP residuals from fit to CPUE. Upper panels=CELR fit; middle panels=FSU fit; lower panels=CR fit.**

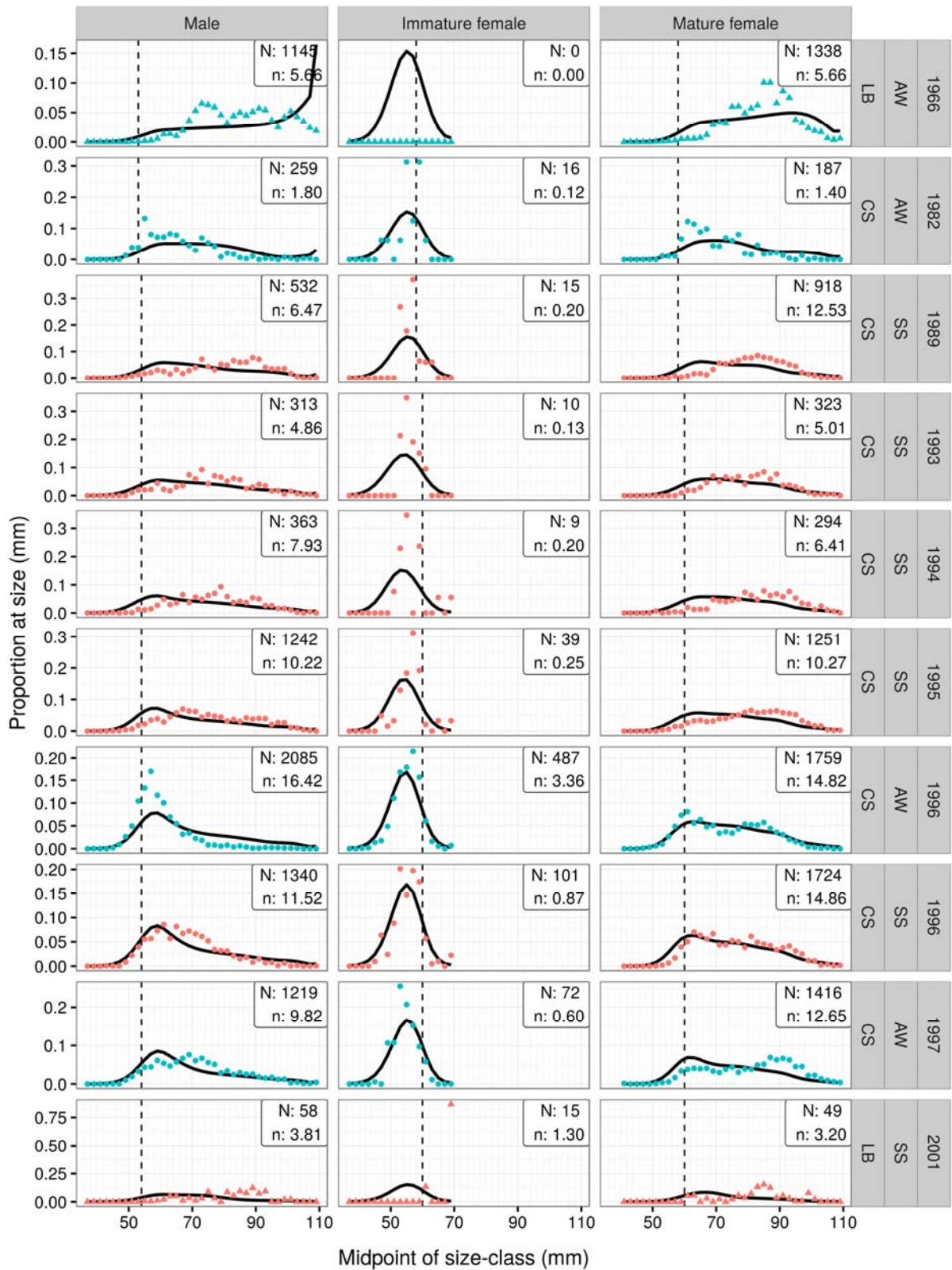


Figure 5: CRA 6 base case MAP: Model fits to LFs from 1966 AW LB – 2001 SS LB.

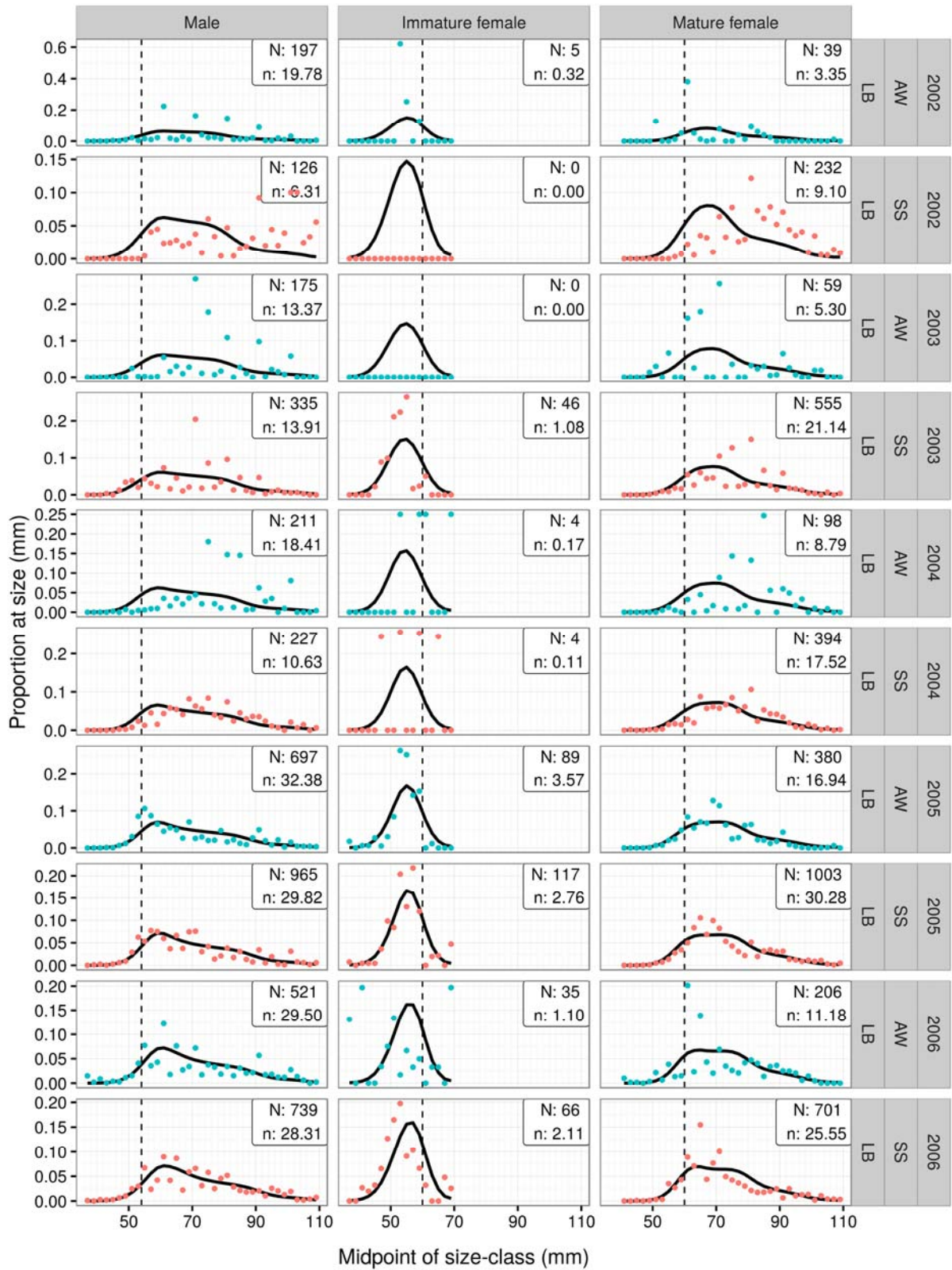


Figure 6: CRA 6 base case MAP: Model fits to LFs from 2002 AW LB – 2006 SS LB.

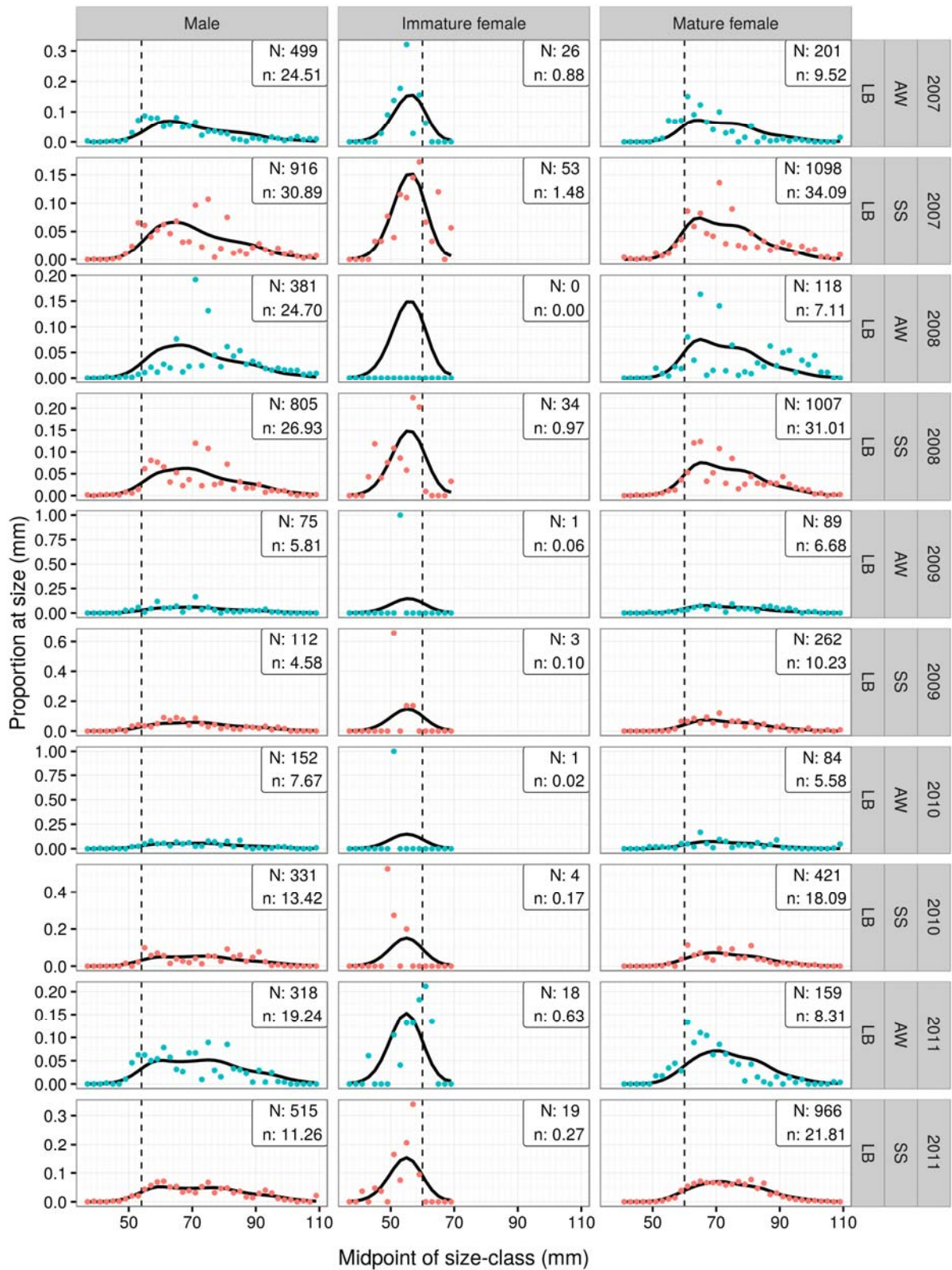


Figure 7: CRA 6 base case MAP: Model fits to LFs from 2007 AW LB – 2011 SS LB.

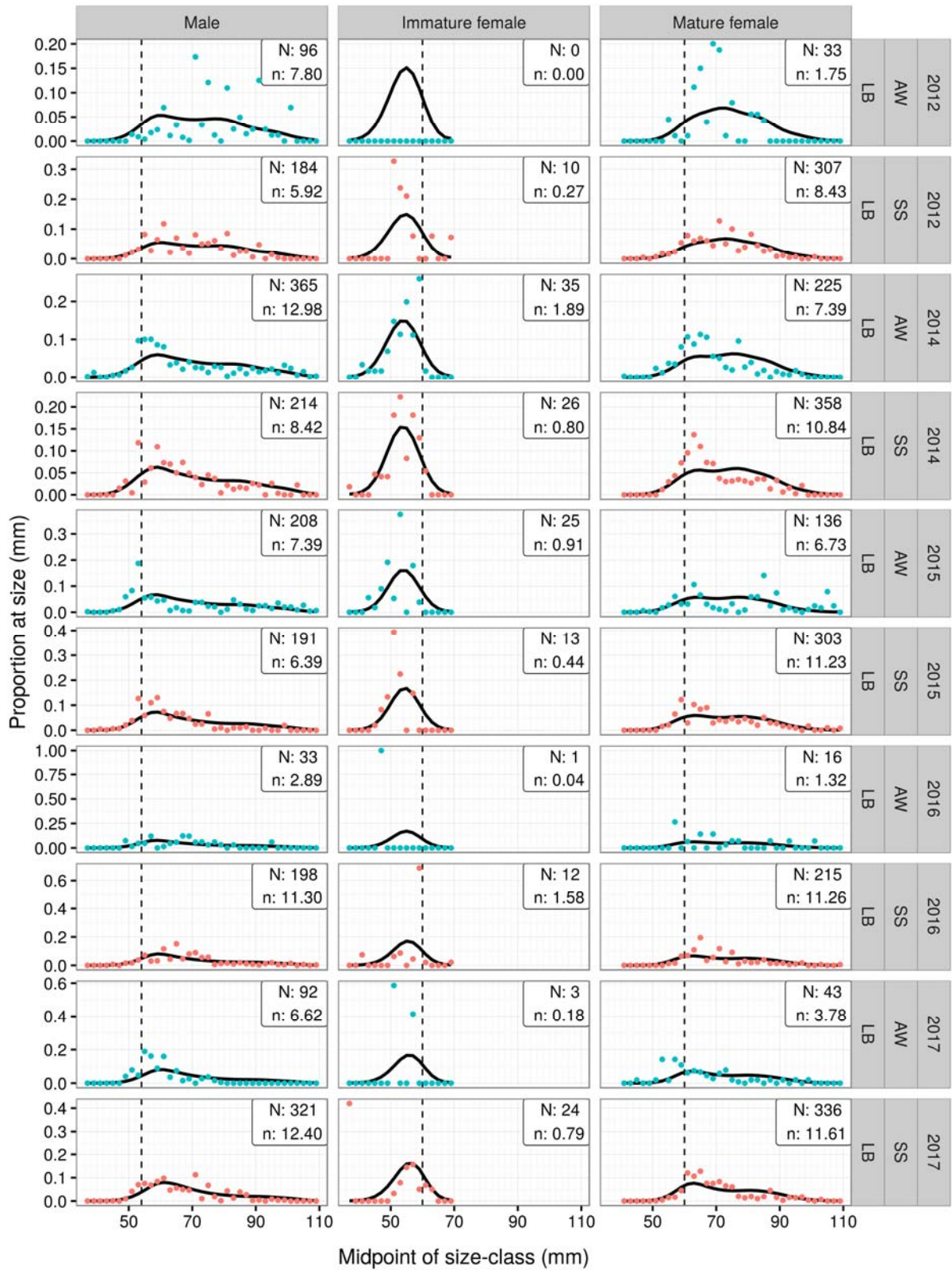
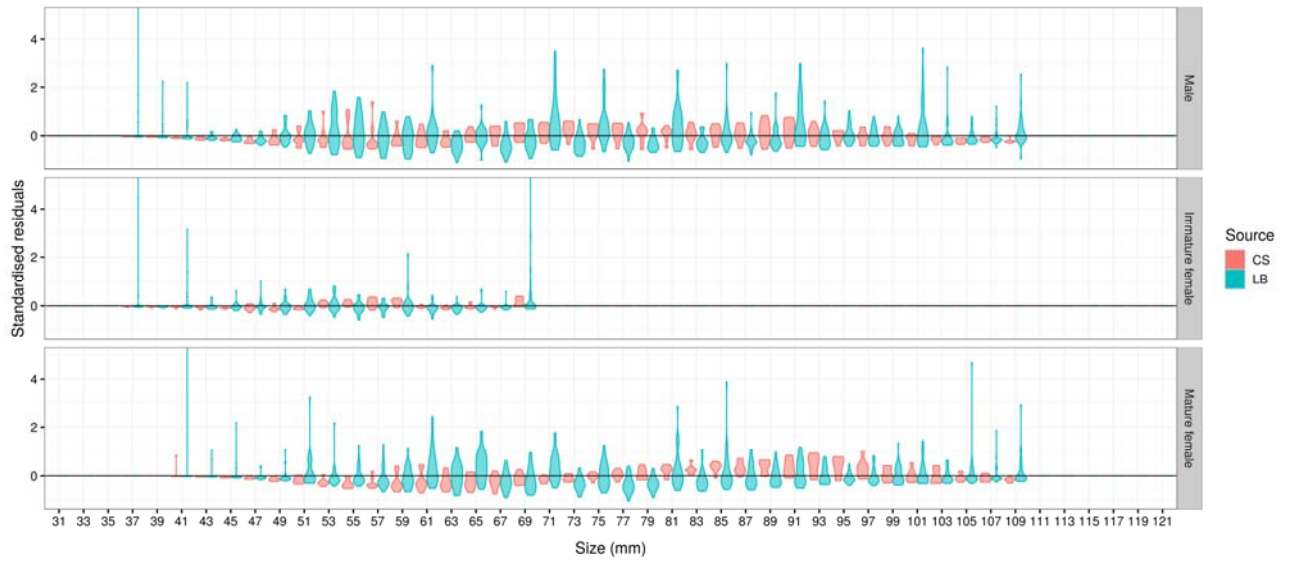
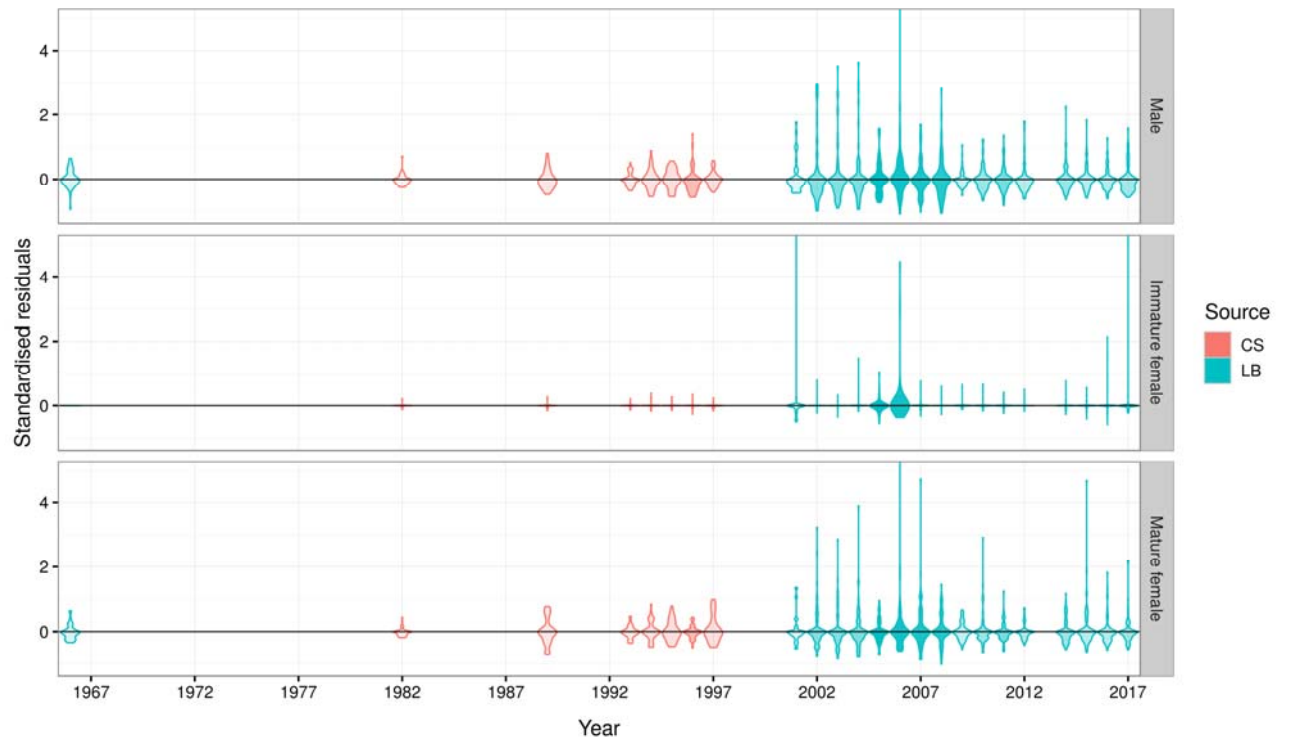


Figure 8: CRA 6 base case MAP: Model fits to LFs from 2012 AW LB – 2017 SS LB.



**Figure 9: CRA 6 base case: MAP residuals from fit to the LF data, showing residuals by sex, 2 mm size bin and sampling source.**



**Figure 10: CRA 6 base case: MAP residuals from fit to the LF data, showing residuals by sex, year and sampling source.**

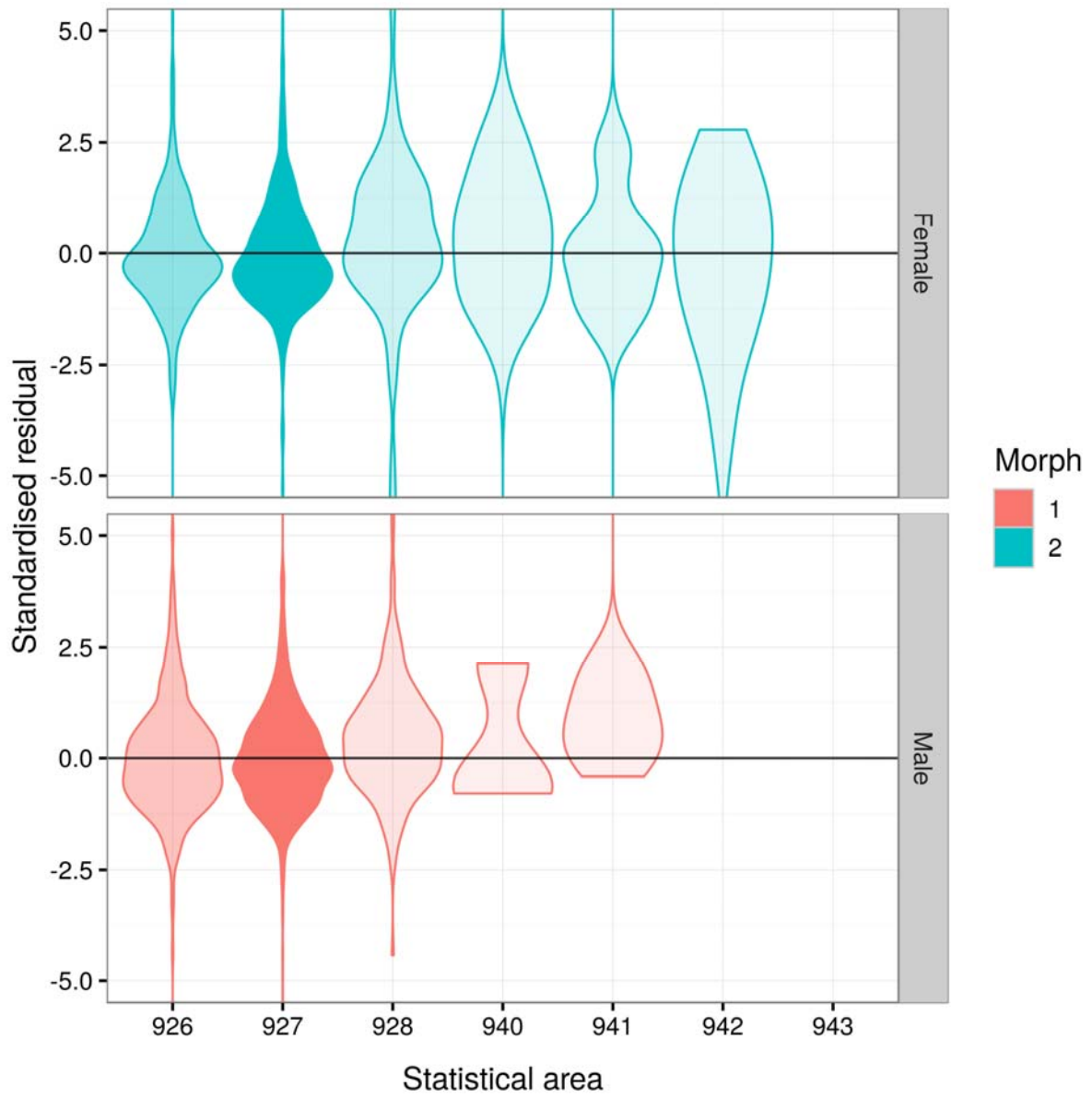


**Figure 11: CRA 6 base case MAP: tag residuals by statistical area of release. Darker shading represents a higher number of tags by area.**

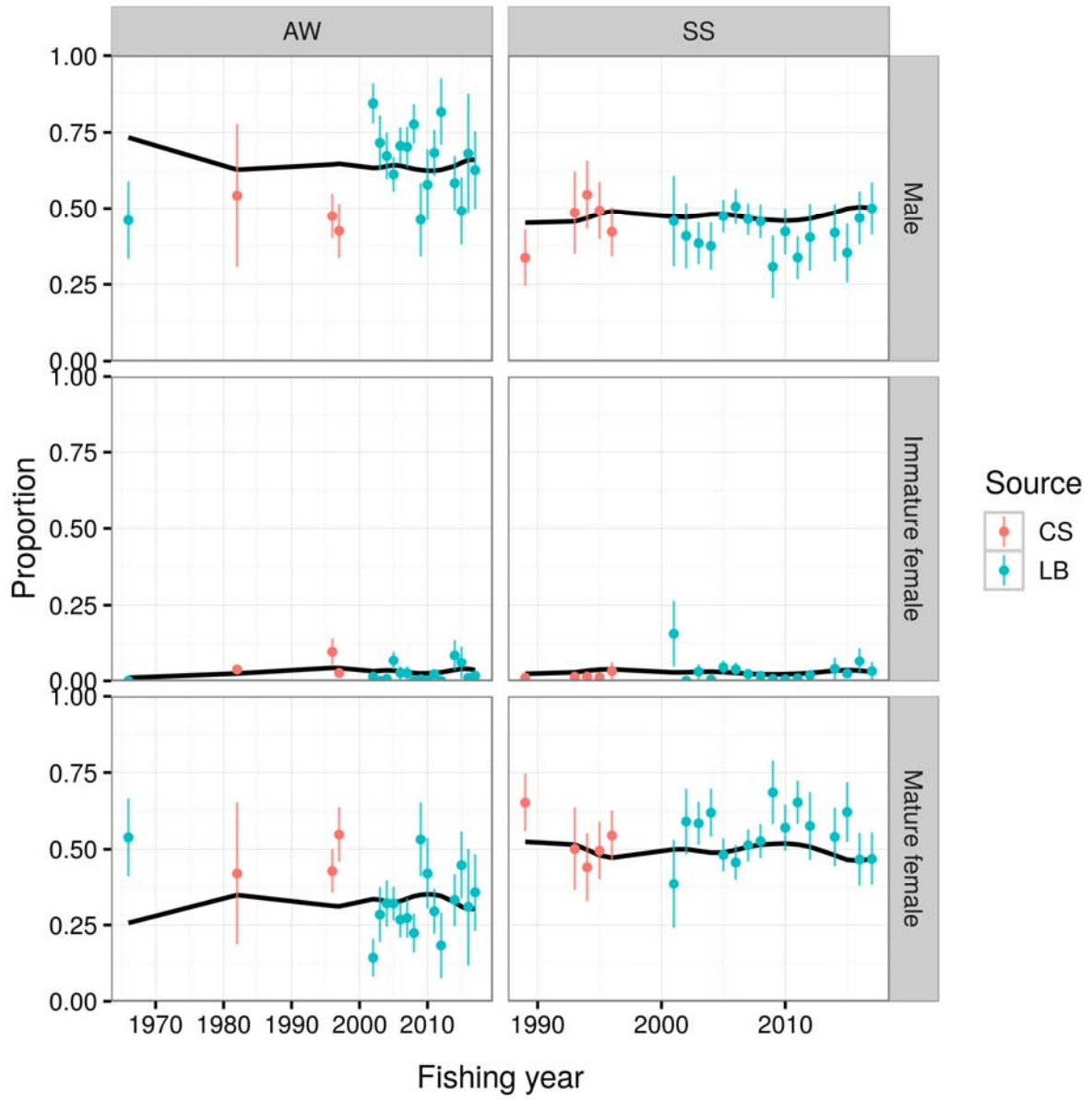


Figure 12: CRA 6 base case MAP: model fit to sex ratios, by year and LF data source.

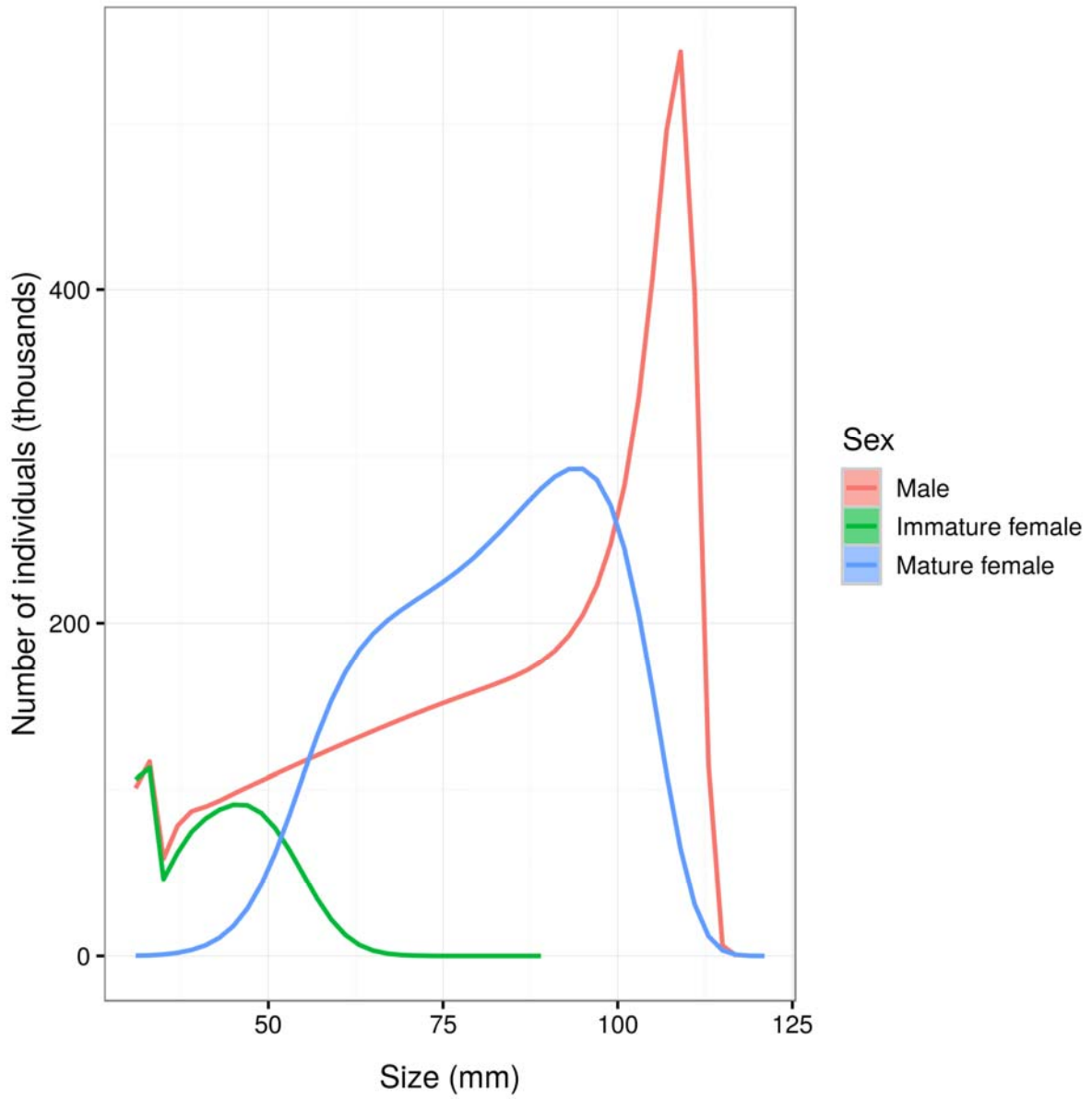
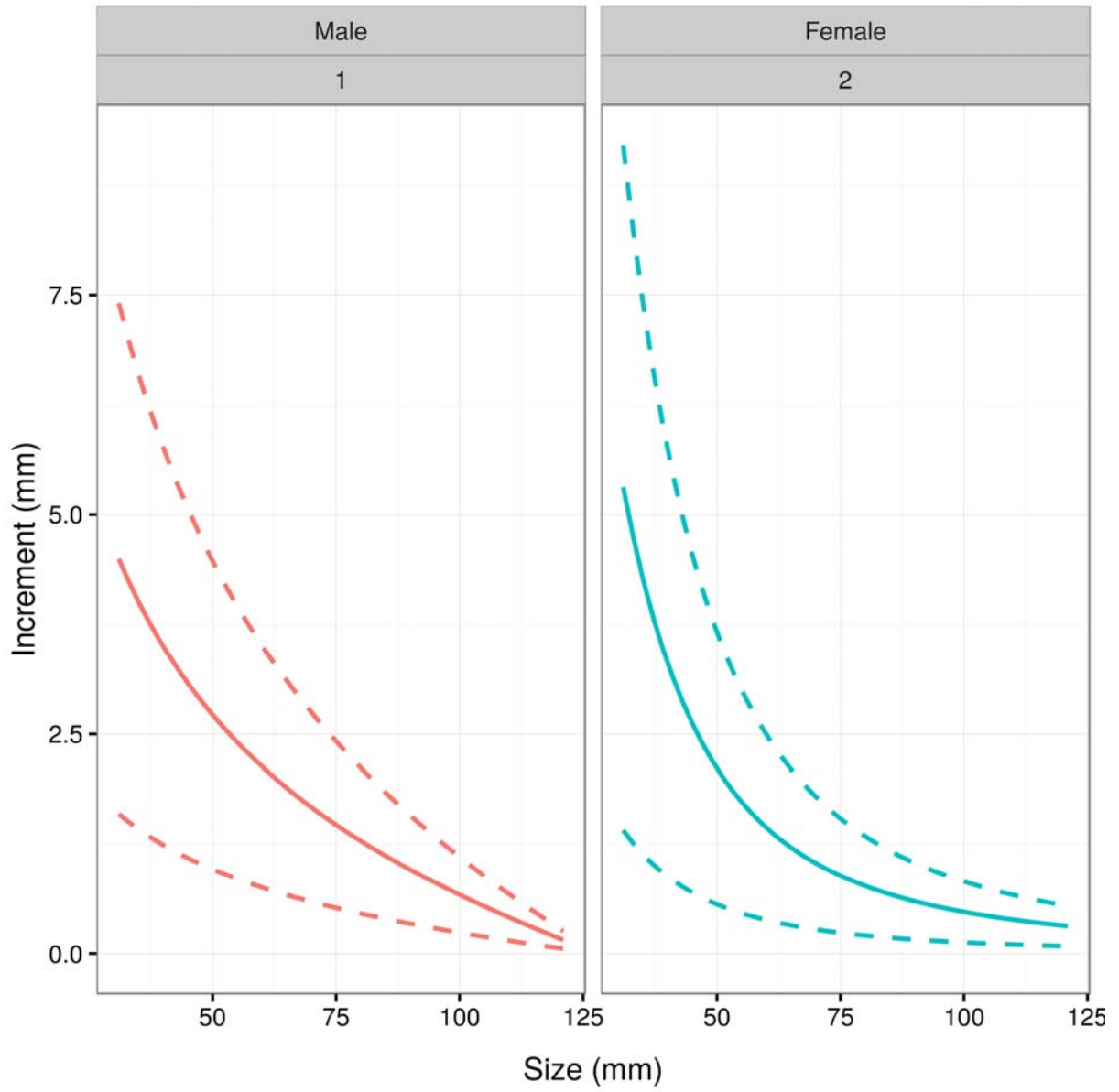
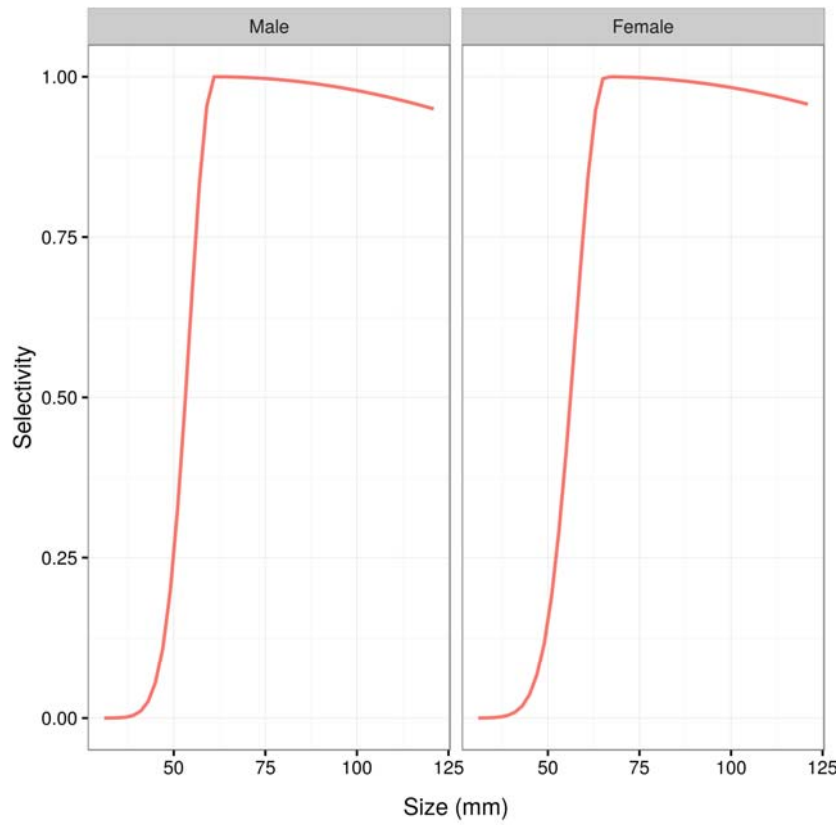


Figure 13: CRA 6 base case MAP: Initial number of individuals by sex category.



**Figure 14: CRA 6 base case MAP: Predicted increments-at-length and  $\pm 1$  standard deviation.**



**Figure 15: CRA 6 base case MAP: selectivity by sex.**

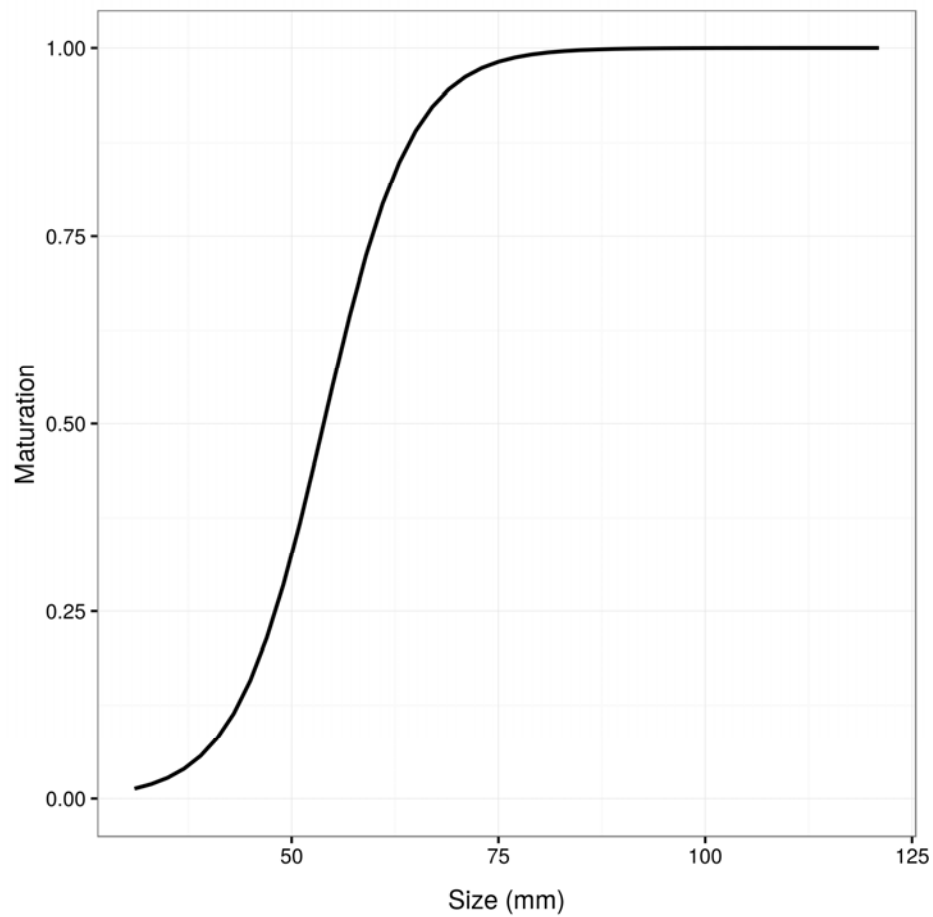


**Figure 16: CRA 6 base case MAP: female maturation curve.**

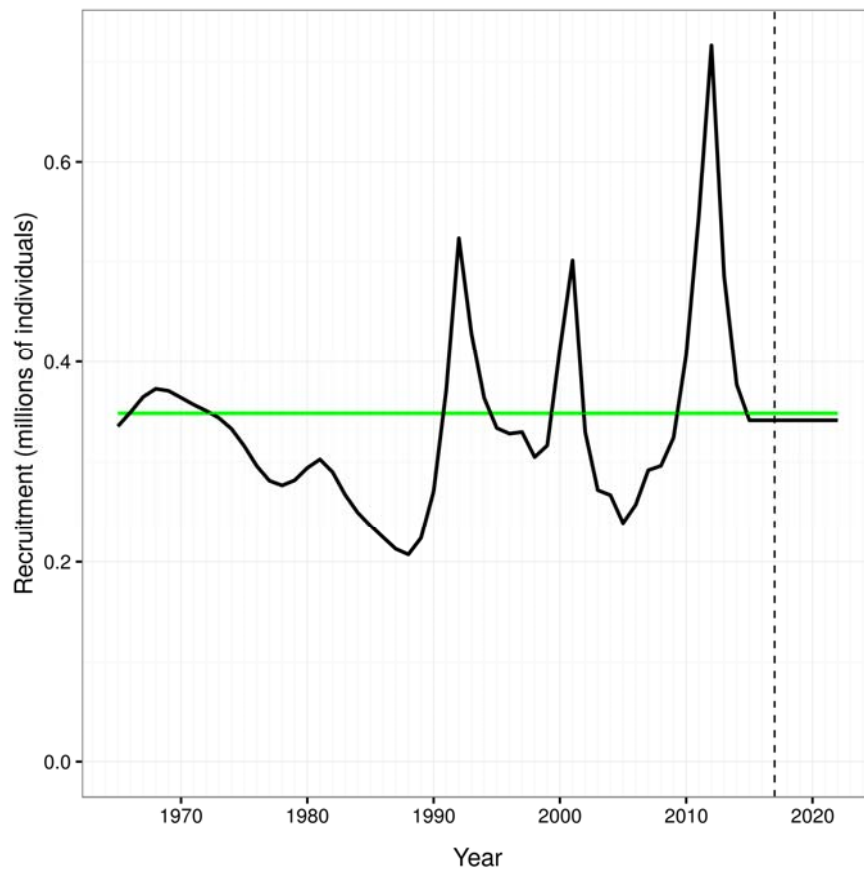


**Figure 17: CRA 6 base case MAP: recruitment in 000 000's. Horizontal line is  $R_0$  and vertical dashed line is the final year of the reconstruction period.**

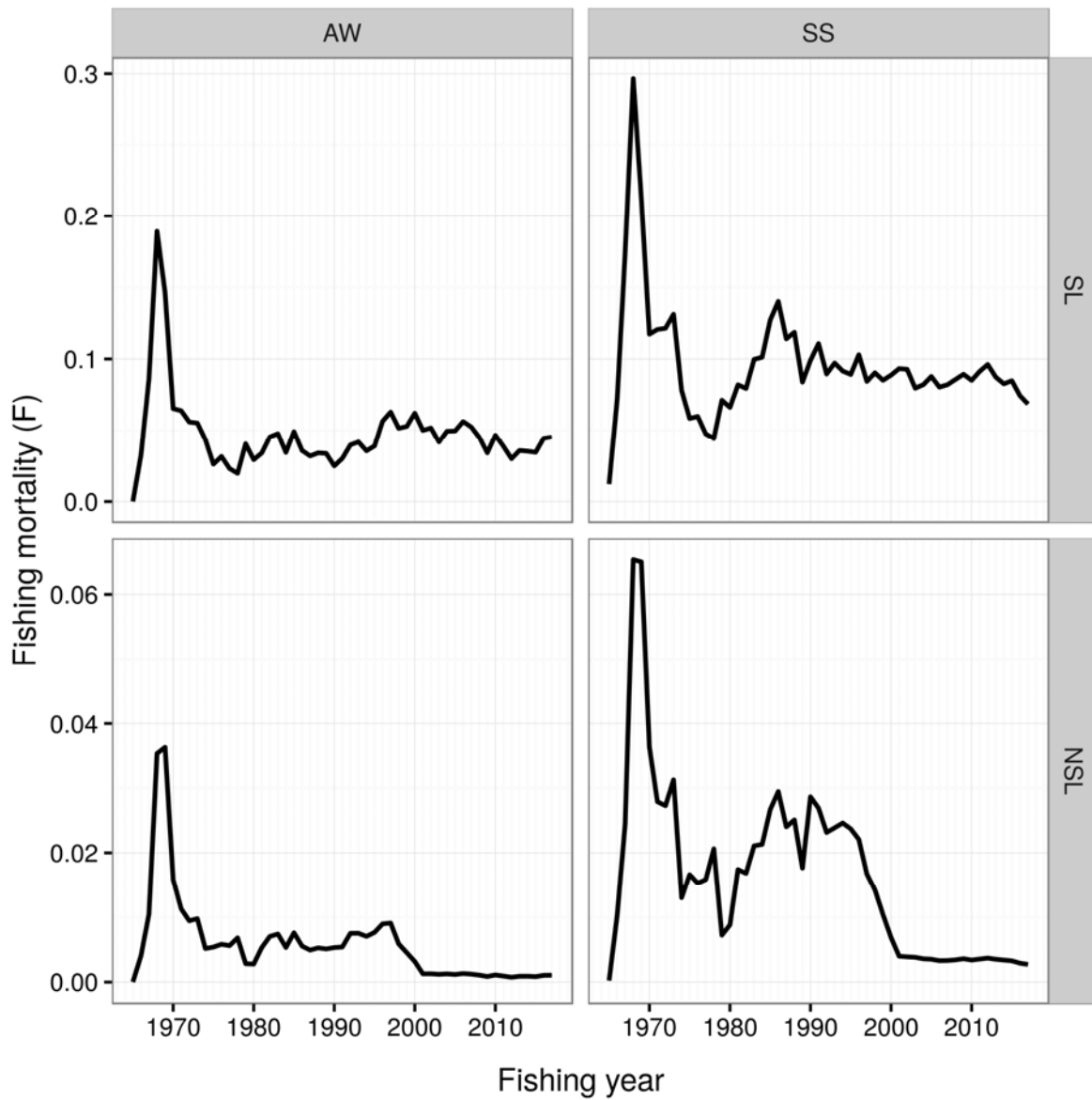
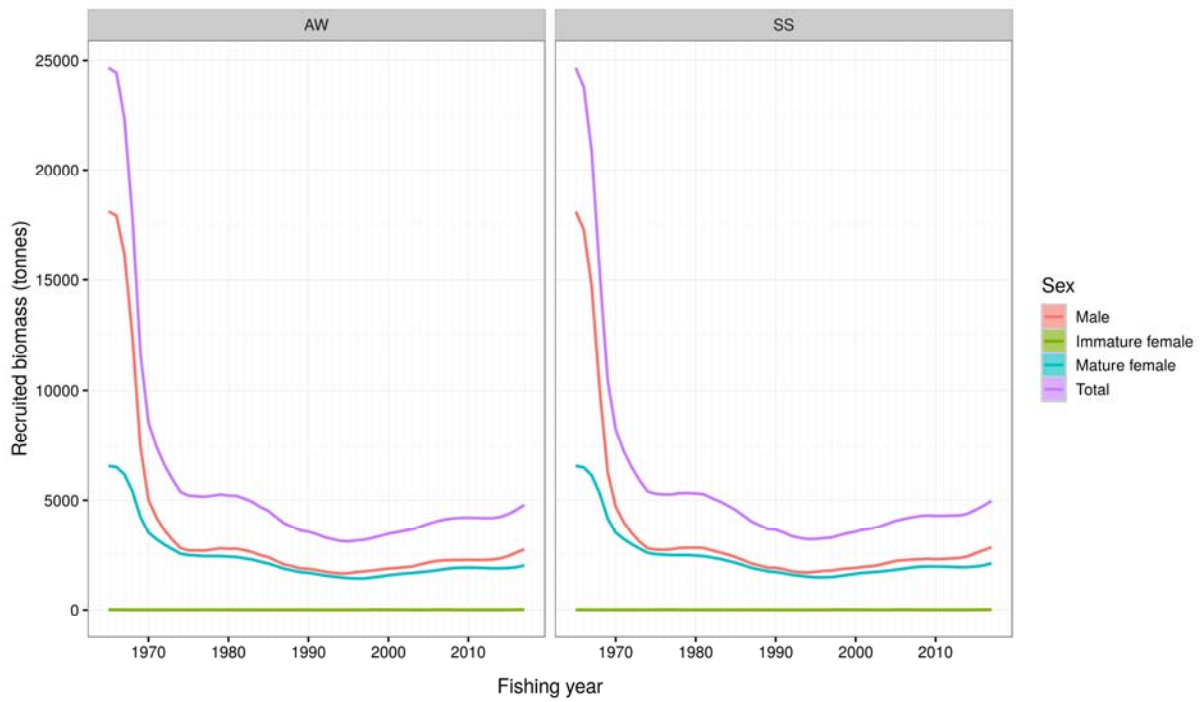
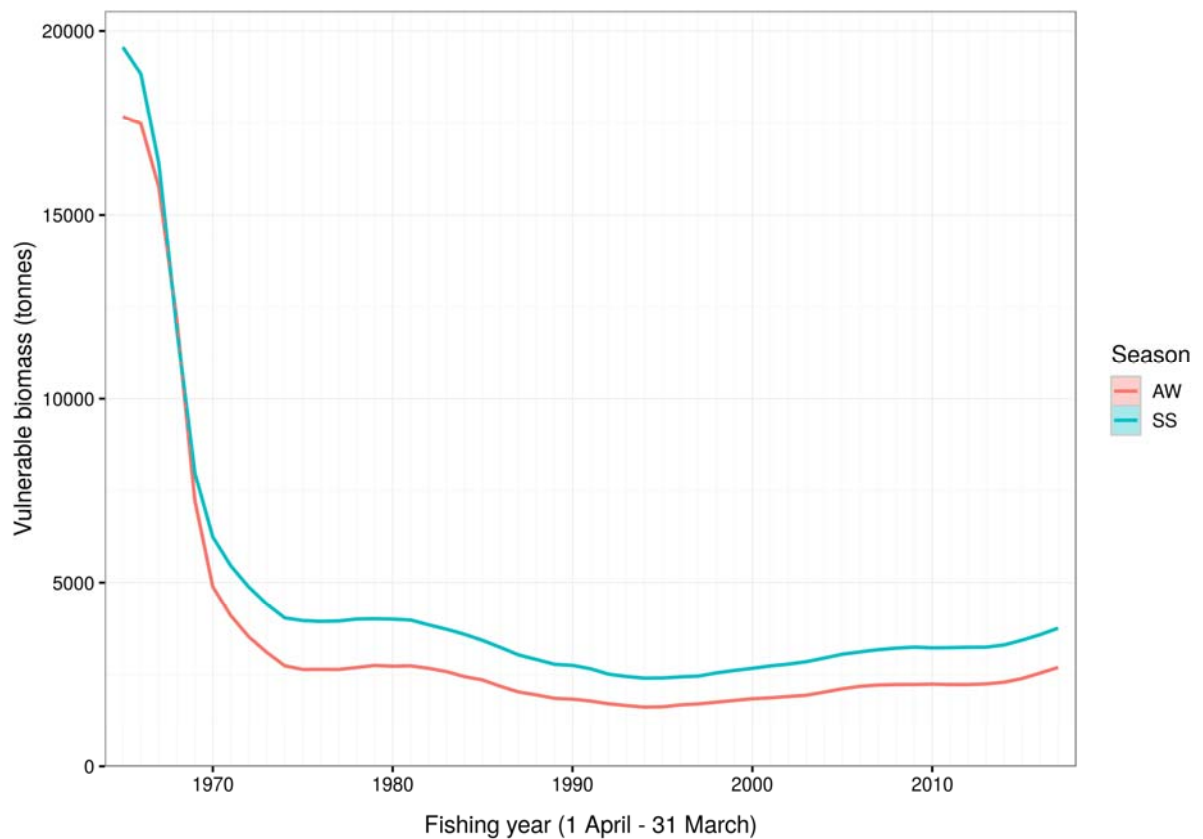


Figure 18: CRA 6 base case MAP: fishing mortality by year, season and catch category.



**Figure 19: CRA 6 base case MAP: trajectory of recruited biomass by sex category and season. The total biomass across all three sex categories is shown as a purple line.**



**Figure 20: CRA 6 base case MAP: trajectory of vulnerable biomass by season.**

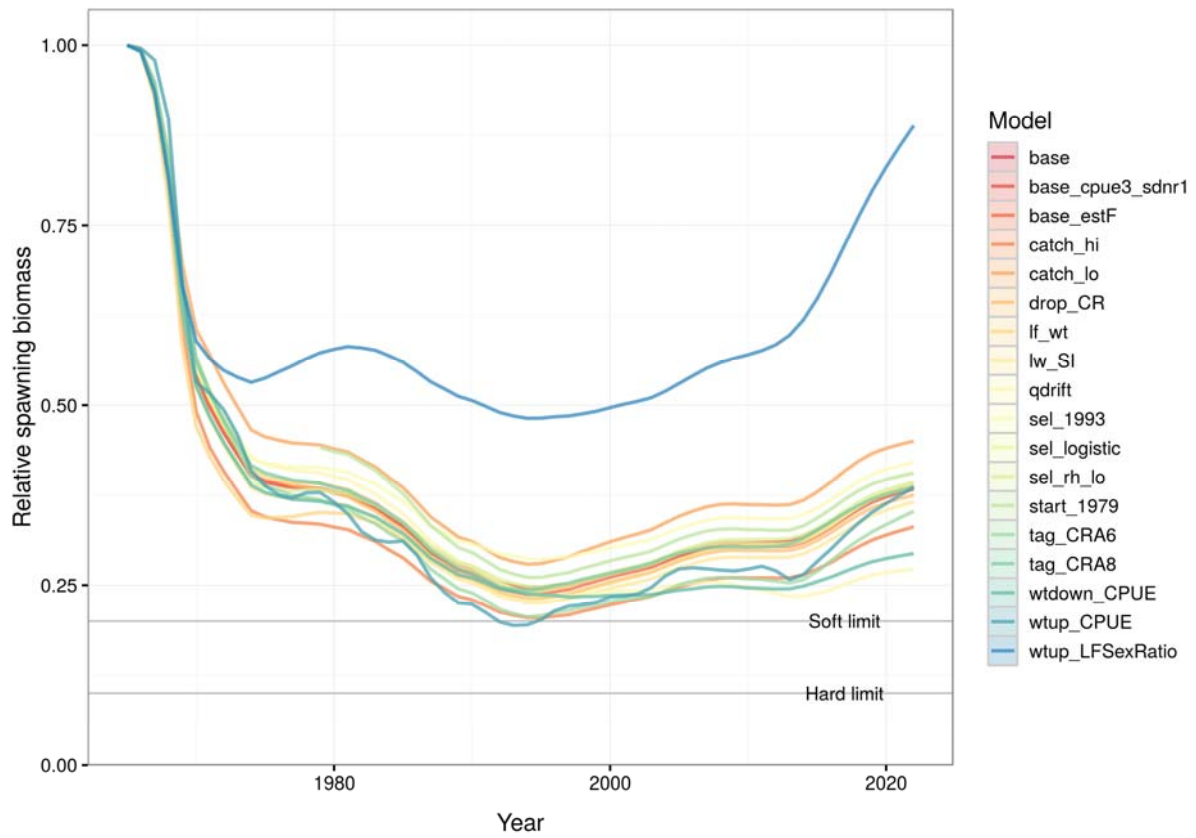
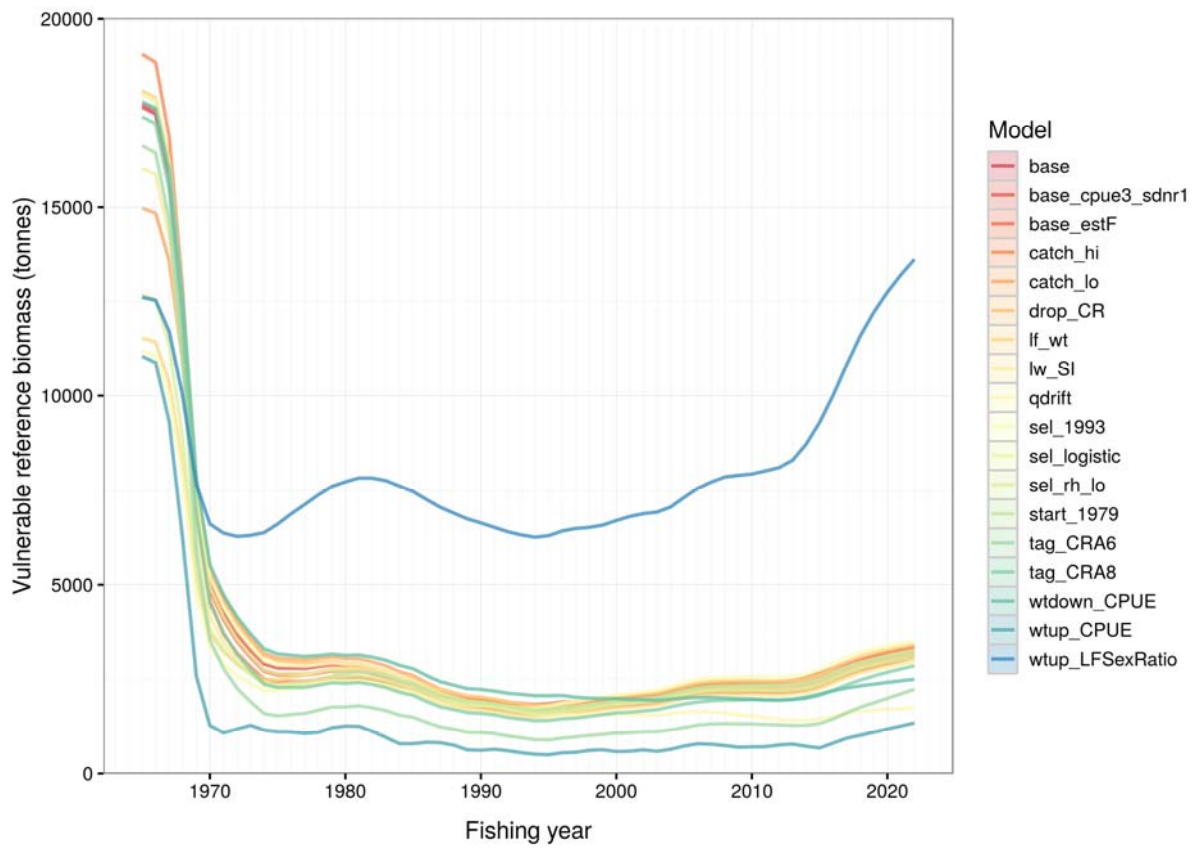


**Figure 21: MAP comparisons showing all sensitivity runs with the base case for vulnerable reference biomass [top panel] and relative spawning biomass [bottom panel].**

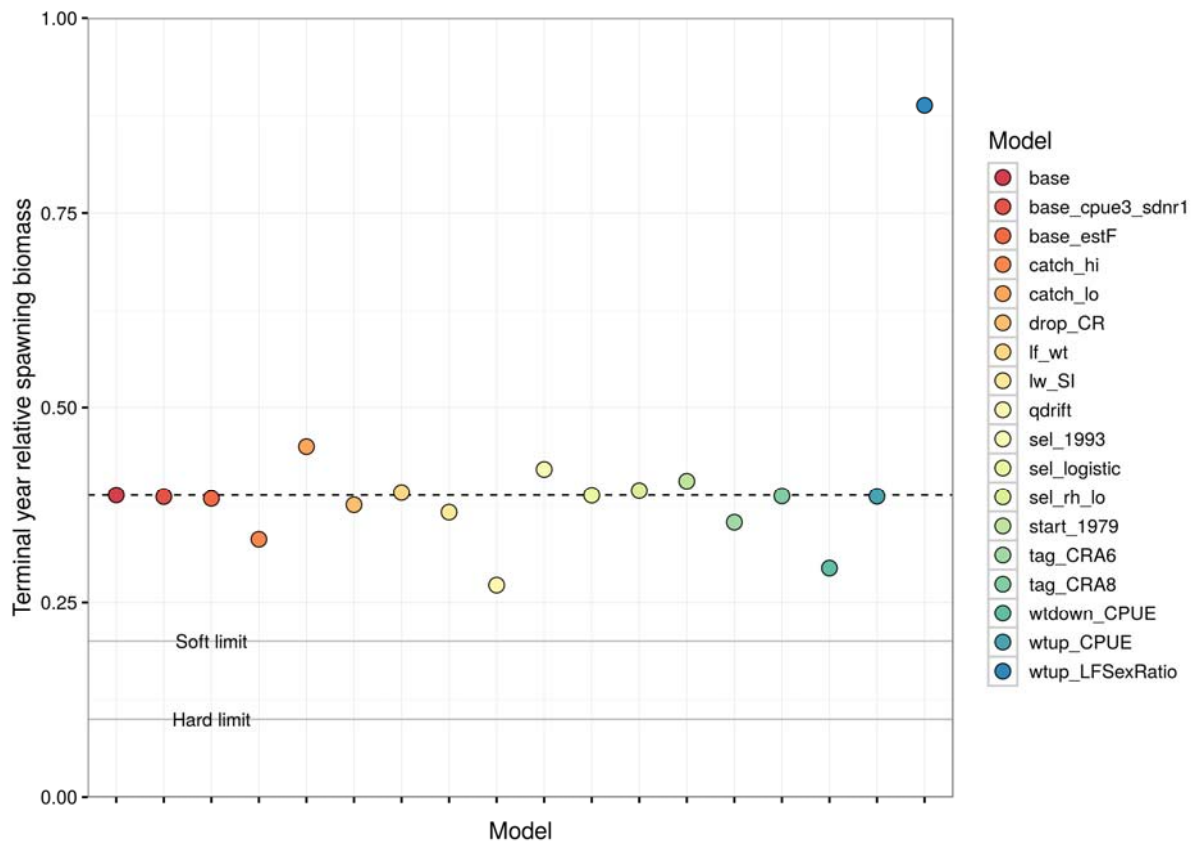


Figure 22: MAP comparisons of  $SSB_{2018}/SSB_0$  for all sensitivity runs with the base case. Dashed line shows the base case value for  $SSB_{2018}/SSB_0$ .

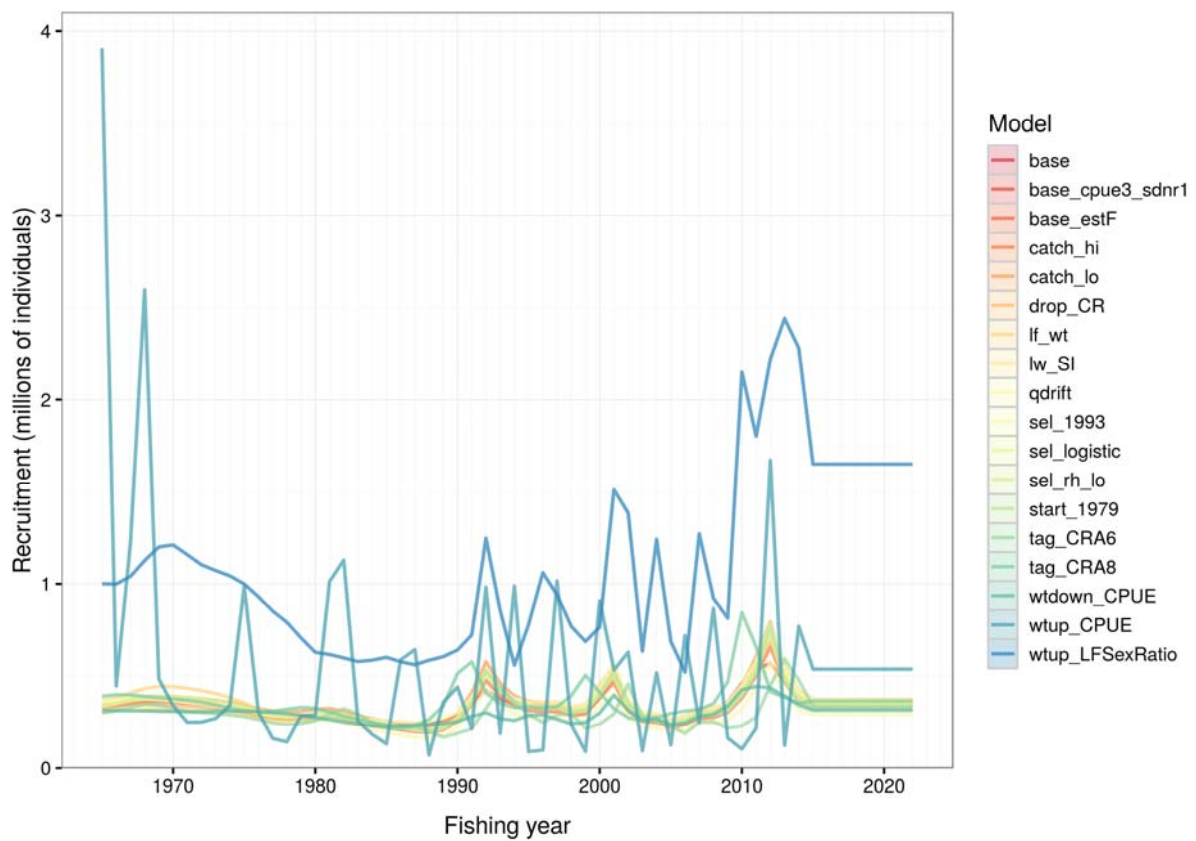
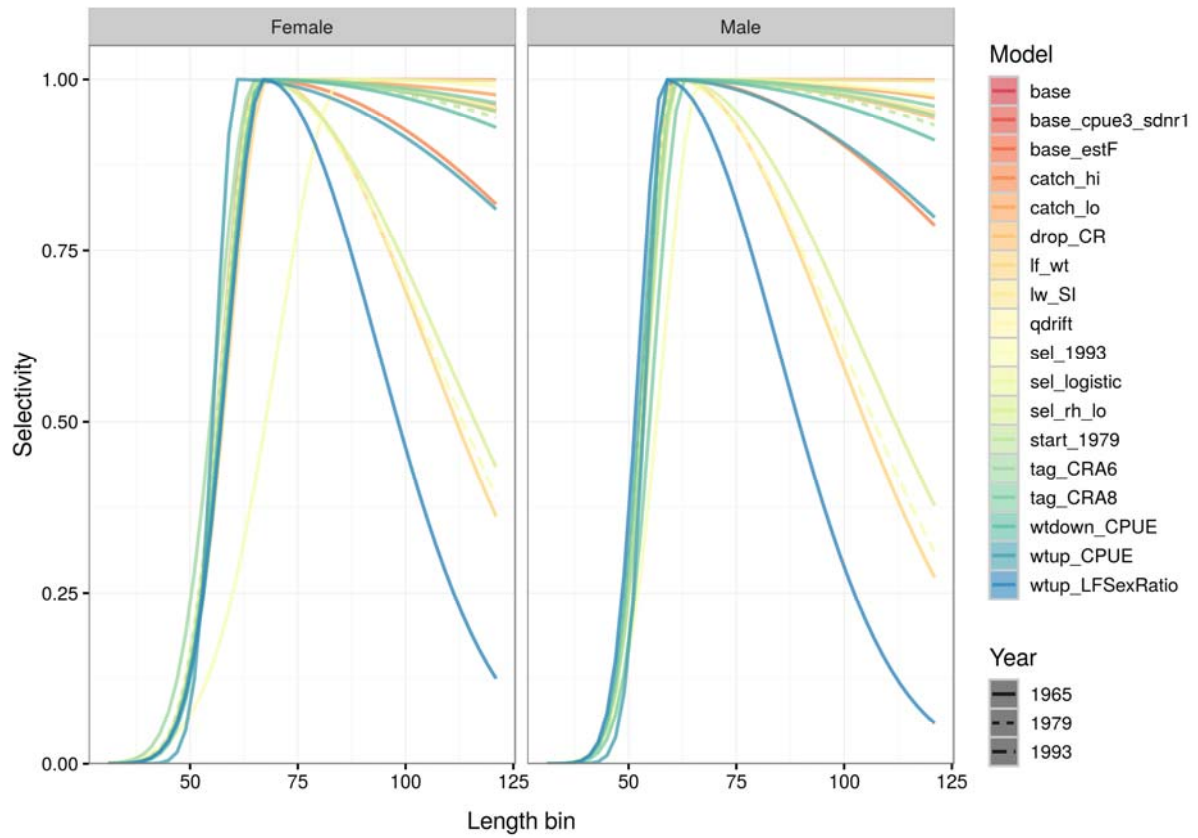
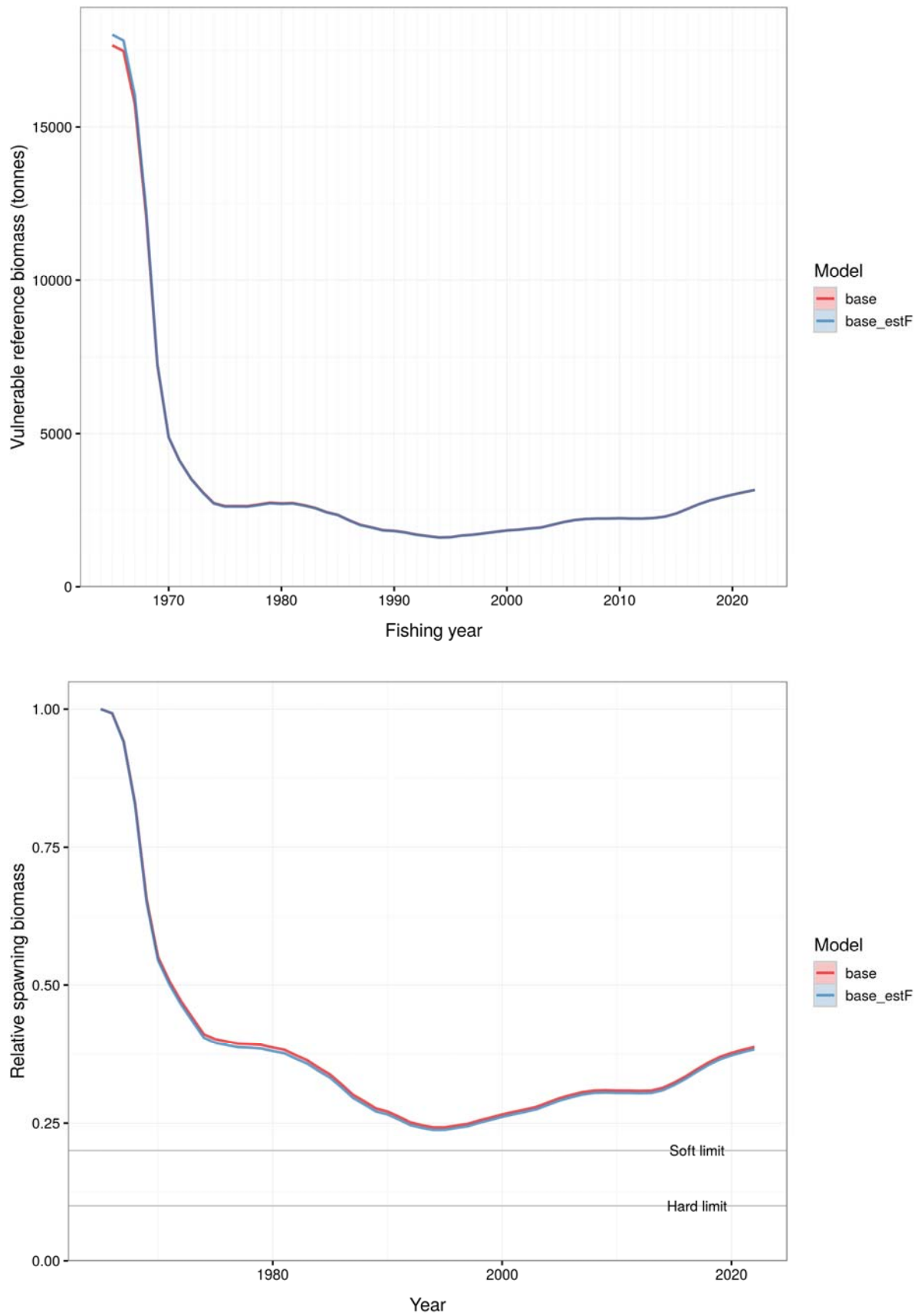


Figure 23: MAP comparisons of recruitment showing all sensitivity runs with the base case.



**Figure 24: MAP comparisons of selectivity curves showing all sensitivity runs with the base case.**



**Figure 25: MAP comparisons of the base case (using Newton-Raphson) with the version estimating fishing mortality rates: [top panel]: absolute vulnerable biomass; [bottom panel] relative spawning biomass.**

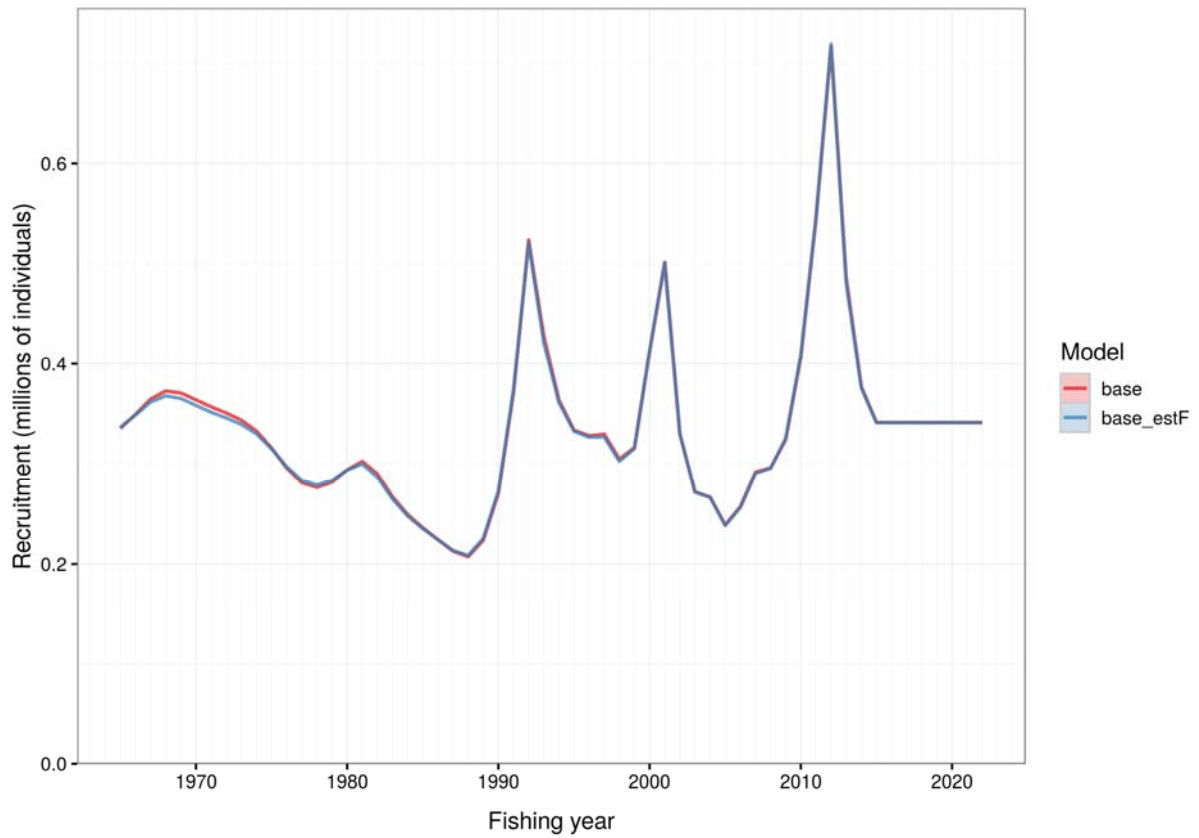


**Figure 26: MAP comparisons of the base case (using Newton-Raphson) with the version estimating fishing mortality rates: recruitment trajectories.**

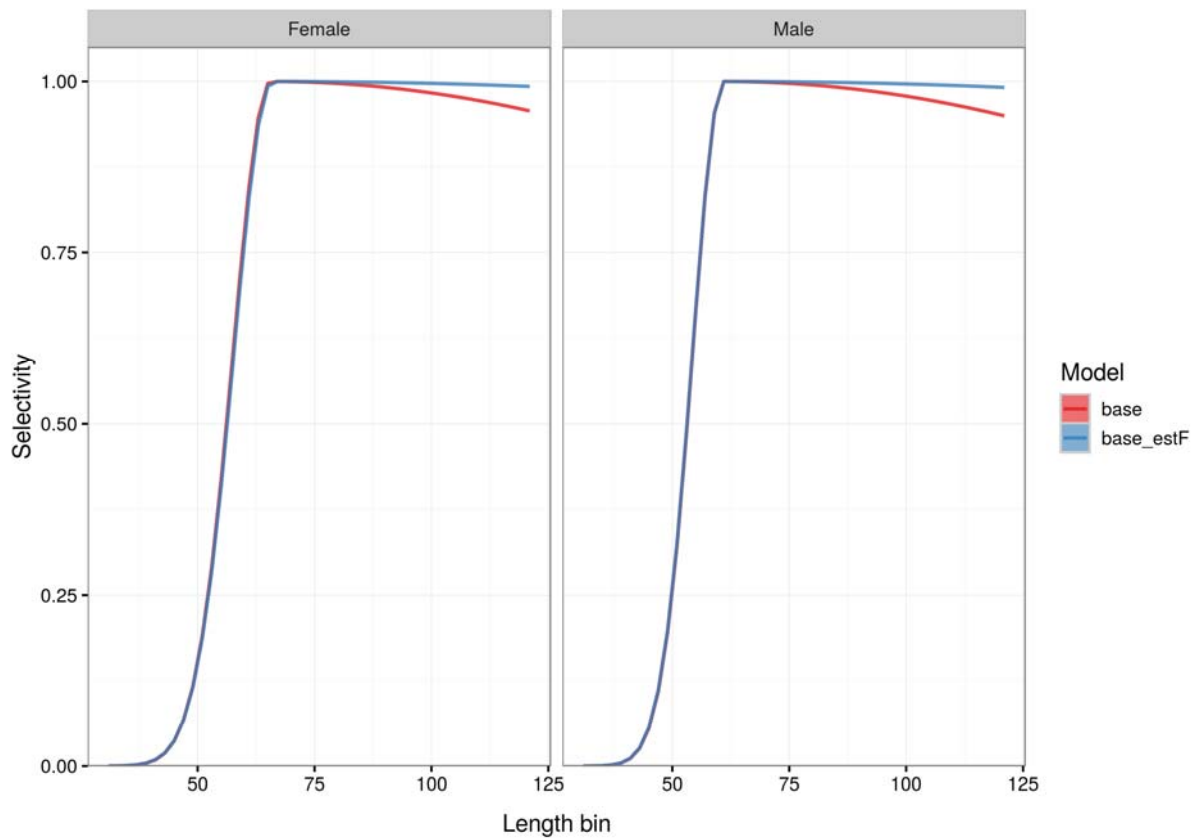


**Figure 27: MAP comparisons of the base case (using Newton-Raphson) with the version estimating fishing mortality rates: selectivity curves.**

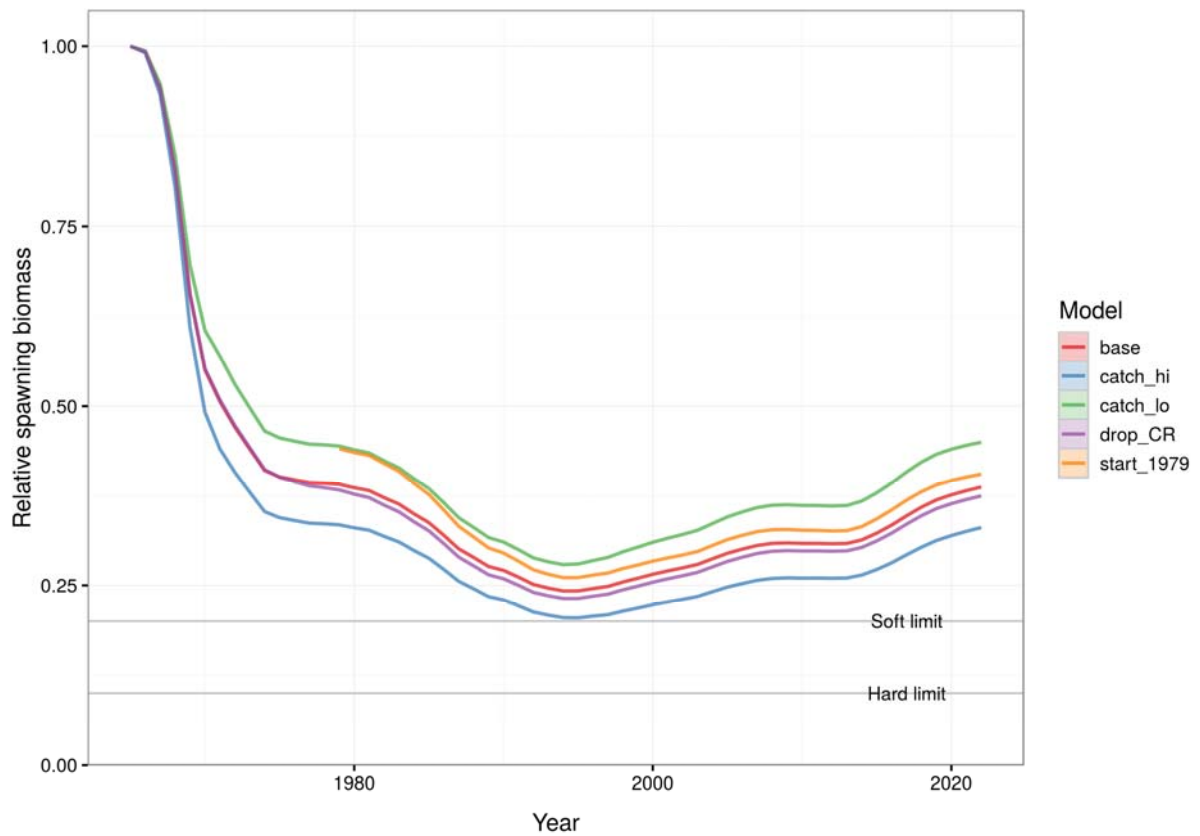
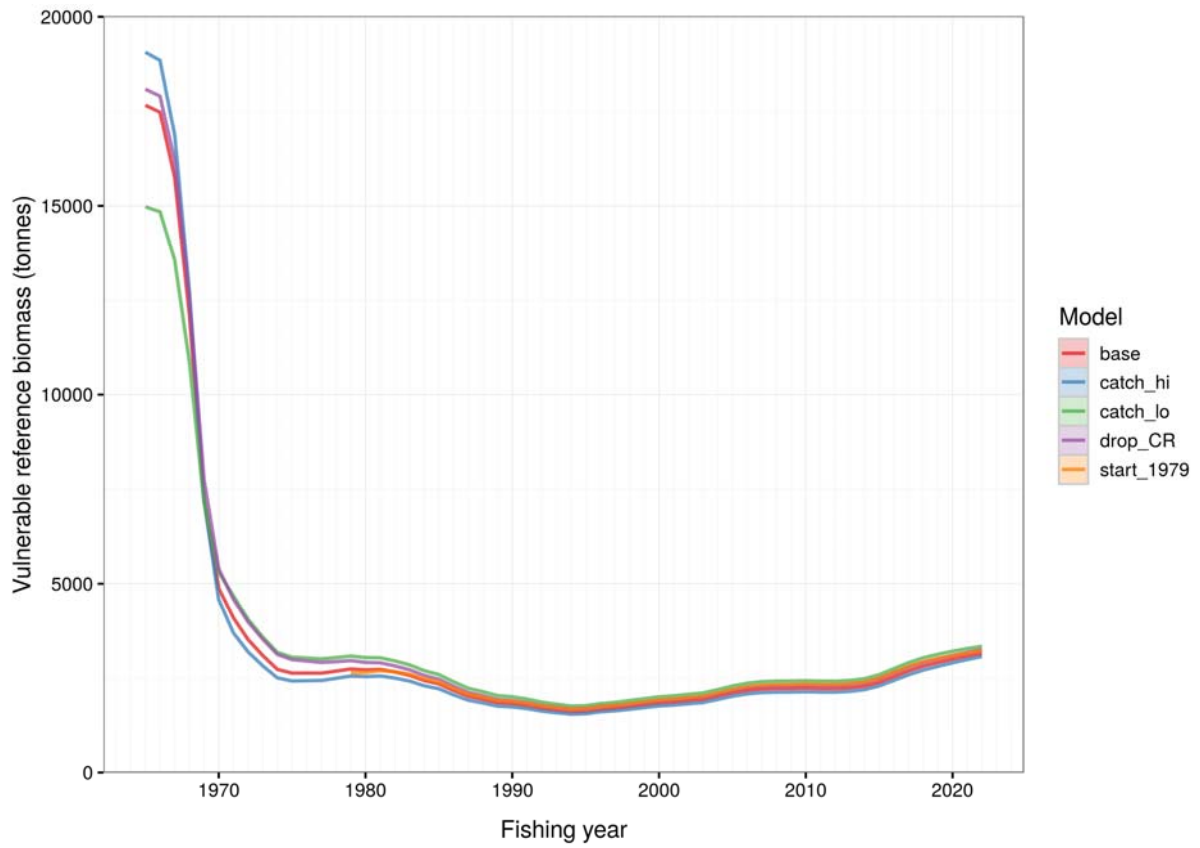


**Figure 28: MAP comparisons of four catch-related sensitivities with the base case: [top panel] vulnerable reference biomass; [bottom panel] relative spawning biomass.**

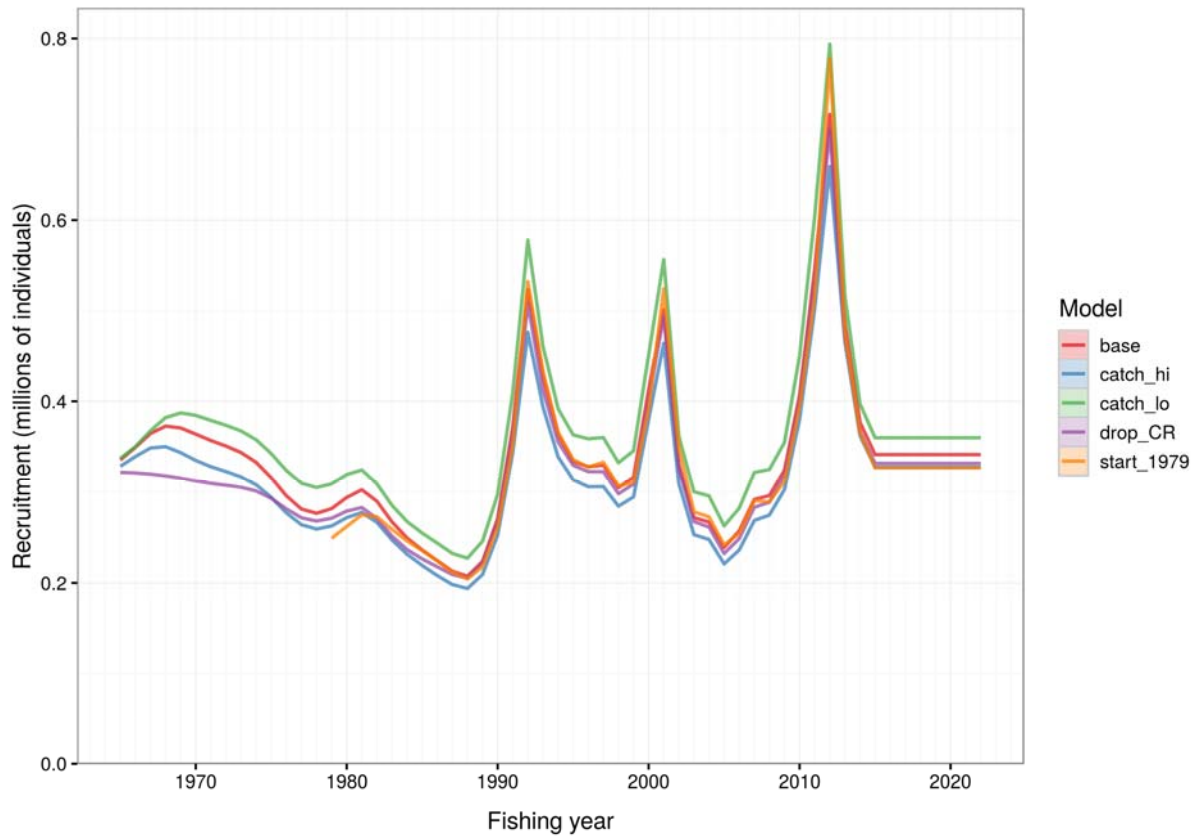


**Figure 29: MAP comparisons of four catch-related sensitivity runs with the base case: recruitment trajectories.**

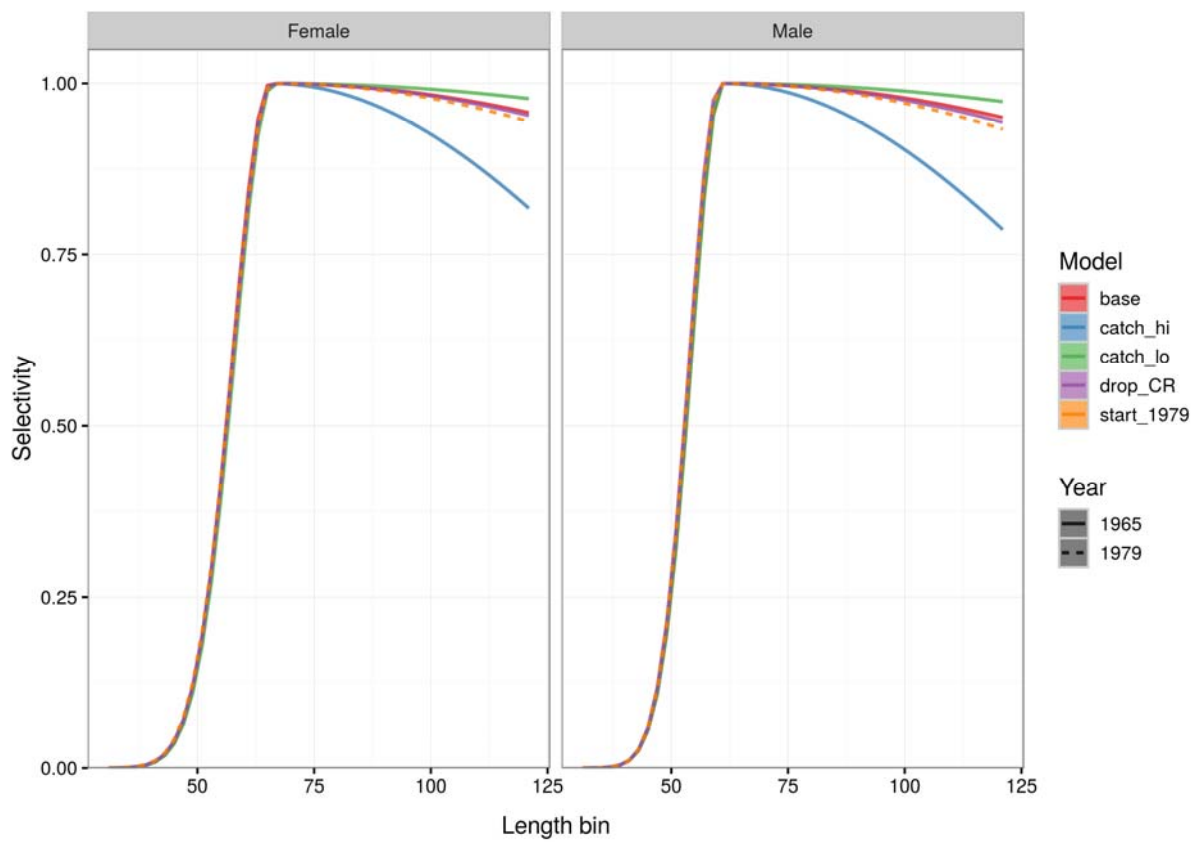


**Figure 30: MAP comparisons of four catch-related sensitivity runs with the base case: selectivity curves.**

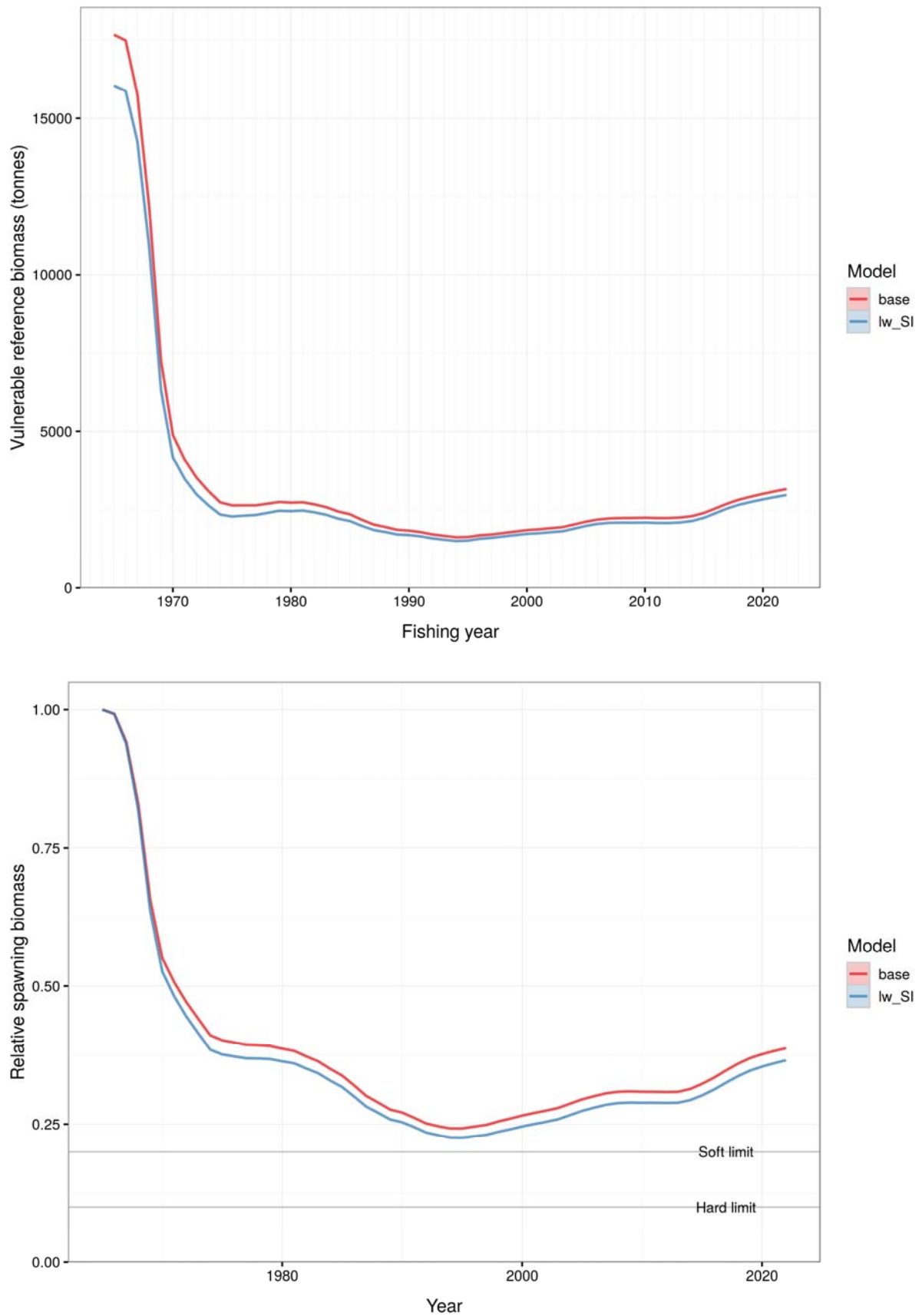
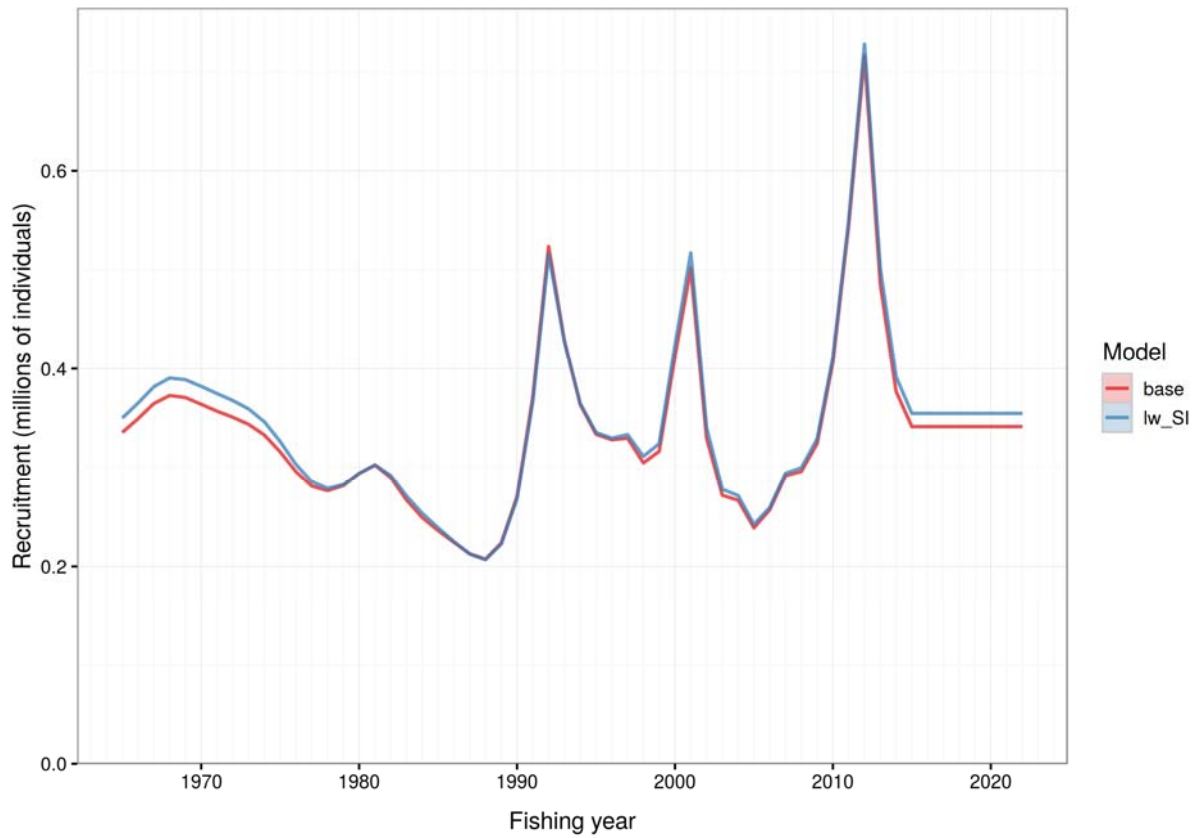
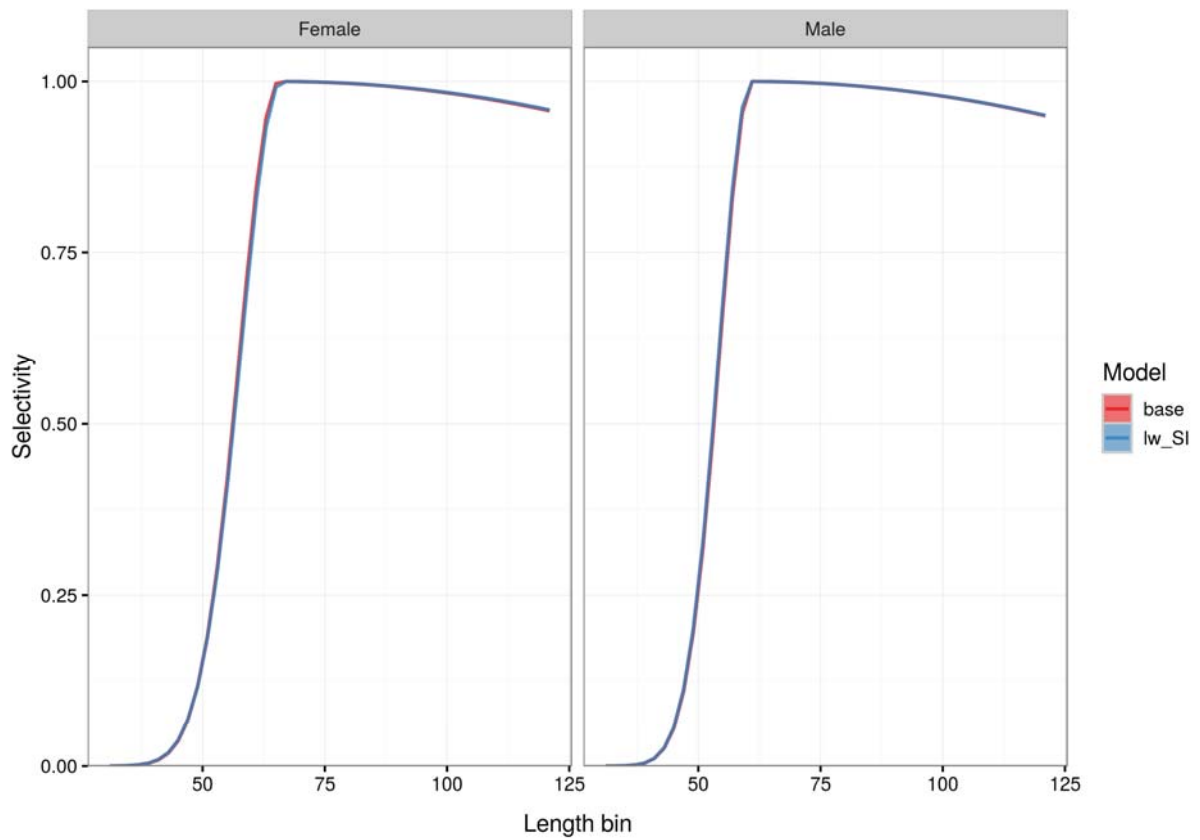


Figure 31: MAP comparisons of the length-weight sensitivity run with the base case: [top panel] vulnerable reference biomass; [bottom panel] relative spawning biomass.



**Figure 32: MAP comparisons of the length-weight sensitivity run with the base case: recruitment trajectories.**



**Figure 33: MAP comparisons of length-weight sensitivity run with the base case: selectivity curves.**

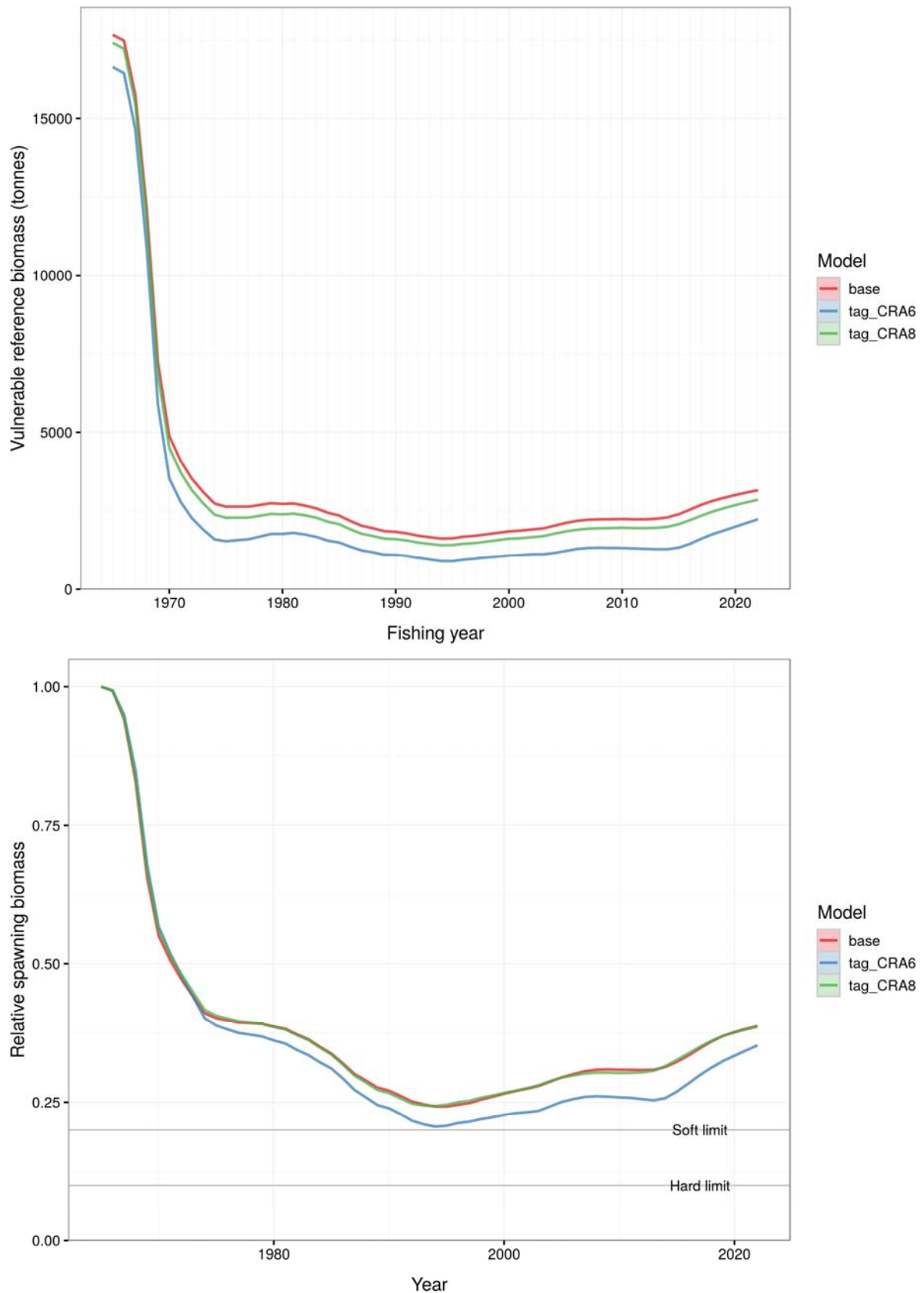


**Figure 34: MAP comparisons of the tag data sensitivity runs with the base case: [top panel] vulnerable reference biomass; [bottom panel] relative spawning biomass.**

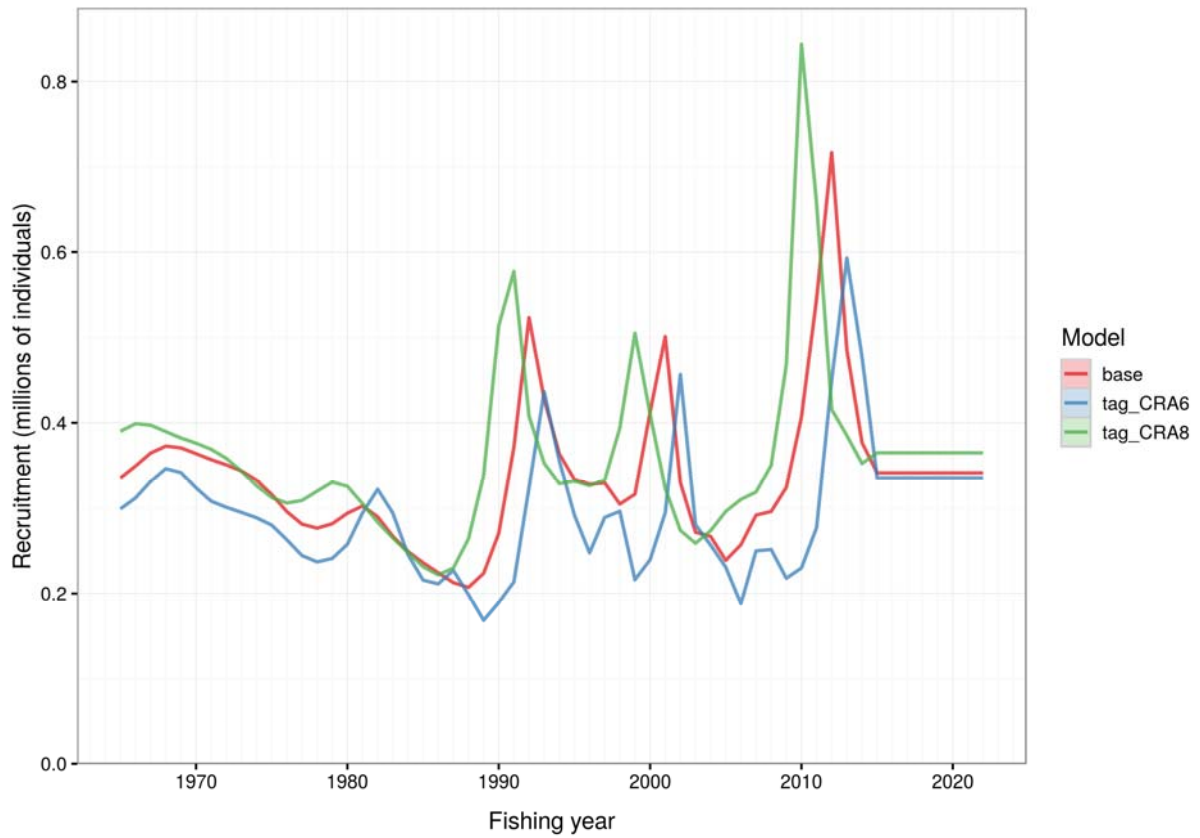


Figure 35: MAP comparisons of the tag data sensitivity runs with the base case: recruitment trajectories.

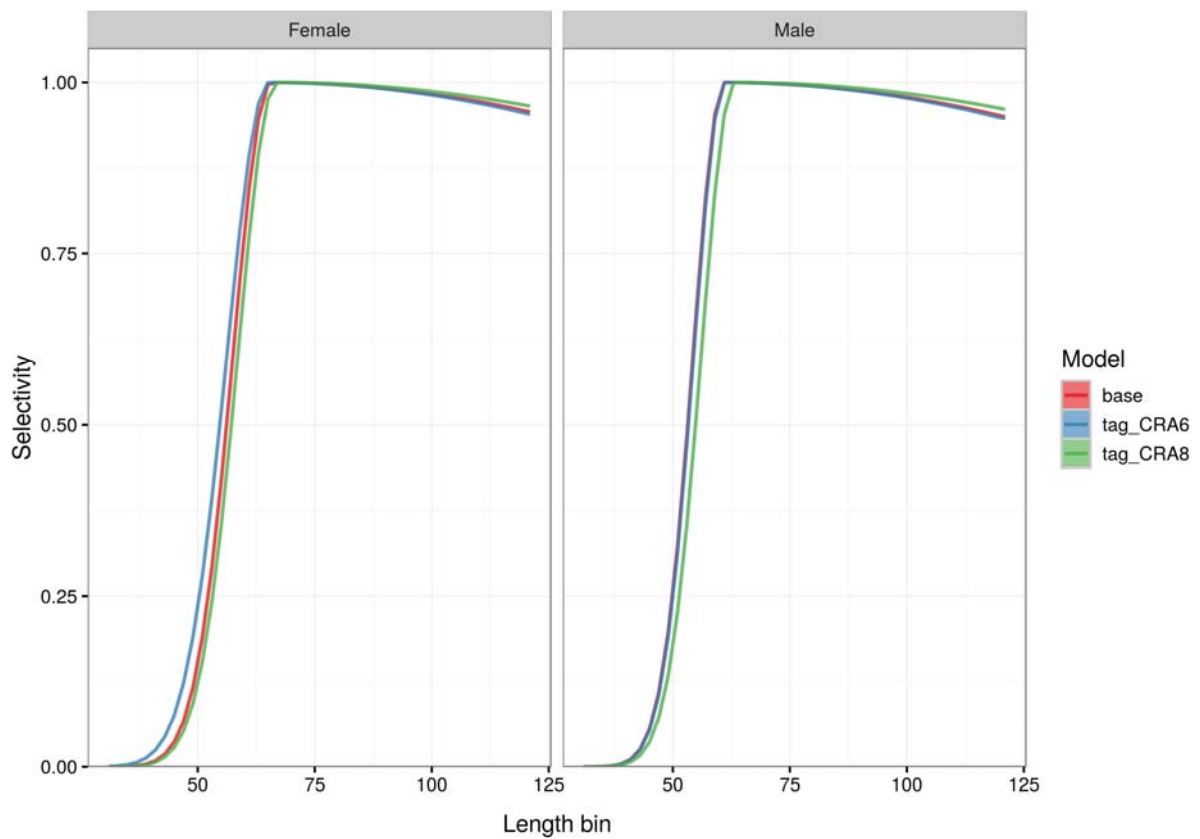
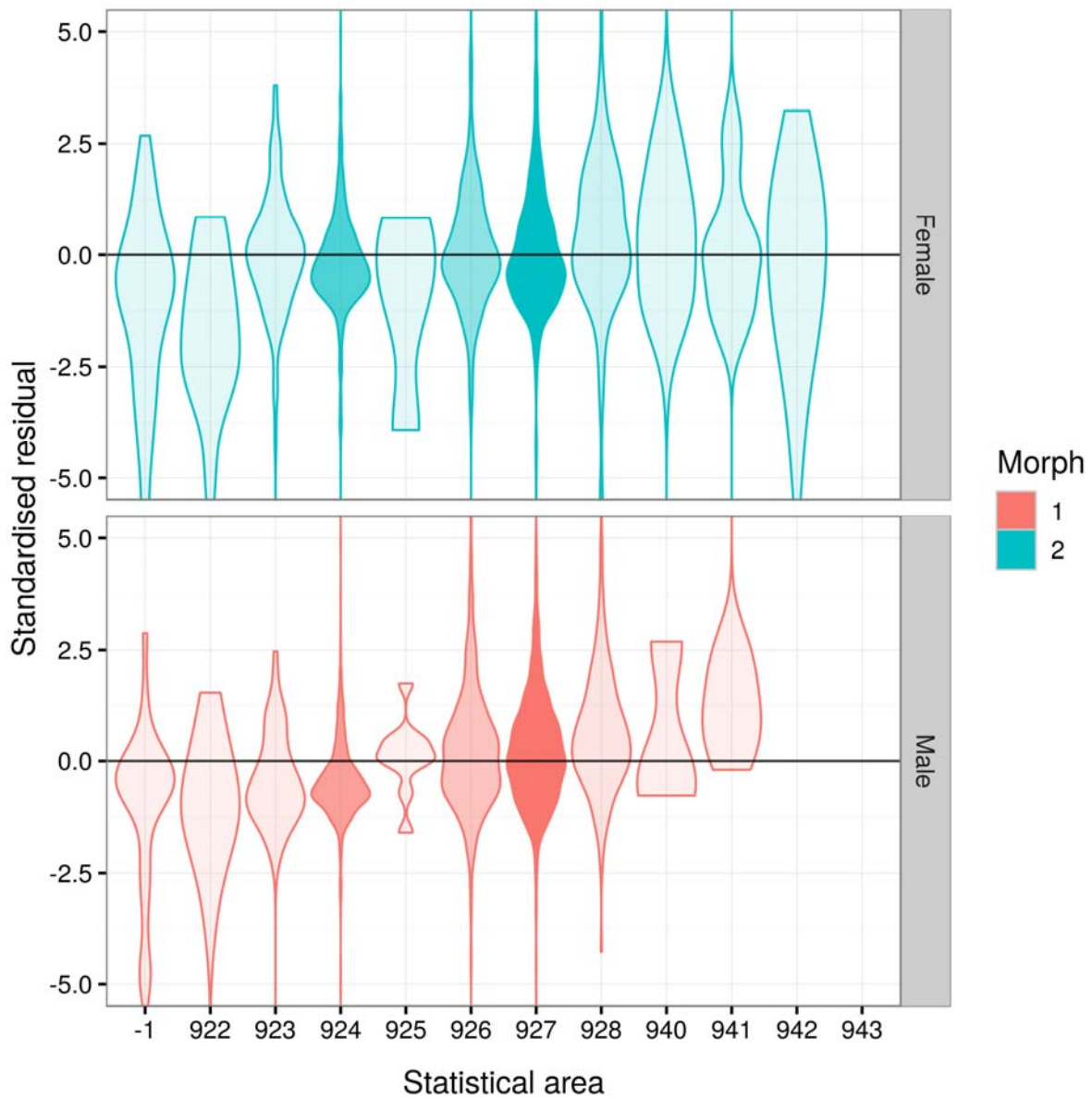
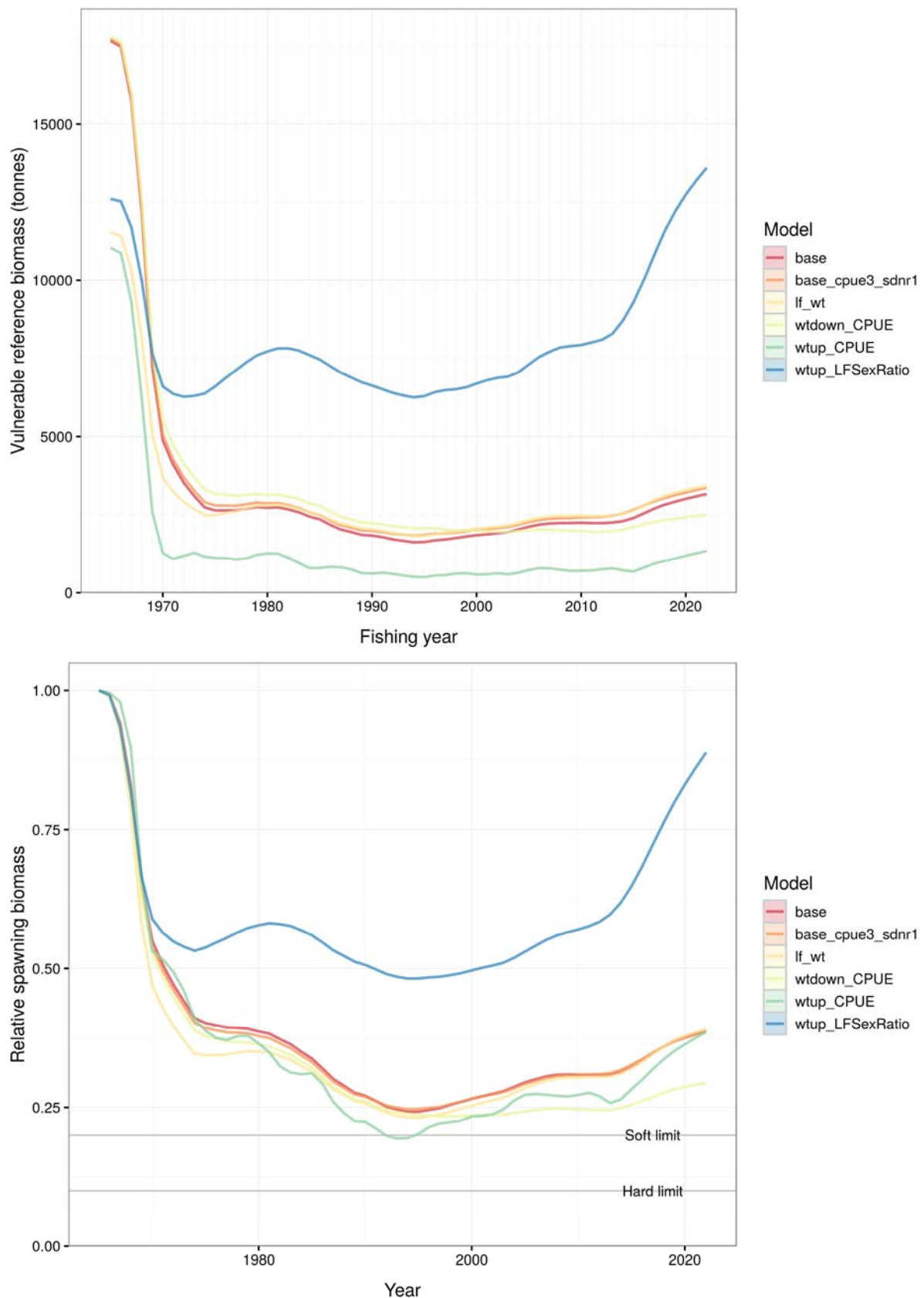


Figure 36: MAP comparisons of tag data sensitivity runs: selectivity curves.



**Figure 37: MAP Tag\_CRA8 sensitivity run: tag residuals by statistical area of release for Tag\_CRA8 sensitivity. Darker shading represents a higher number of tags by area. The inclusion of CRA 8 tag data for areas 926, 927 and 928 was based on their better fit and reasonable amount of data compared to the other CRA 8 areas.**



**Figure 38: MAP comparisons of the data weighting sensitivity runs with the base case: [top panel] vulnerable reference biomass; [bottom panel] relative spawning biomass.**

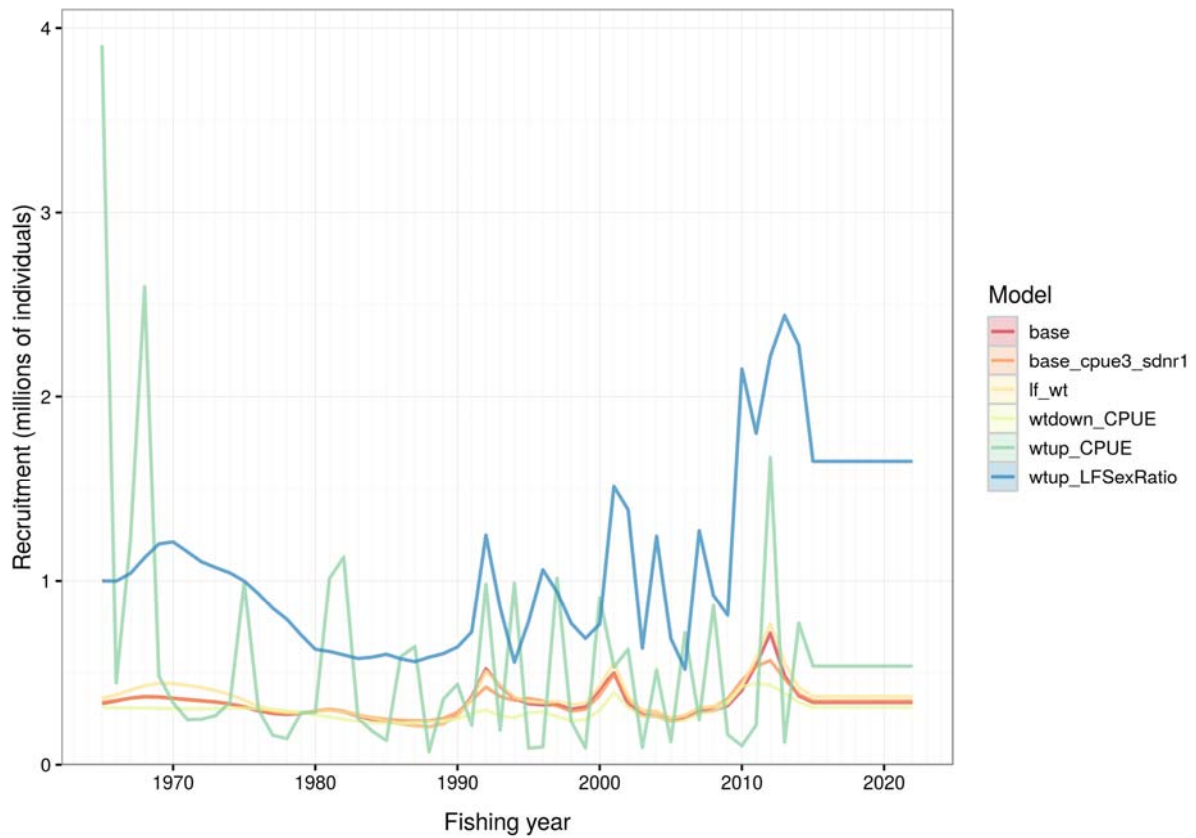


**Figure 39: MAP comparisons of the data weighting sensitivity runs with the base case: recruitment trajectories.**

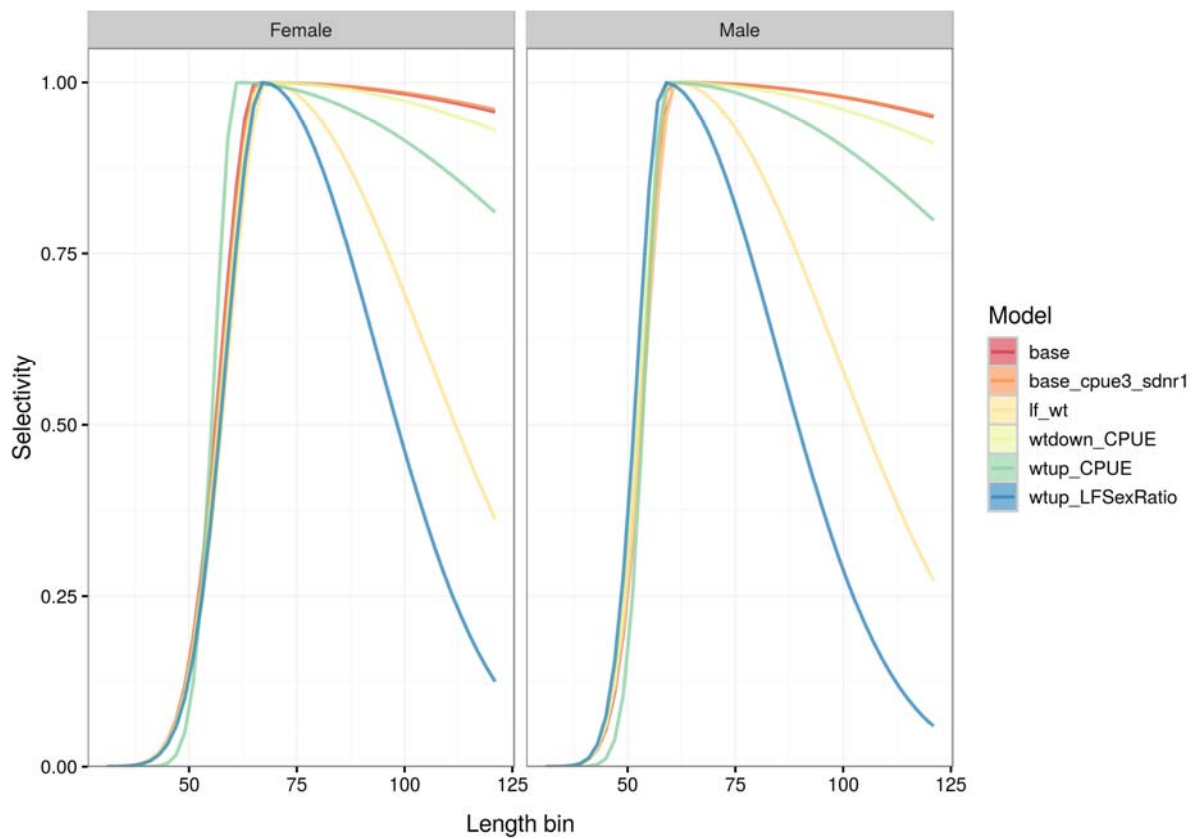


**Figure 40: MAP comparisons of the data weighting sensitivity runs with the base case: selectivity curves.**

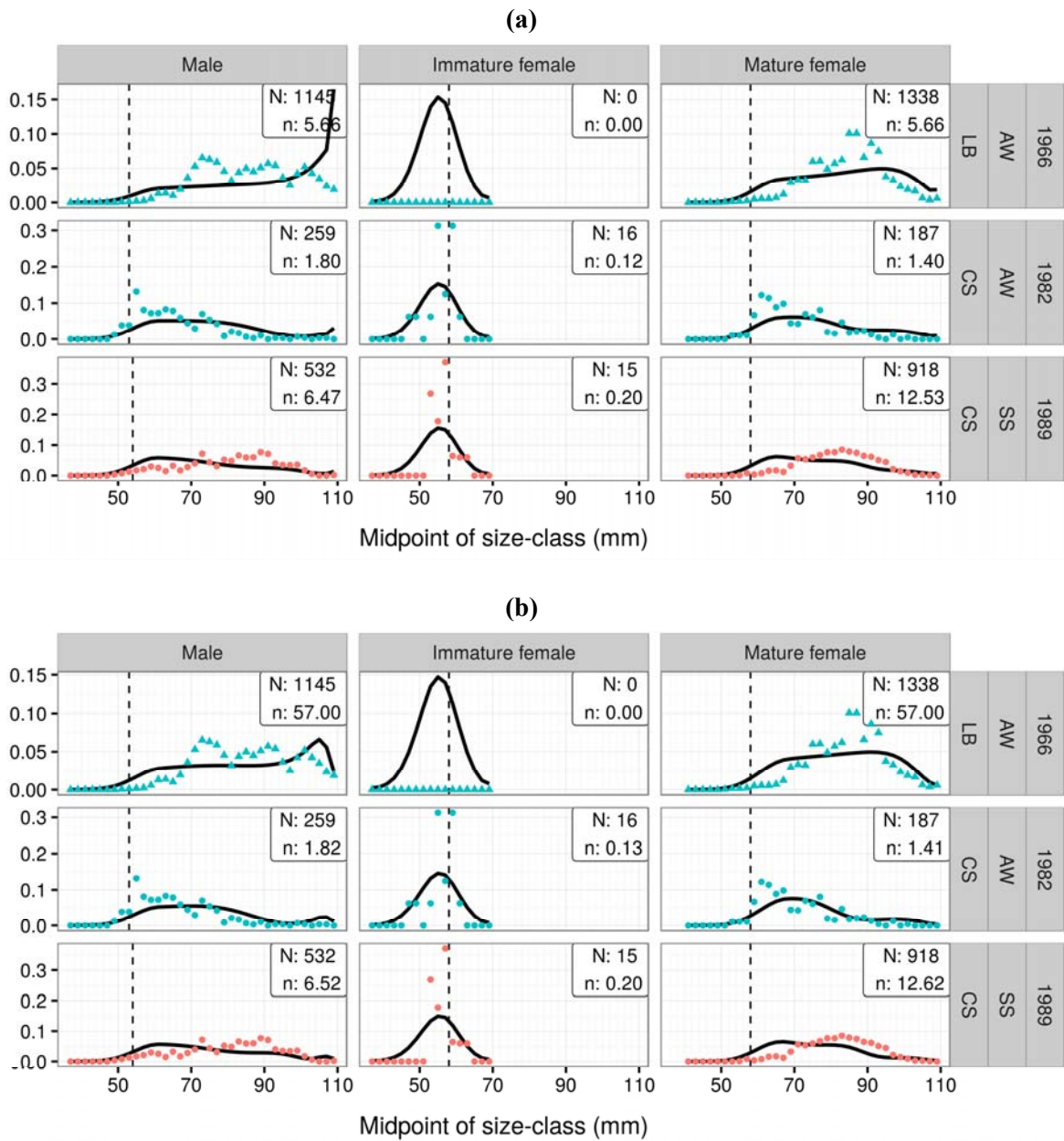


**Figure 41: CRA 6 MAP: Model fits to LFs from 1966 SS LB, 1982 AW LB and 1989 SS LB for (a) base case, and (b)  $lf\_wt$  sensitivity. Upweighting the 1966 LF from 1 to 10 for males and mature females improves the fit to these data somewhat, however it has little bearing on the overall model fit.**

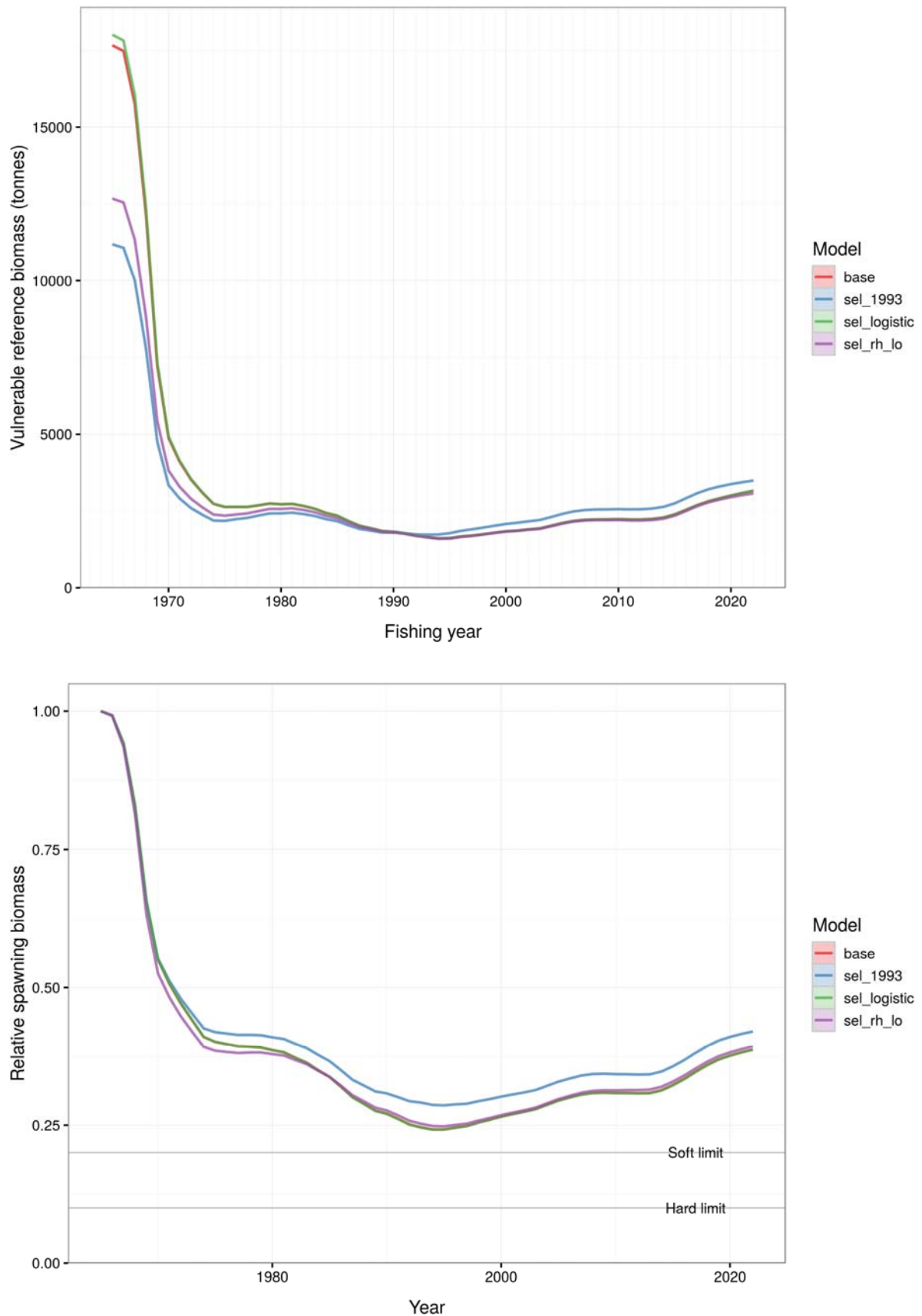


**Figure 42: MAP comparisons of the selectivity sensitivity runs with the base case: [top panel] vulnerable reference biomass; [bottom panel] relative spawning biomass.**

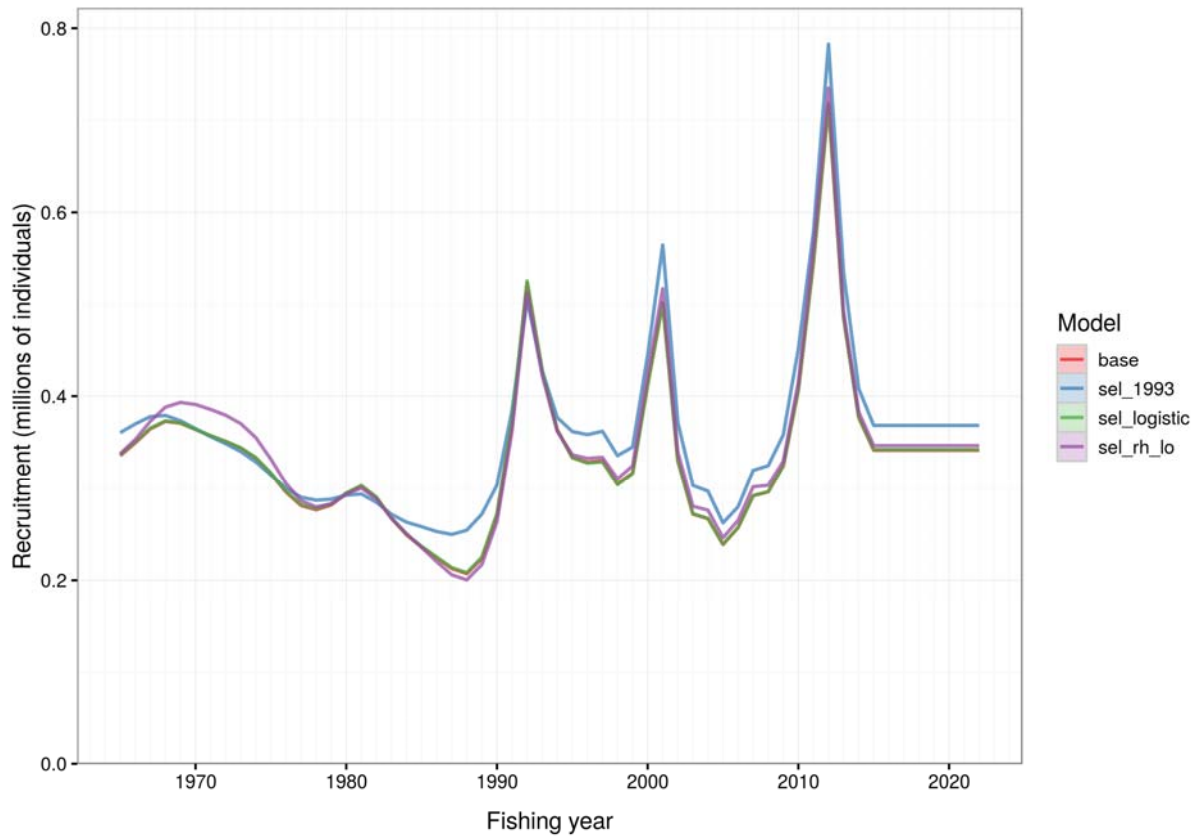


**Figure 43: MAP comparisons of the selectivity sensitivity runs with the base case: recruitment trajectories.**

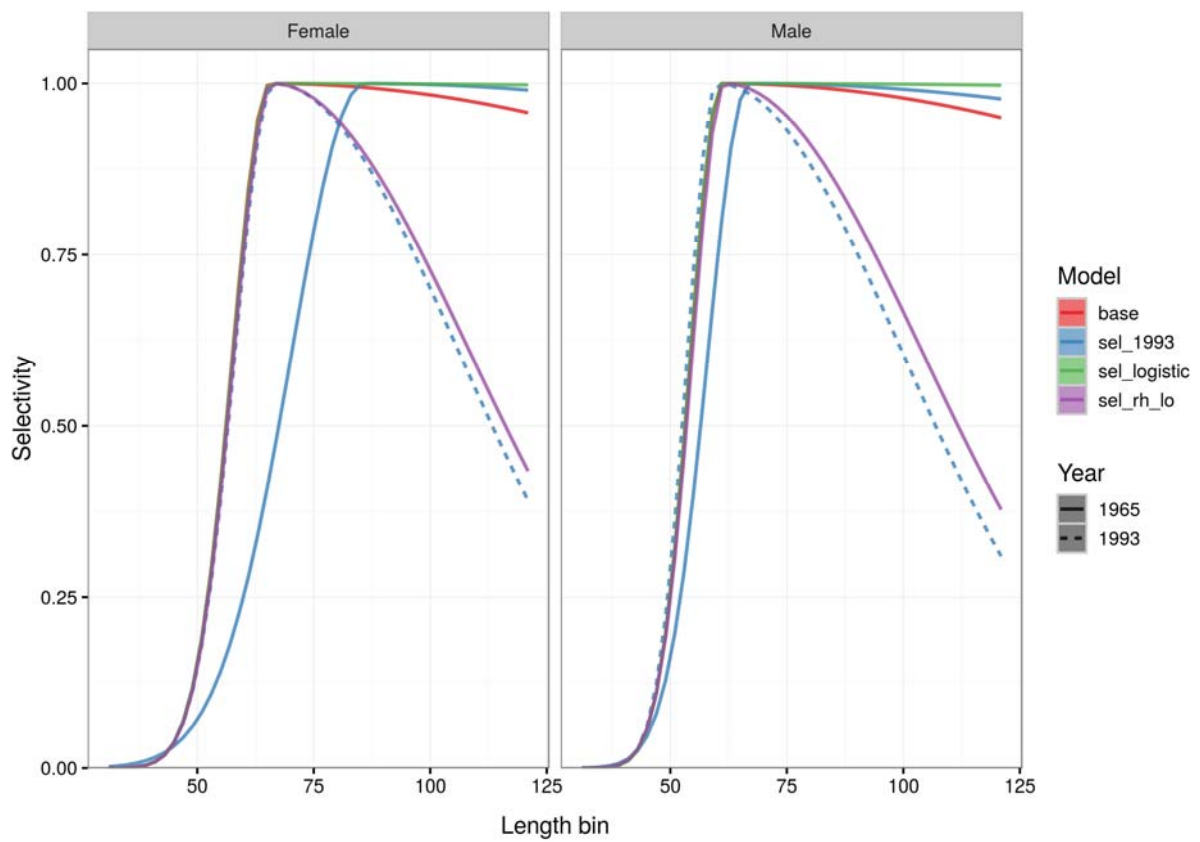


**Figure 44: MAP comparisons of the selectivity sensitivity runs with the base case: selectivity curves.**

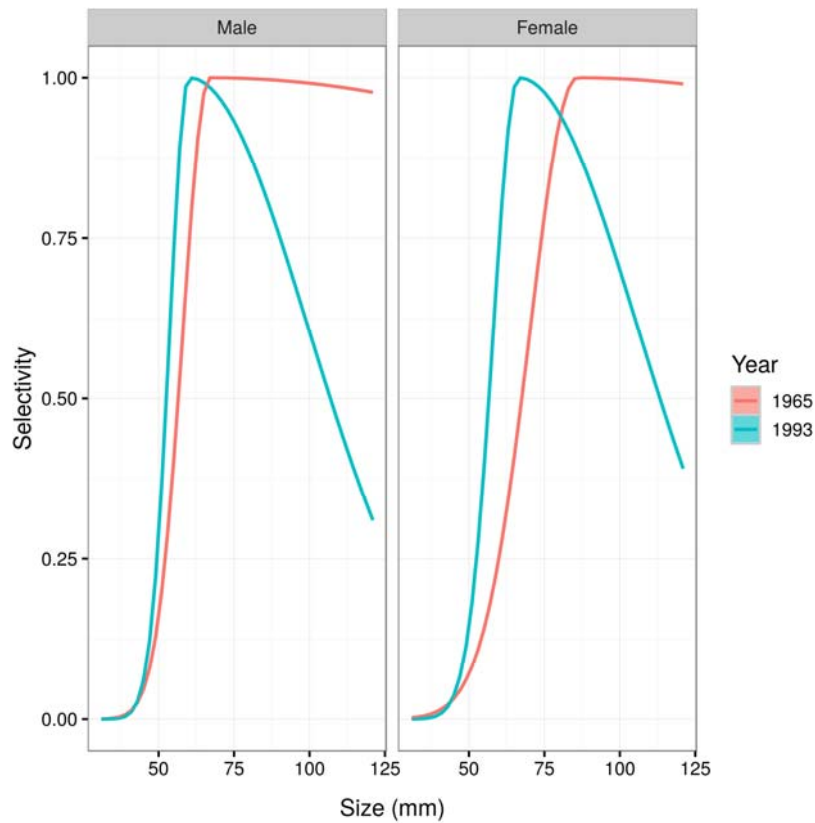


**Figure 45: CRA 6 *sel\_1993* MAP sensitivity run: tested model response to changes in escape gap regulations implemented in 1993. The model estimated a shift left in selectivity, resulting in selecting smaller lobster (males and females) after 1993, along with a strong downward shift in the right-hand limb. The left-shift was more pronounced for females.**

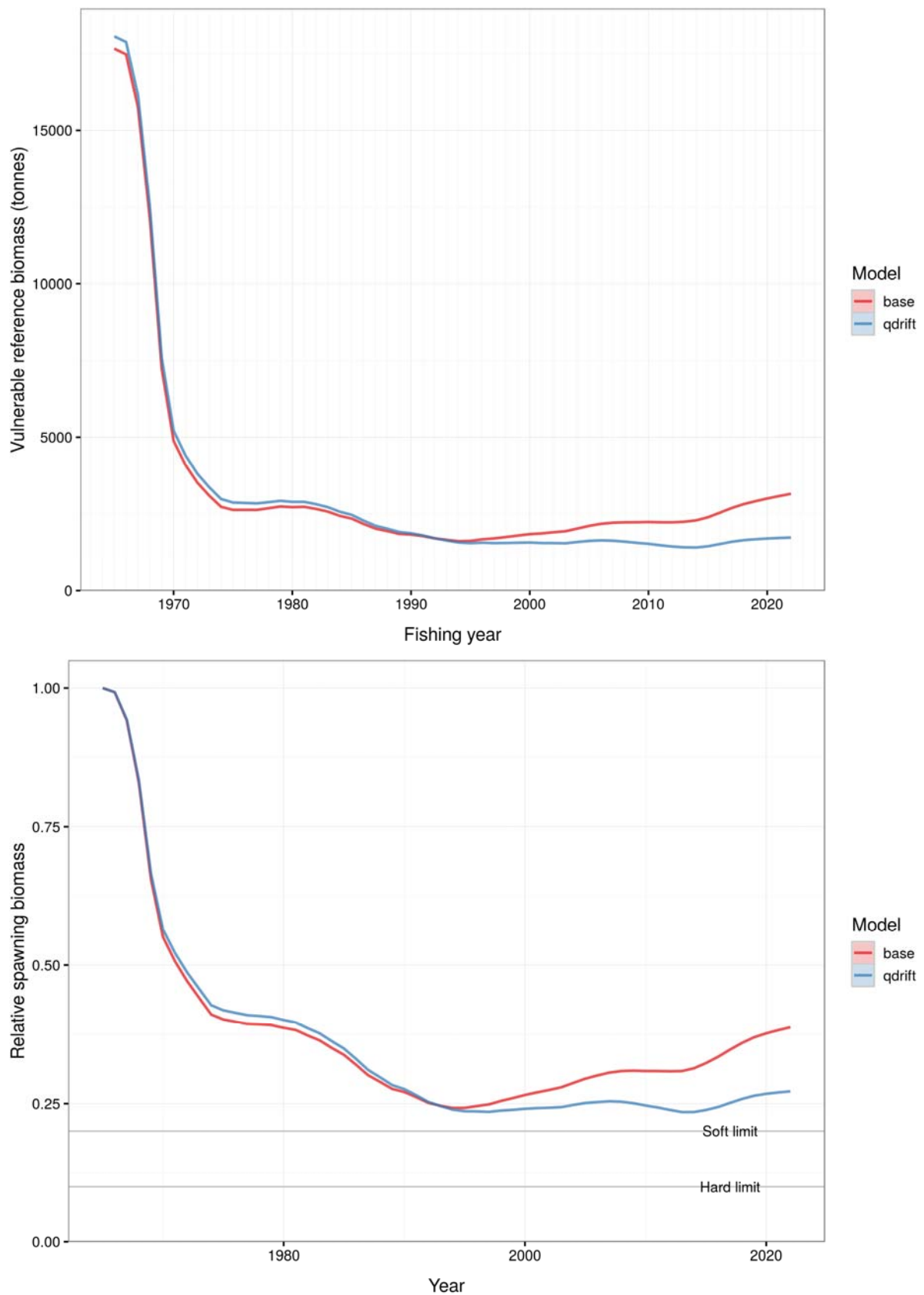


**Figure 46: MAP comparisons of the *q-drift* sensitivity run with the base case: [top panel] vulnerable reference biomass; [bottom panel] relative spawning biomass.**

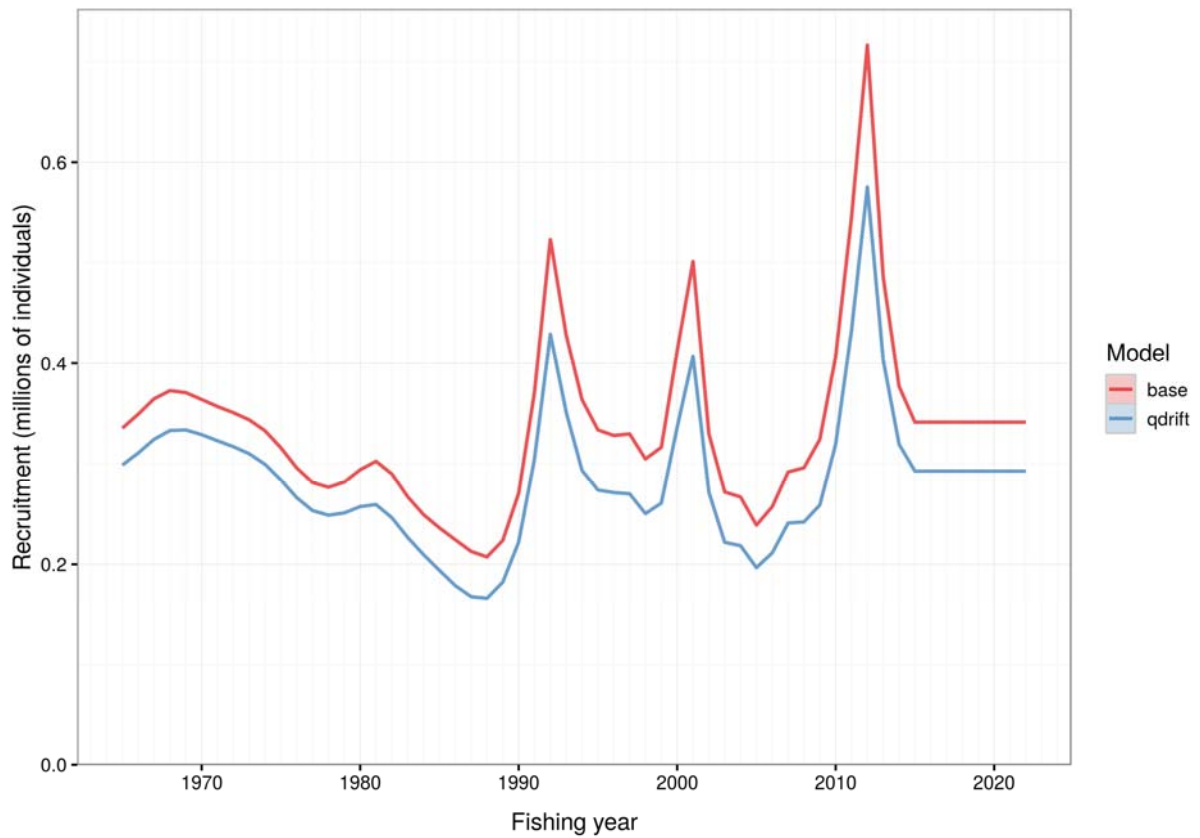


Figure 47: MAP comparisons of the q-drift sensitivity run with the base case: recruitment trajectories.

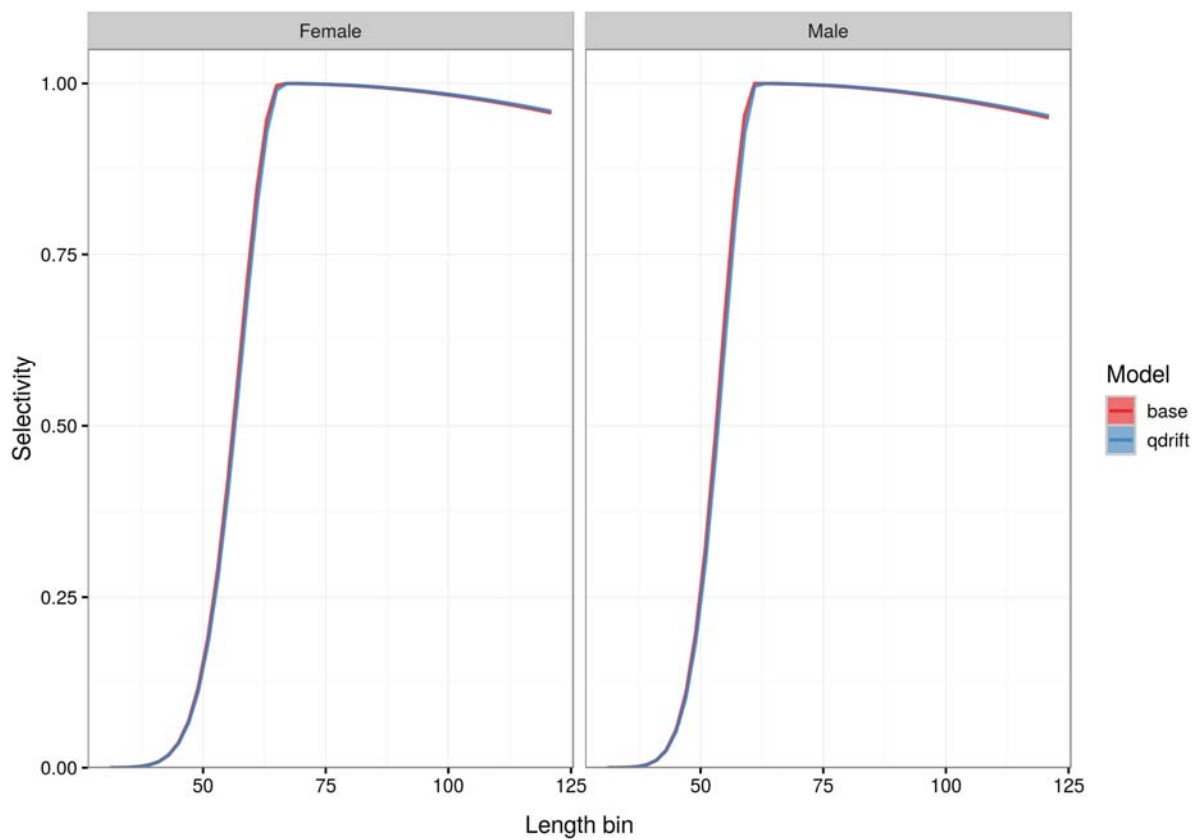
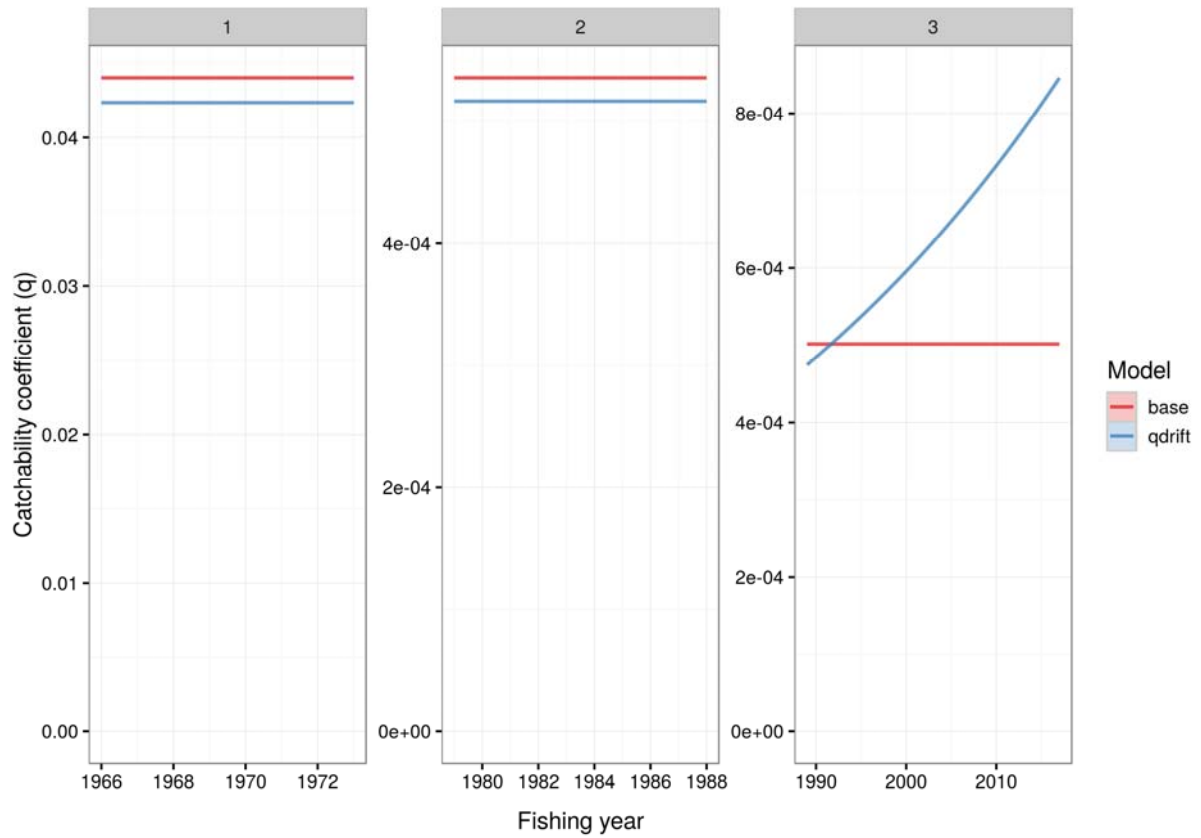
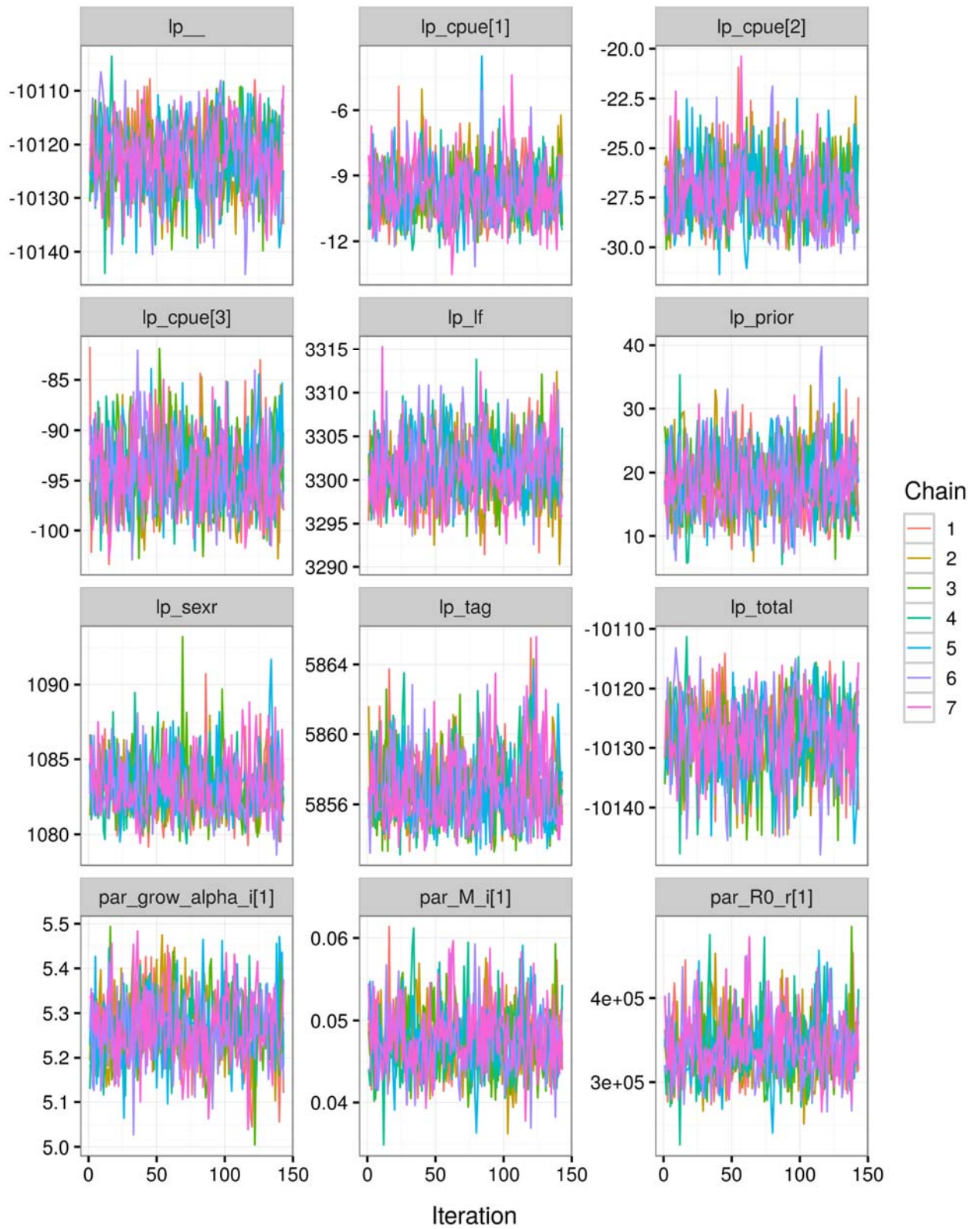


Figure 48: MAP comparisons of q-drift sensitivity run with the base case: selectivity curves.



**Figure 49: MAP comparisons of q-drift sensitivity with the base case: CPUE catchability coefficients ( $q$ ) 1=CR; 2= FSU; 3=CELR.**



**Figure 50: CRA 6 base case: MCMC trace plots by independent chain for likelihood components and estimated growth, natural mortality ( $M$ ), and  $R_0$  parameters.**

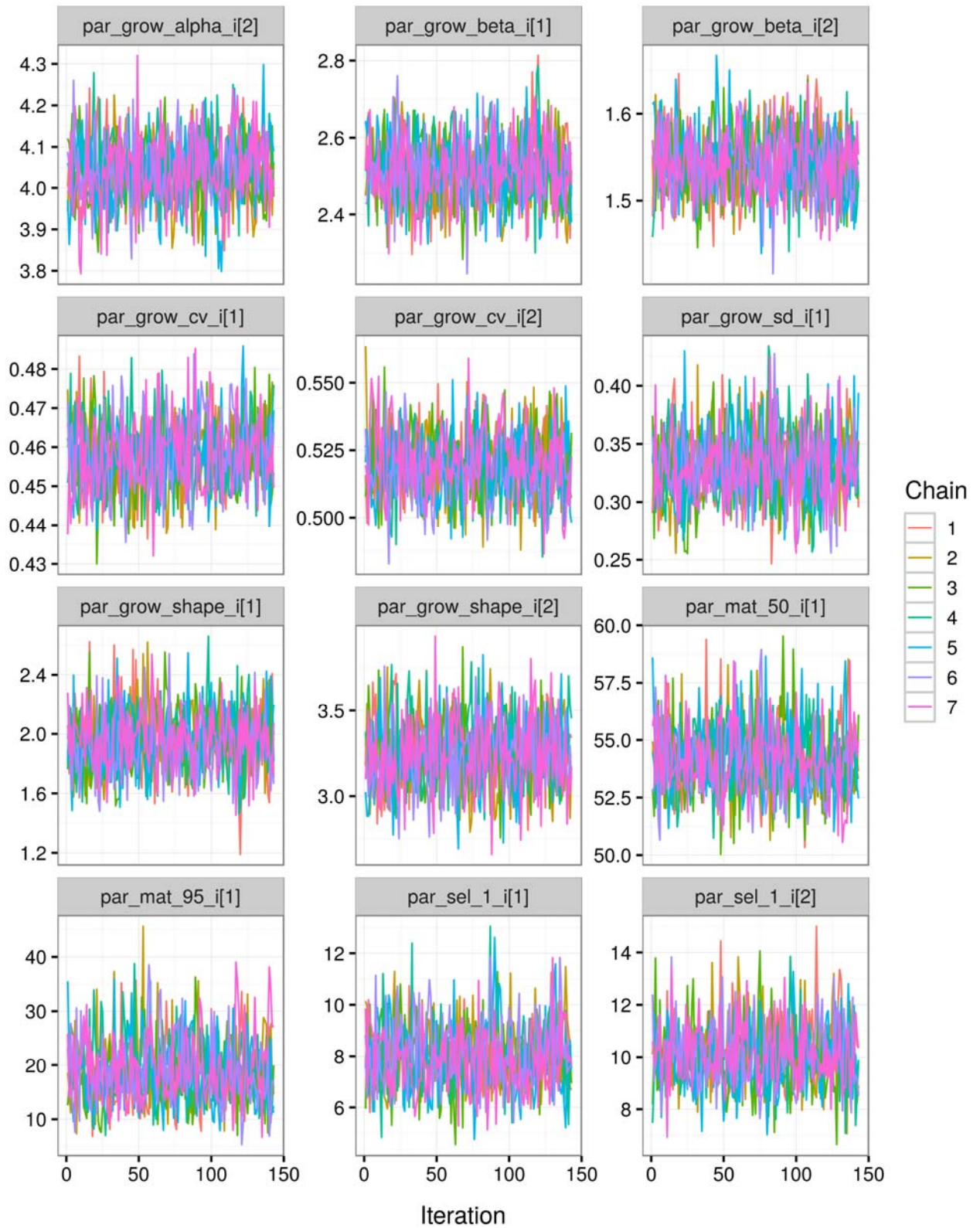


**Figure 51: CRA 6 base case: MCMC trace plots by independent chain for estimated growth, maturity, and selectivity parameters.**

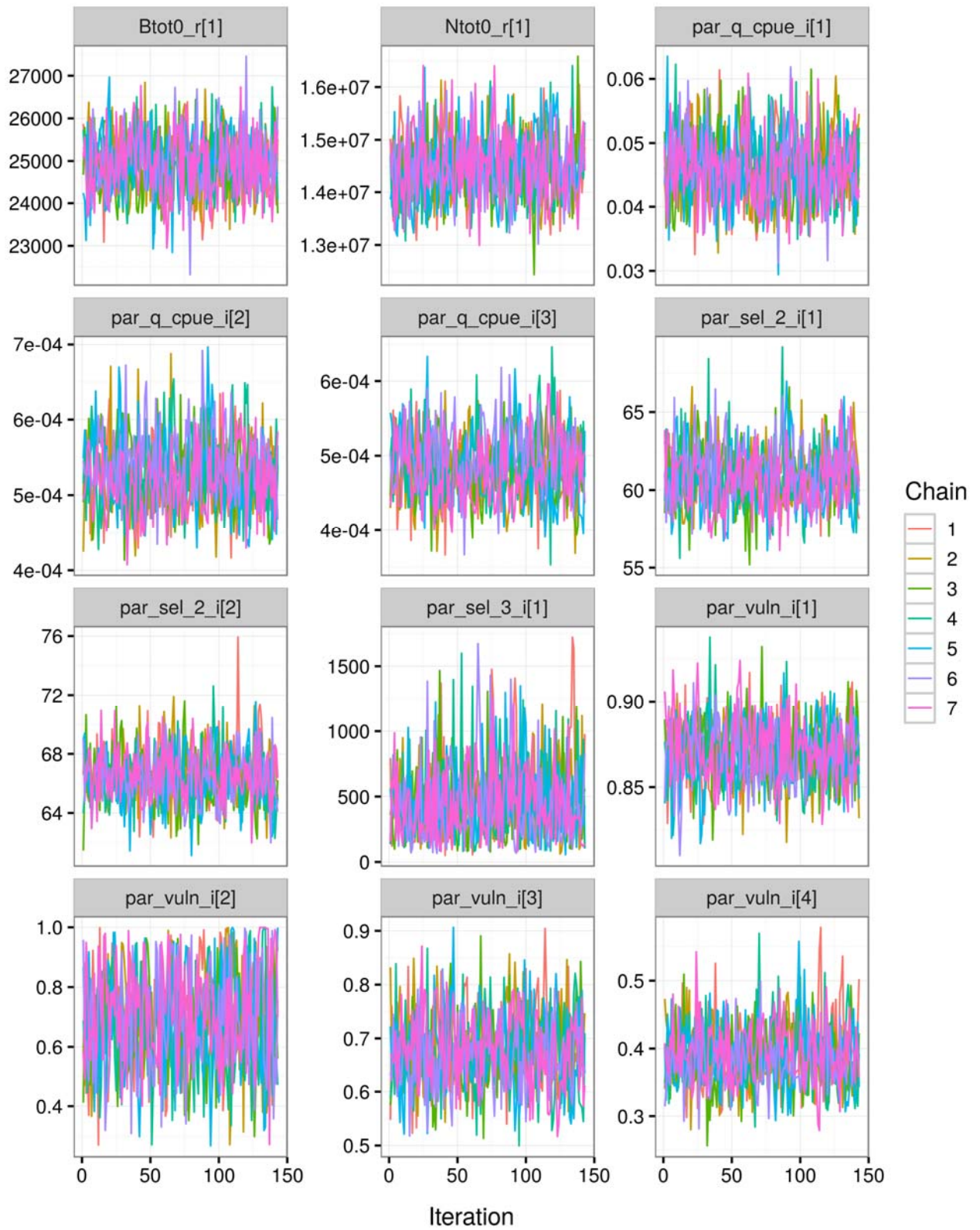


**Figure 52: CRA 6 base case: MCMC trace plots by independent chain for estimated total biomass and numbers,  $q$ , selectivity, and vulnerability parameters.**

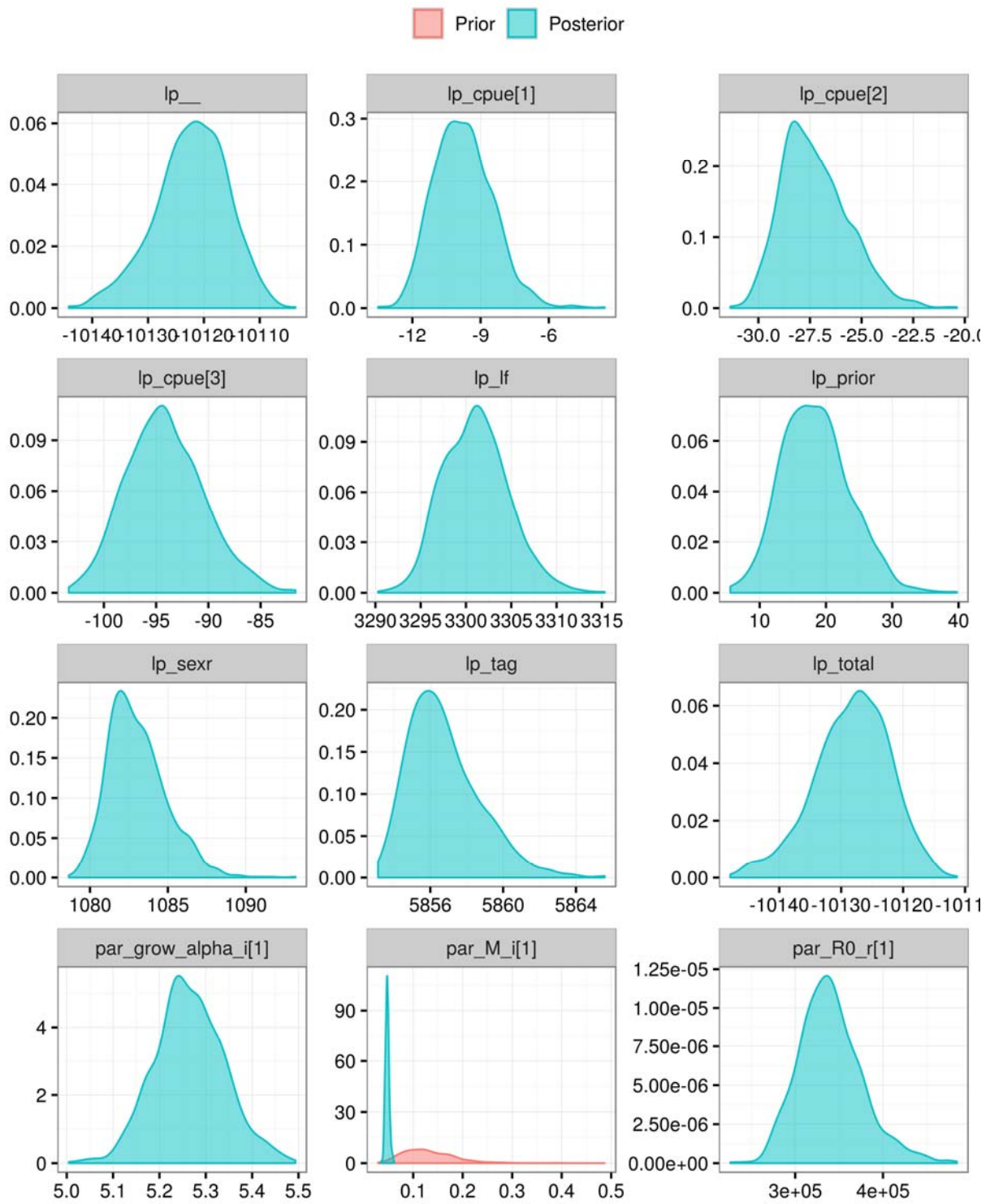


**Figure 53: CRA 6 base case: density plots showing prior (red) and posterior distributions (blue) for likelihood components, growth, natural mortality ( $M$ ), and  $R_0$  parameters.**

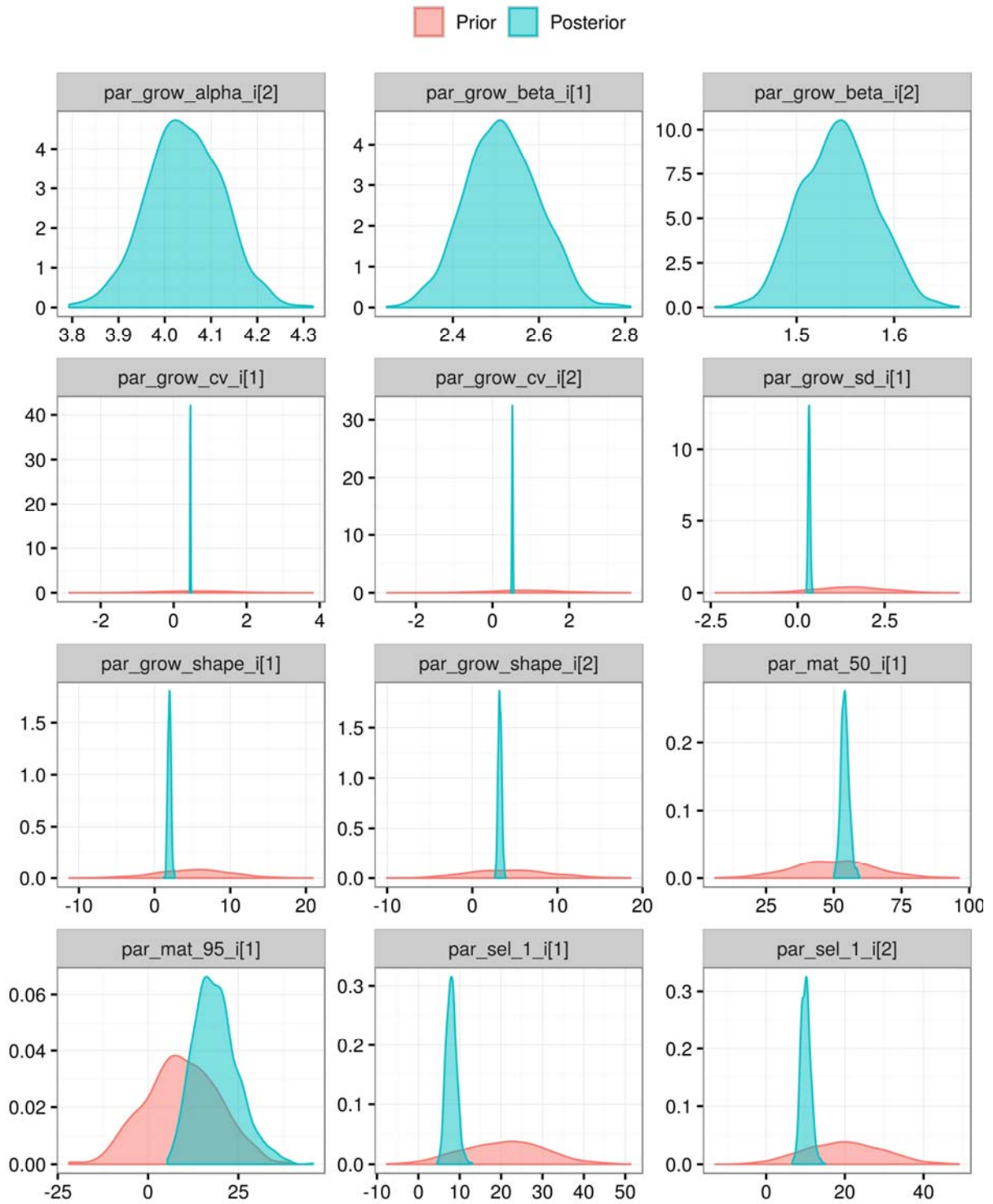


**Figure 54: CRA 6 base case: density plots showing prior (red) and posterior distributions (blue) for growth, maturity, and selectivity parameters.**

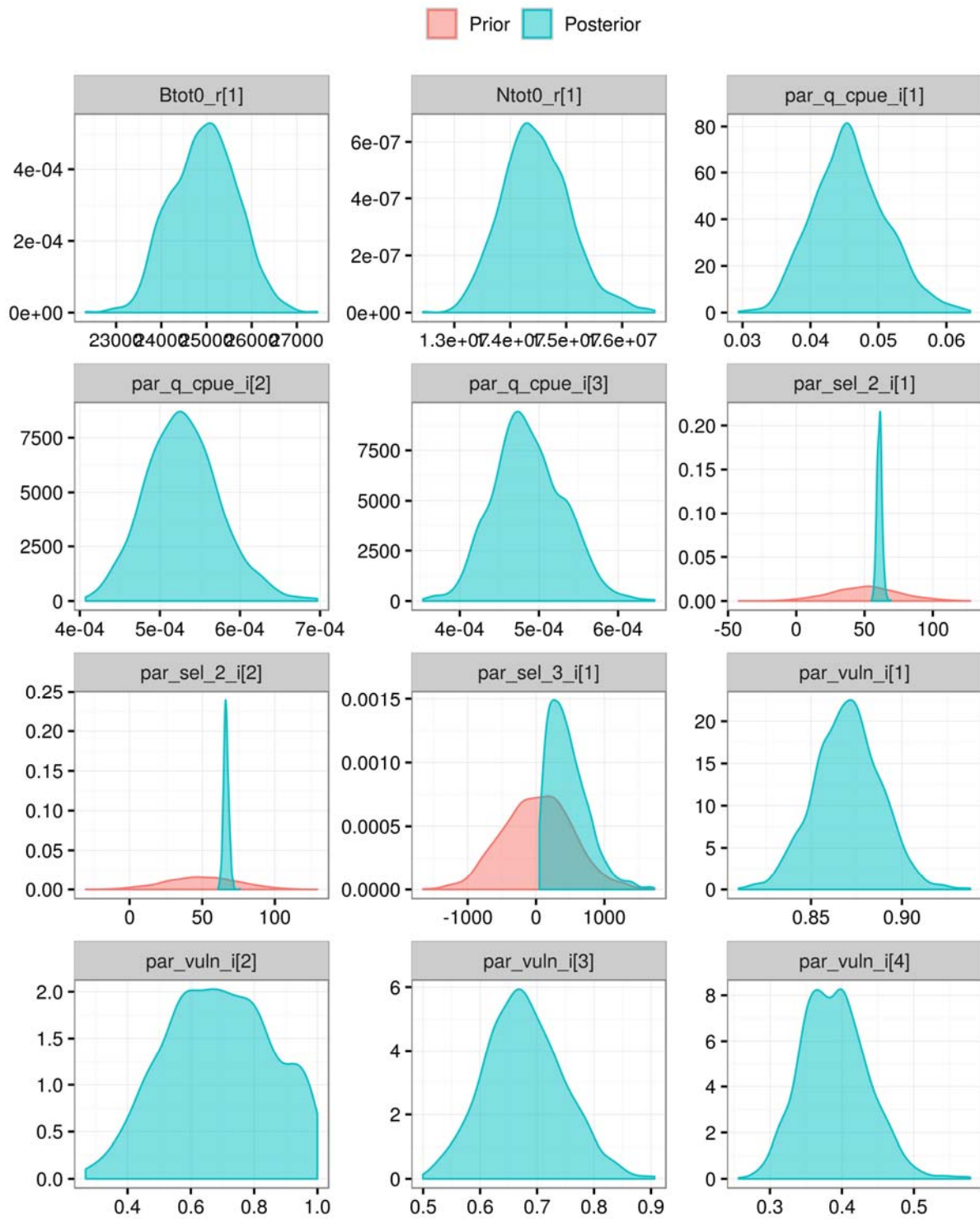


**Figure 55: CRA 6 base case: density plots showing prior (red) and posterior distributions (blue) for total biomass and numbers,  $q$ , selectivity, and vulnerability parameters.**

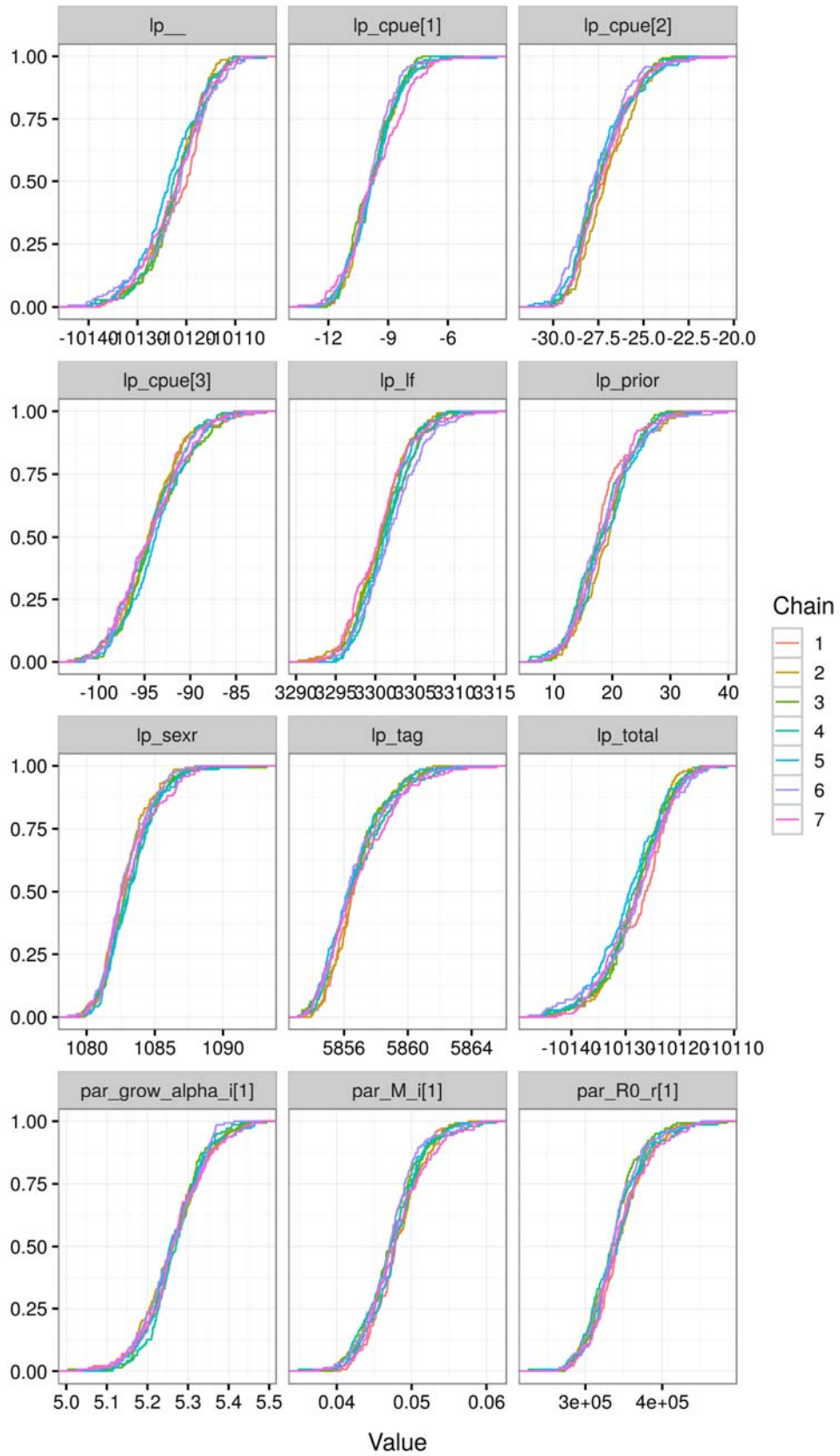
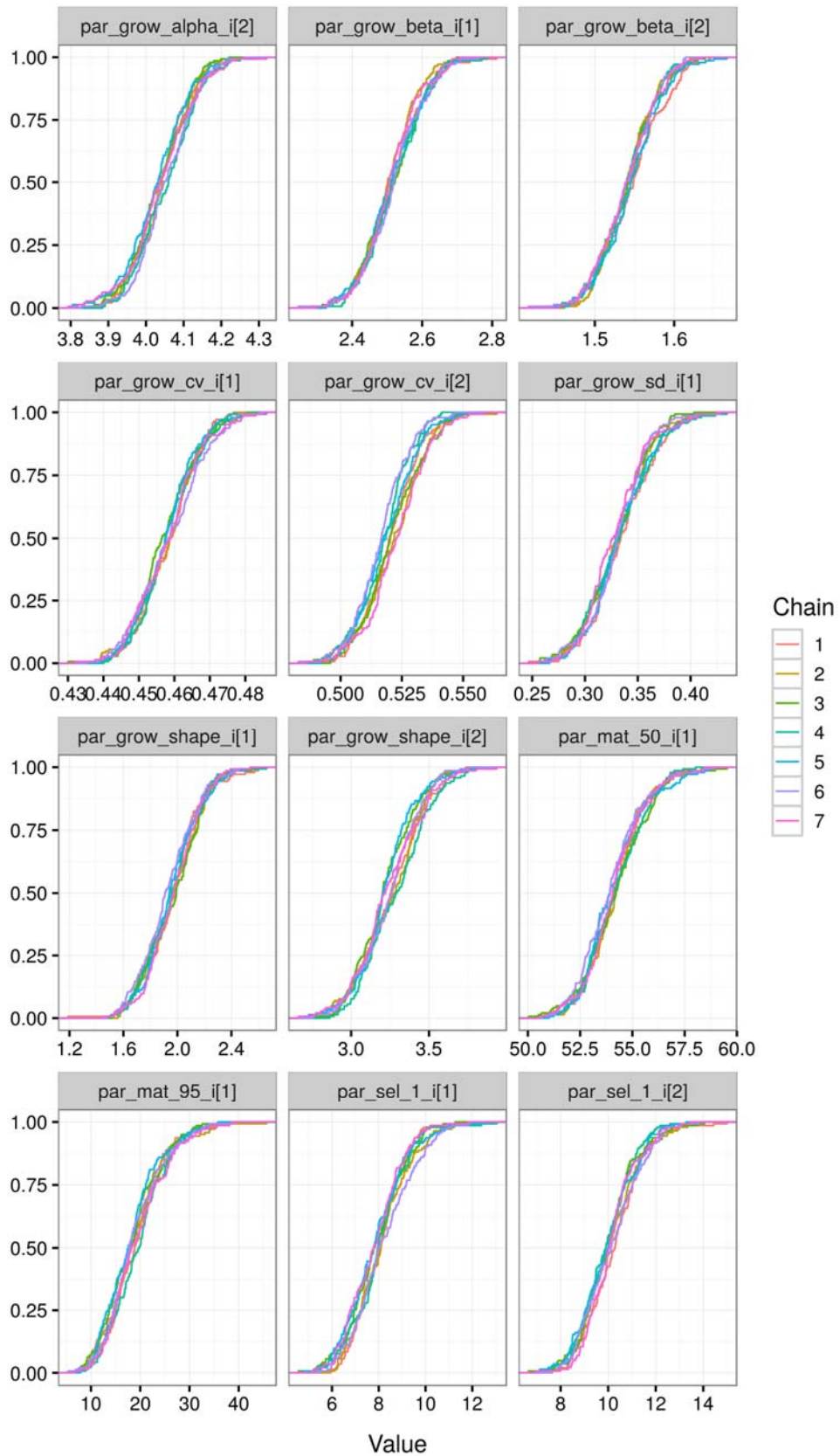


Figure 56: CRA 6 base case: empirical cumulative proportional distributions for each independent MCMC chain for likelihood components and growth, natural mortality ( $M$ ), and  $R_0$  parameters.



**Figure 57: CRA 6 base case: empirical cumulative proportional distributions for each independent MCMC chain for growth, maturity, and selectivity parameters.**

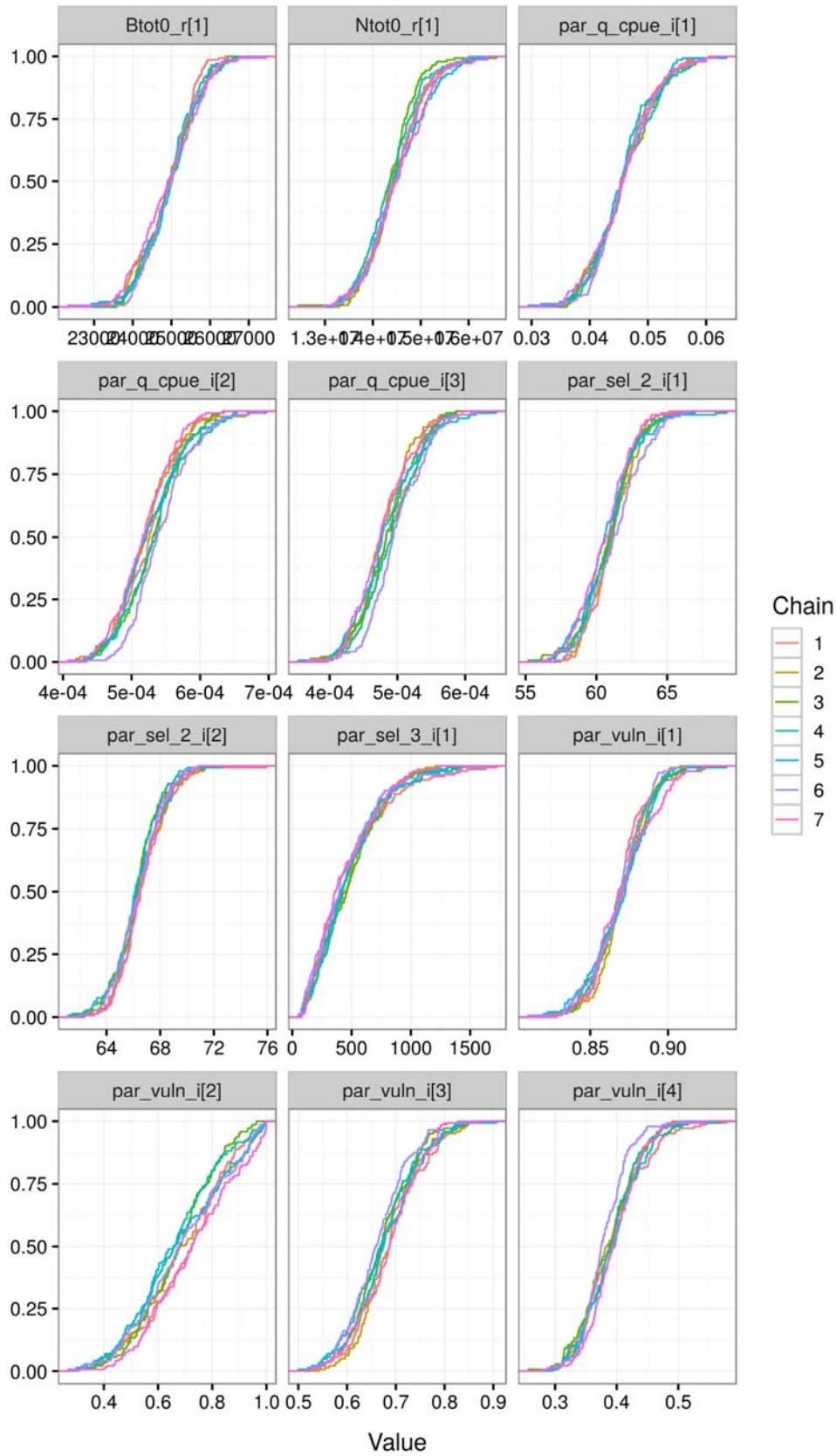
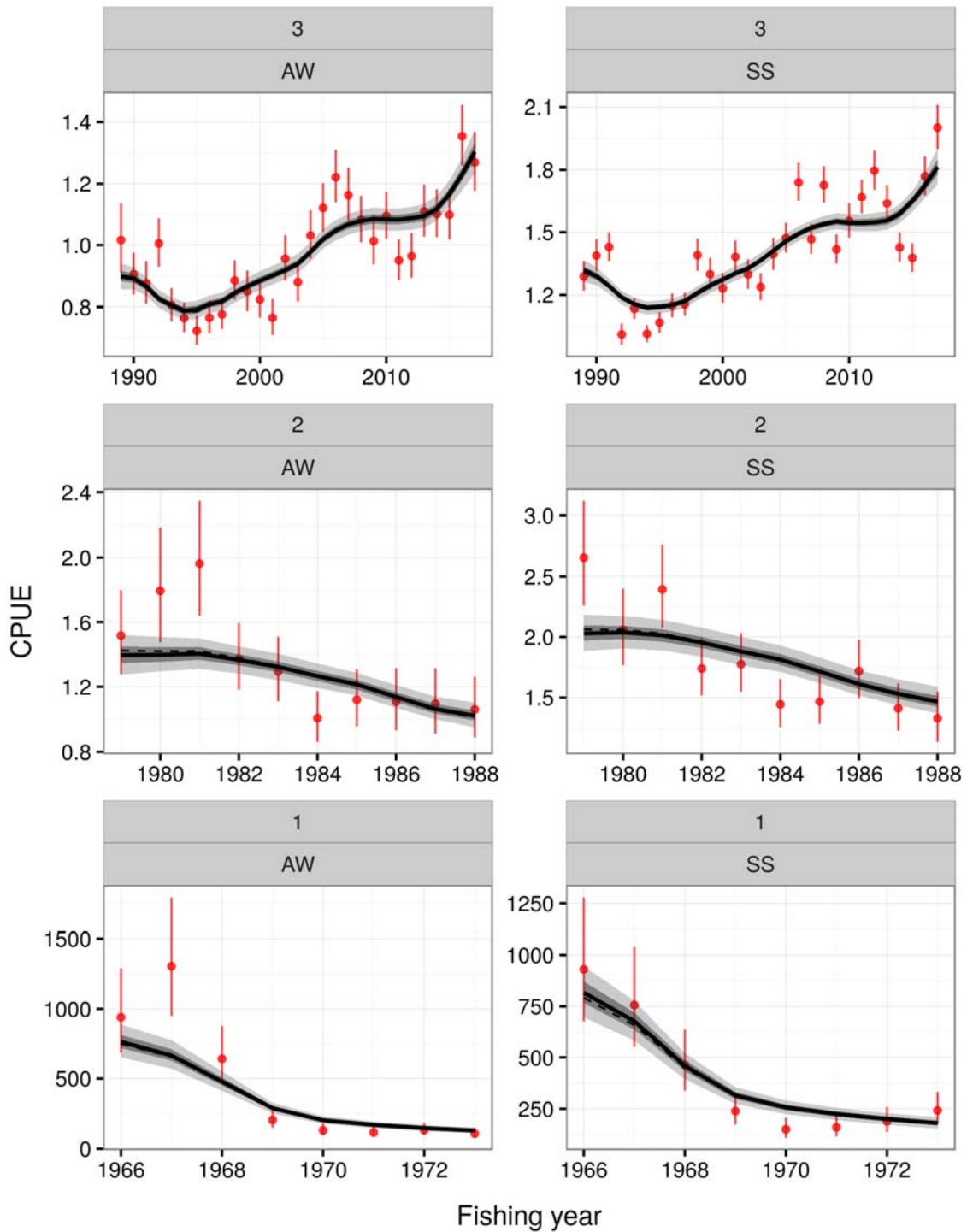
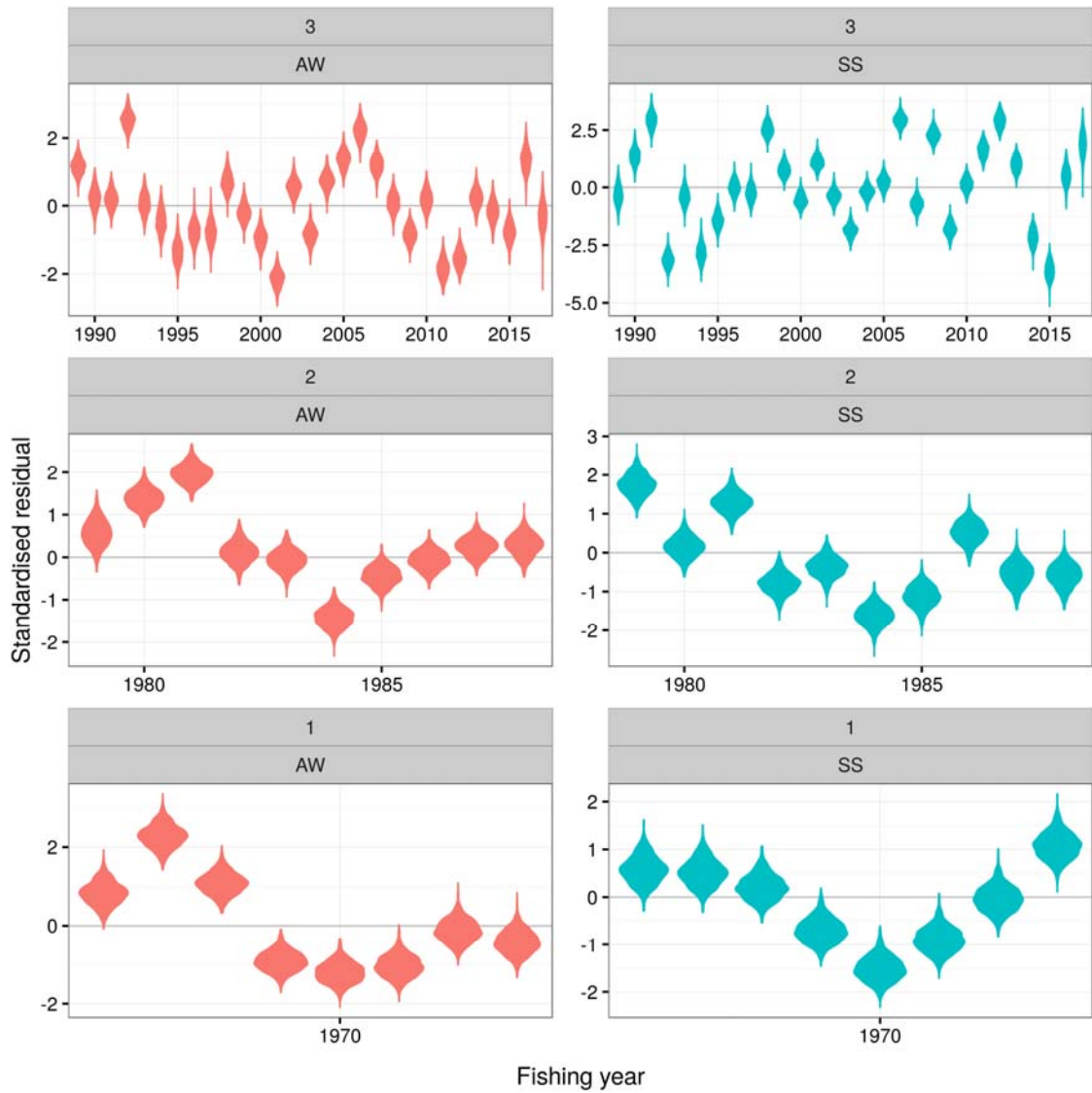


Figure 58: CRA 6 base case: empirical cumulative proportional distributions for each independent MCMC chain for total numbers and biomass,  $q$ , selectivity, and vulnerability parameters.



**Figure 59: CRA 6 base case: posterior of predicted CPUE by season: upper panels=CELR fit; middle panels=FSU fit; lower panels=CR fit. The solid line indicates the posterior median and grey shading with variable intensity indicates the 50% and 90% credible intervals. A dashed line (often not visible) indicates the corresponding MAP estimates.**



**Figure 60: CRA 6 base case: distribution of standardised residuals between the predicted CPUE and observed CPUE by season for each sample from the posterior distribution. Upper panels=CELR fit; middle panels=FSU fit; lower panels=CR fit.**

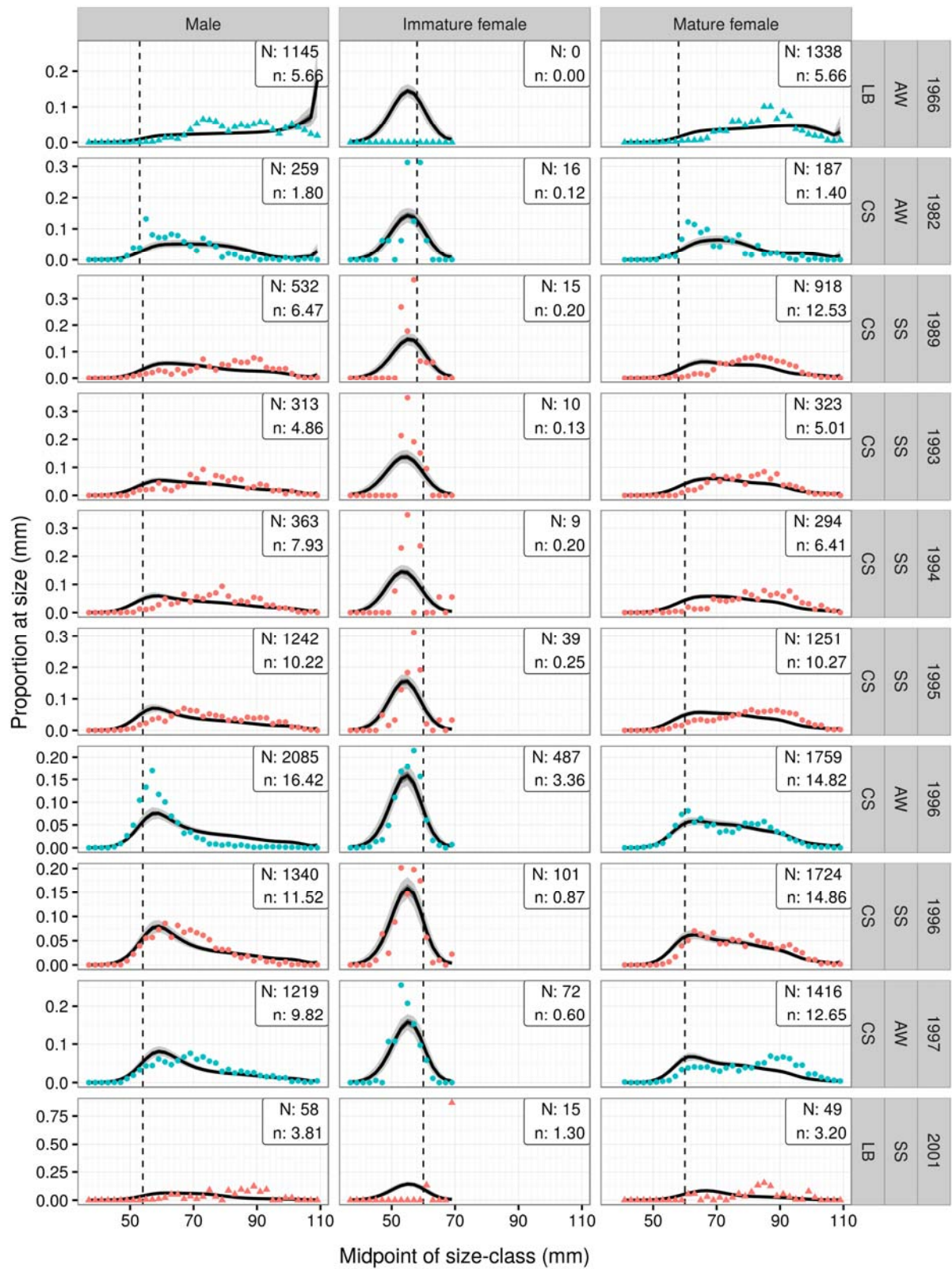


**Figure 61: CRA 6 base case posterior vs. observed LFs from 1966 AW LB – 2001 SS LB. The solid line indicates the posterior median and grey shading with variable intensity indicates the 50% and 90% credible intervals.**

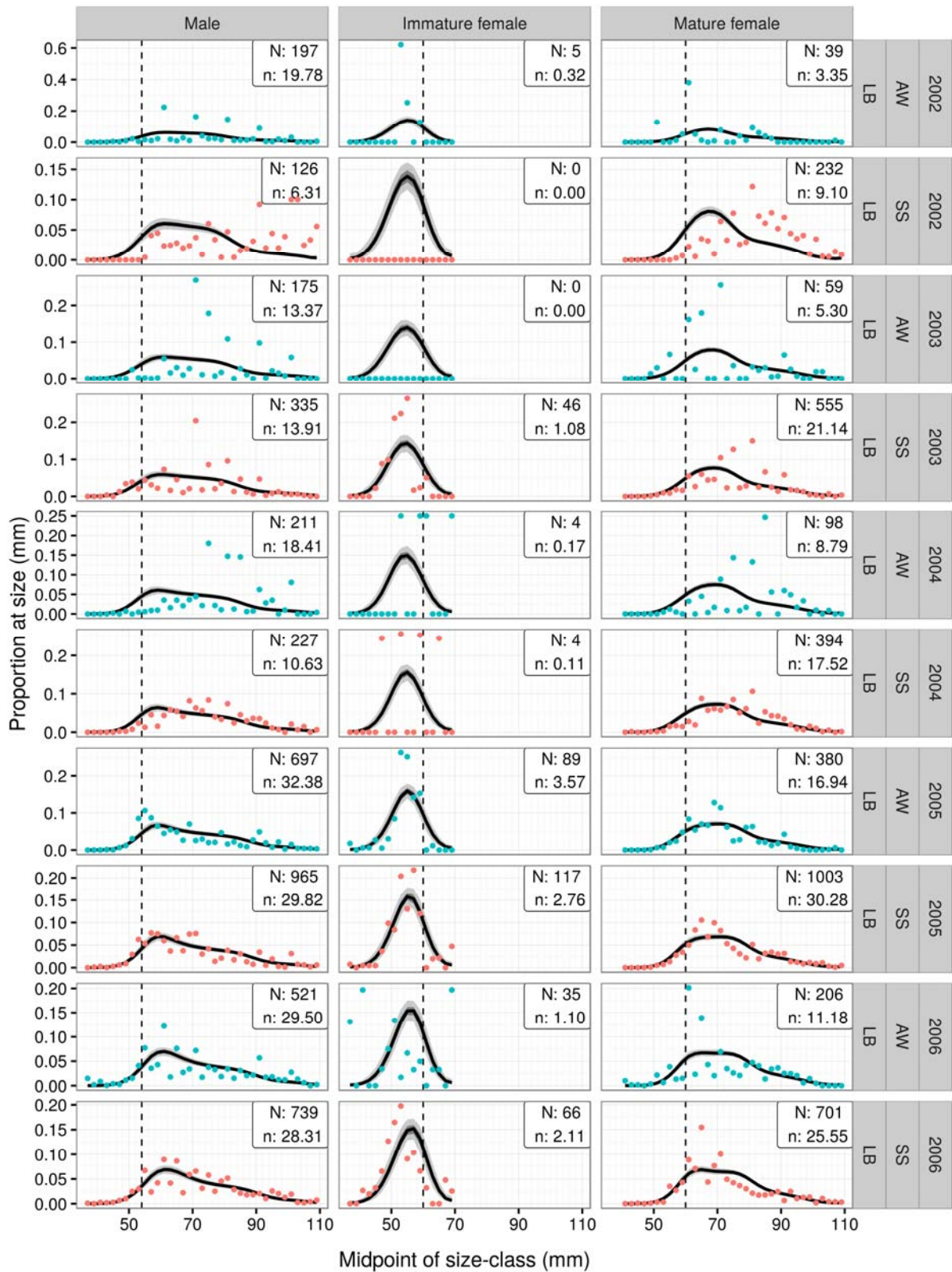


**Figure 62: CRA 6 base case posterior vs. observed LFs from 2002 AW LB – 2006 SS LB. The solid line indicates the posterior median and grey shading with variable intensity indicates the 50% and 90% credible intervals.**

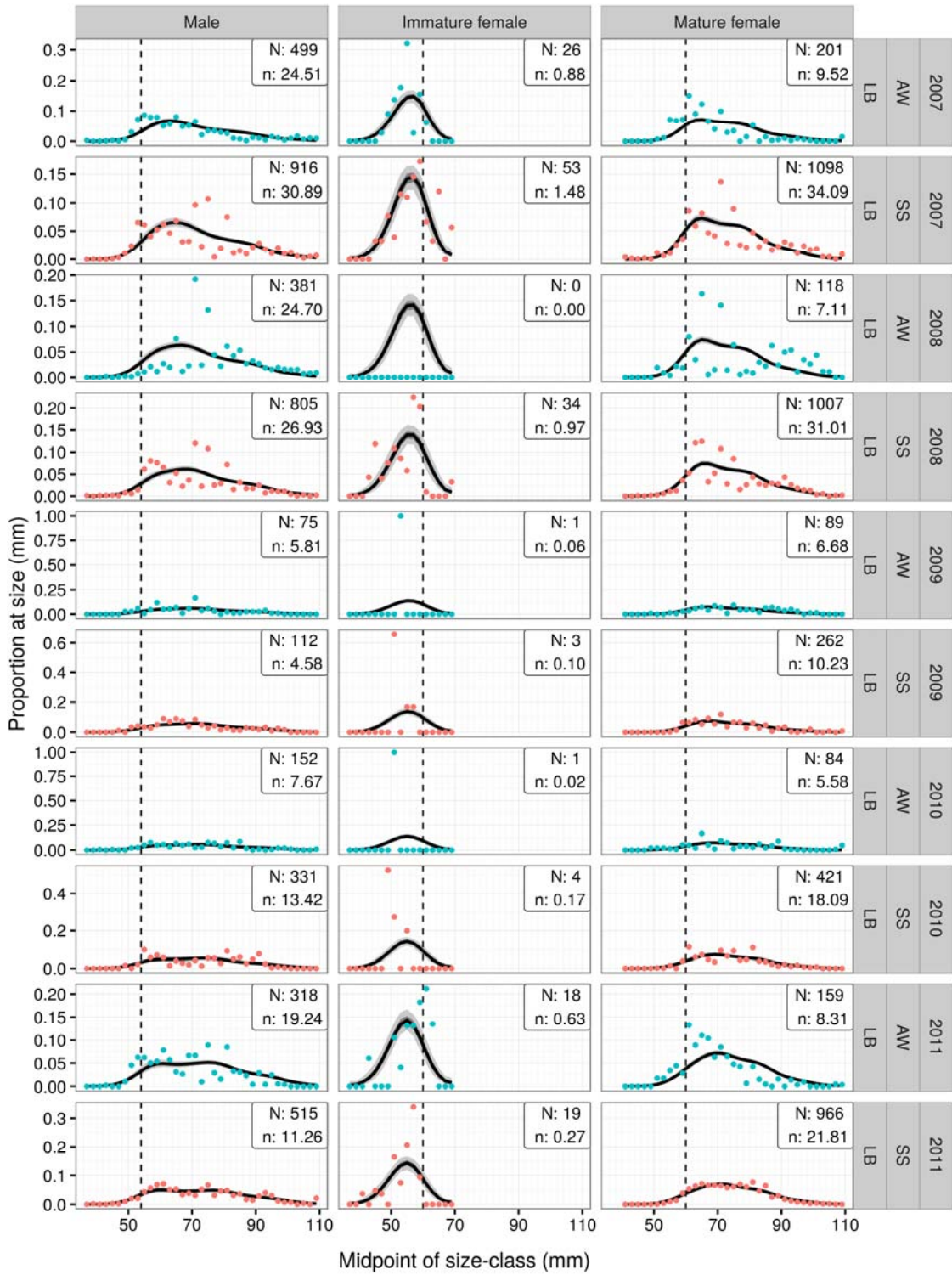


**Figure 63: CRA 6 base case posterior vs. observed LFs from 2007 AW LB – 2011 SS LB. The solid line indicates the posterior median and grey shading with variable intensity indicates the 50% and 90% credible intervals.**

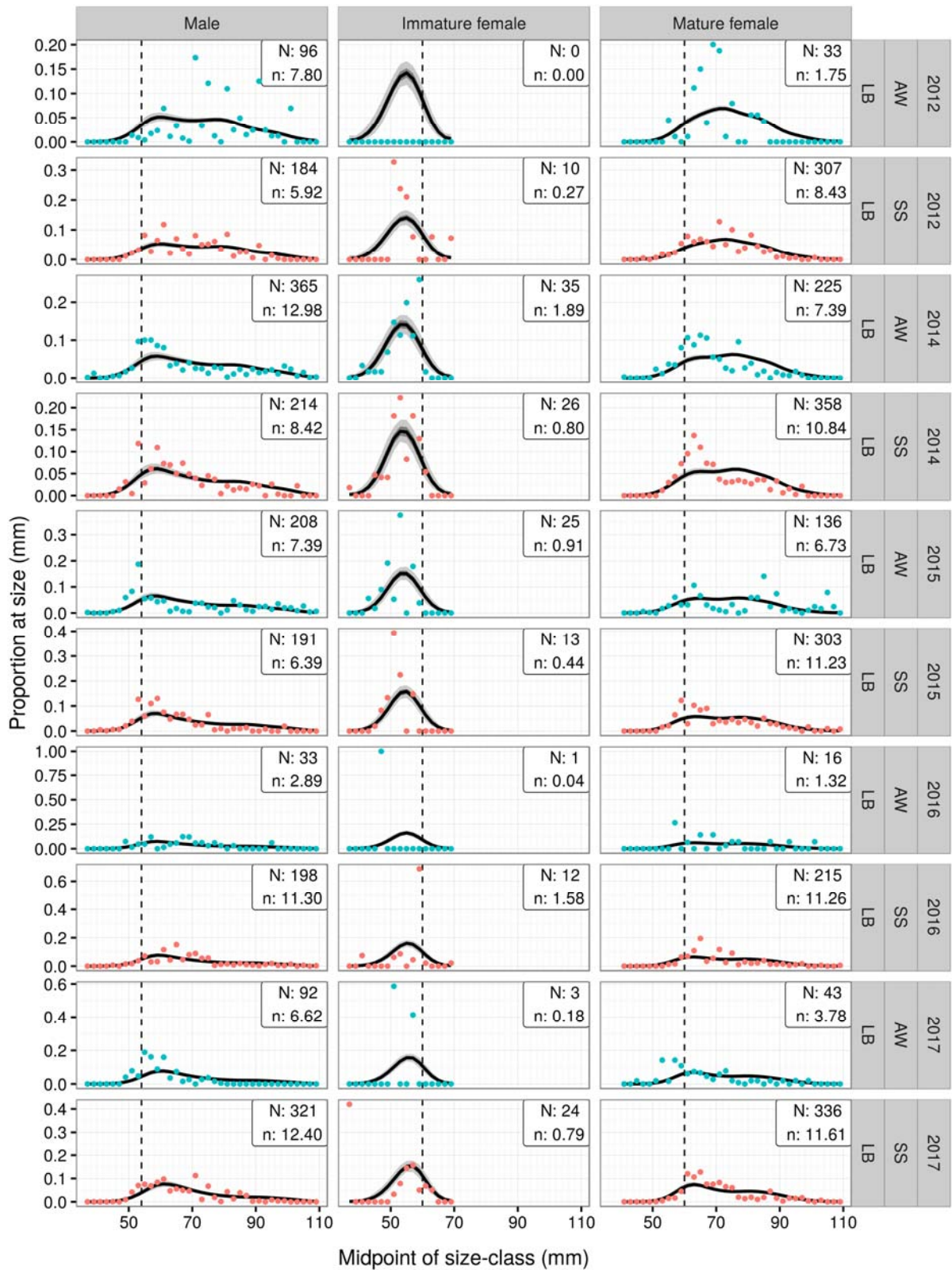


**Figure 64:** CRA 6 base case posterior vs. observed LFs from 2012 AW LB – 2017 SS LB. The solid line indicates the posterior median and grey shading with variable intensity indicates the 50% and 90% credible intervals.

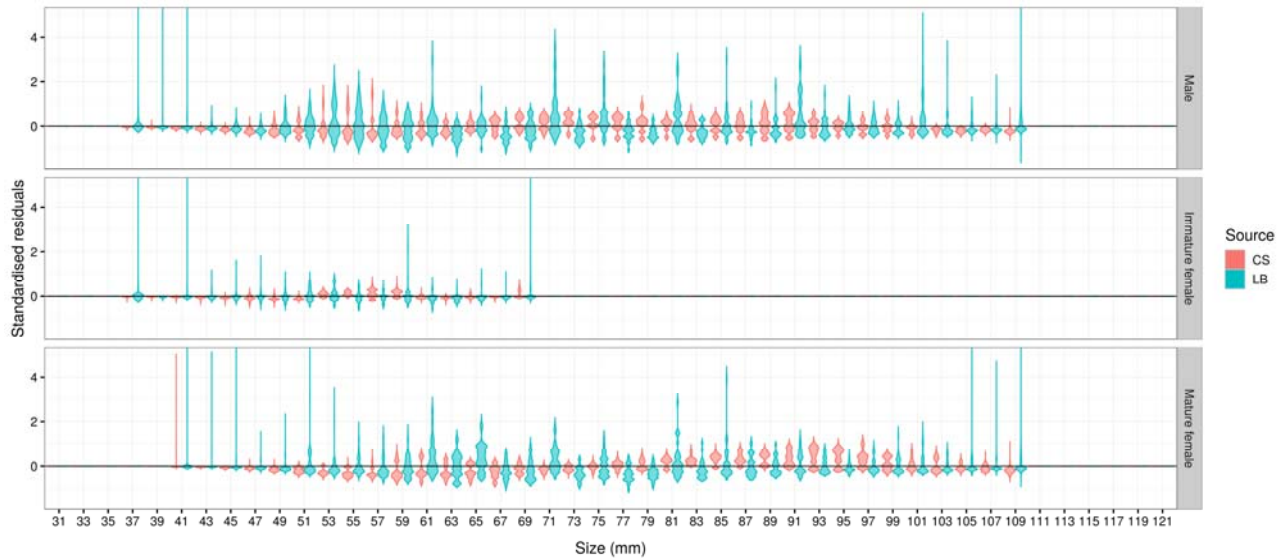


**Figure 65: CRA 6 base case: distribution of standardised residuals between the predicted LF distributions and LF data for each sample from the posterior distribution, showing residuals by sex, 2 mm size bin, and sampling source. Shading intensity varies with number of observations.**

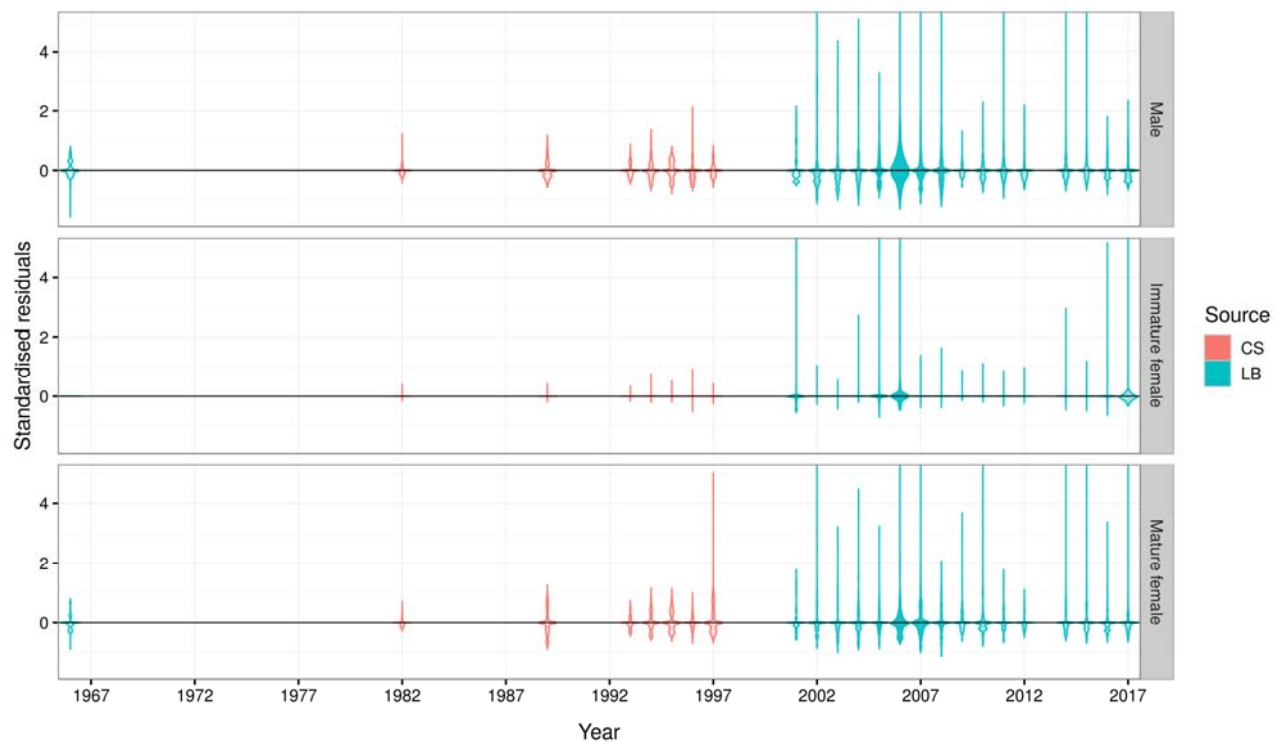


**Figure 66: CRA 6 base case: distribution of standardised residuals between the predicted LF distributions and LF data for each sample from the posterior distribution, showing residuals by sex, year, and sampling source. Shading intensity varies with number of observations.**

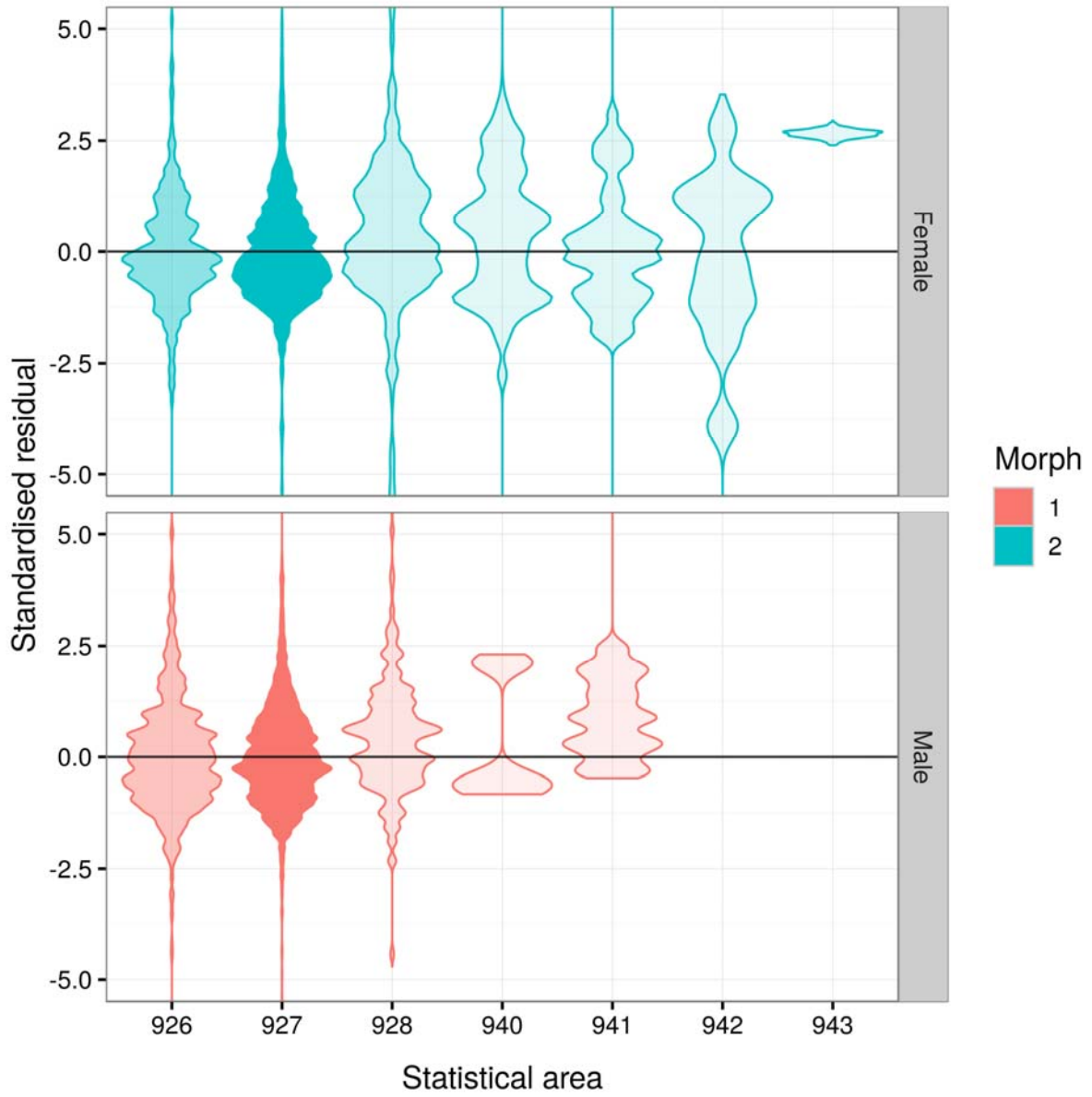


**Figure 67: CRA 6 base case: distribution of tag residuals by statistical area of release for each sample from the posterior distribution. Shading intensity varies with number of observations.**

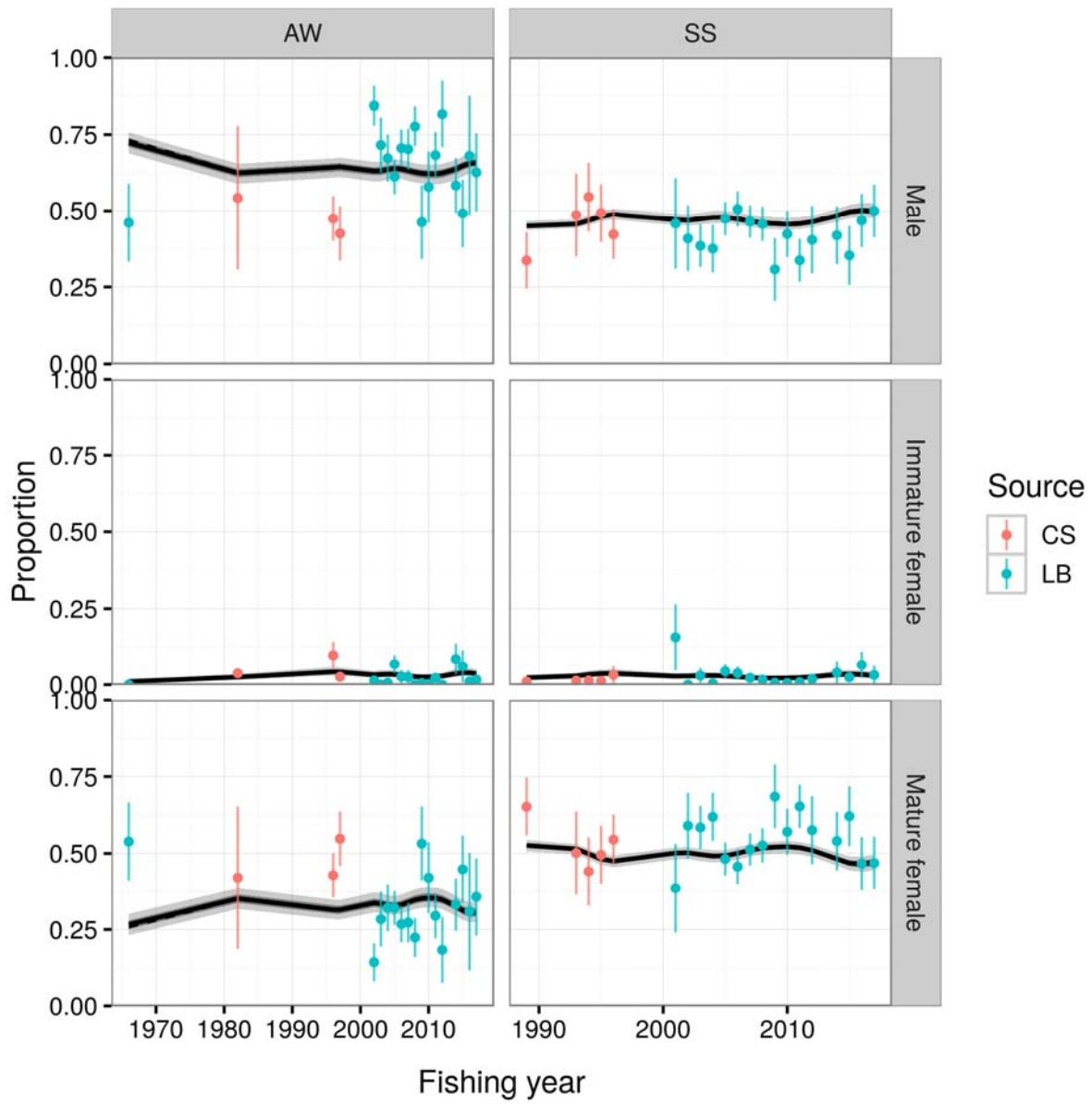


**Figure 68: CRA 6 base case: model fit to sex ratios by year and LF data source. The solid line indicates the posterior median and grey shading with variable intensity indicates the 50% and 90% credible intervals. A dashed line (not visible) indicates the corresponding MAP estimates.**

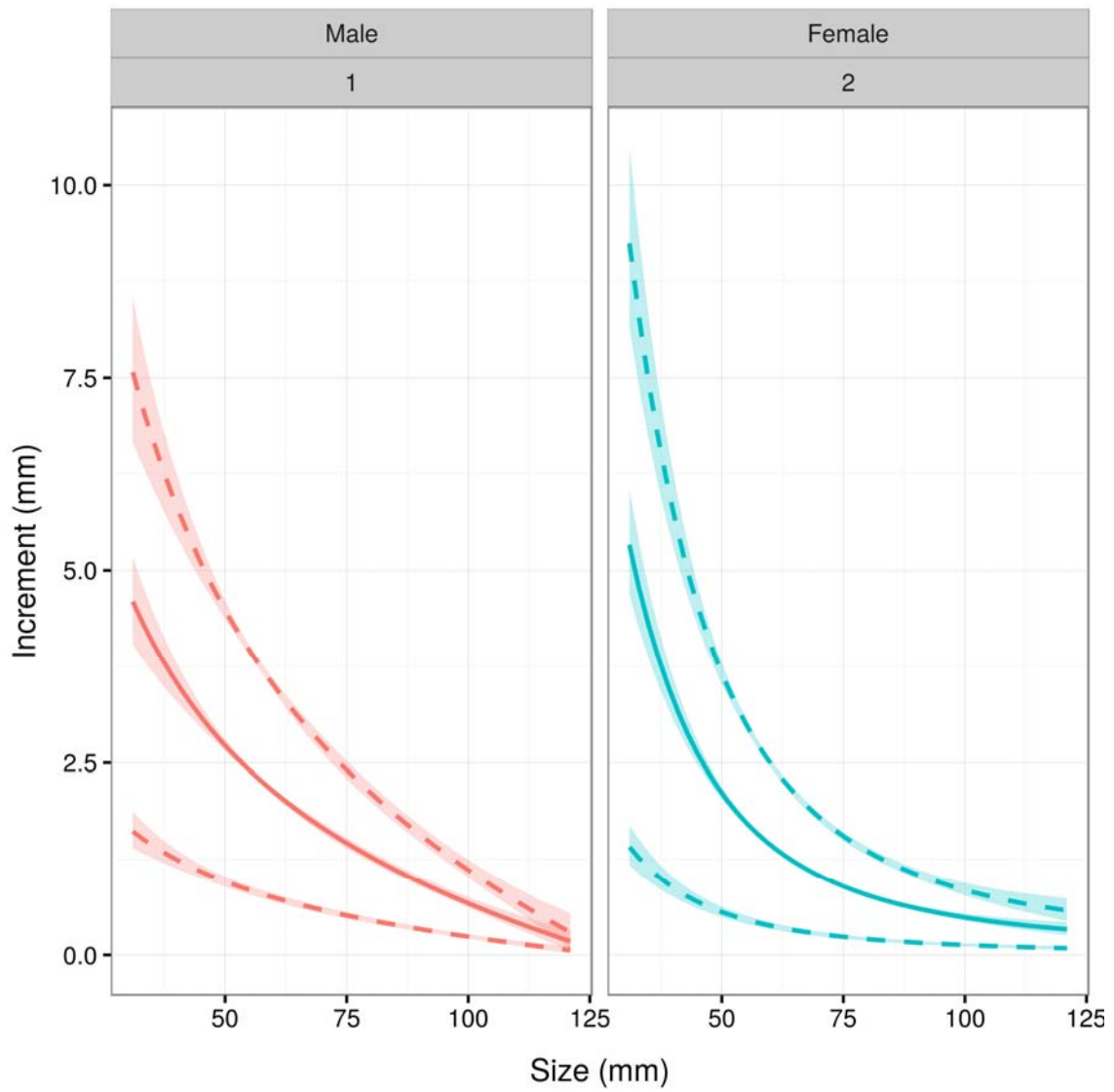


**Figure 69: CRA 6 base case: Predicted increments-at-length and  $\pm 1$  standard deviation (dashed coloured lines), with the solid line indicating the posterior median and the grey bands showing the 90% credible intervals. A dashed line (not visible underneath the posterior median) indicates the corresponding MAP estimates.**

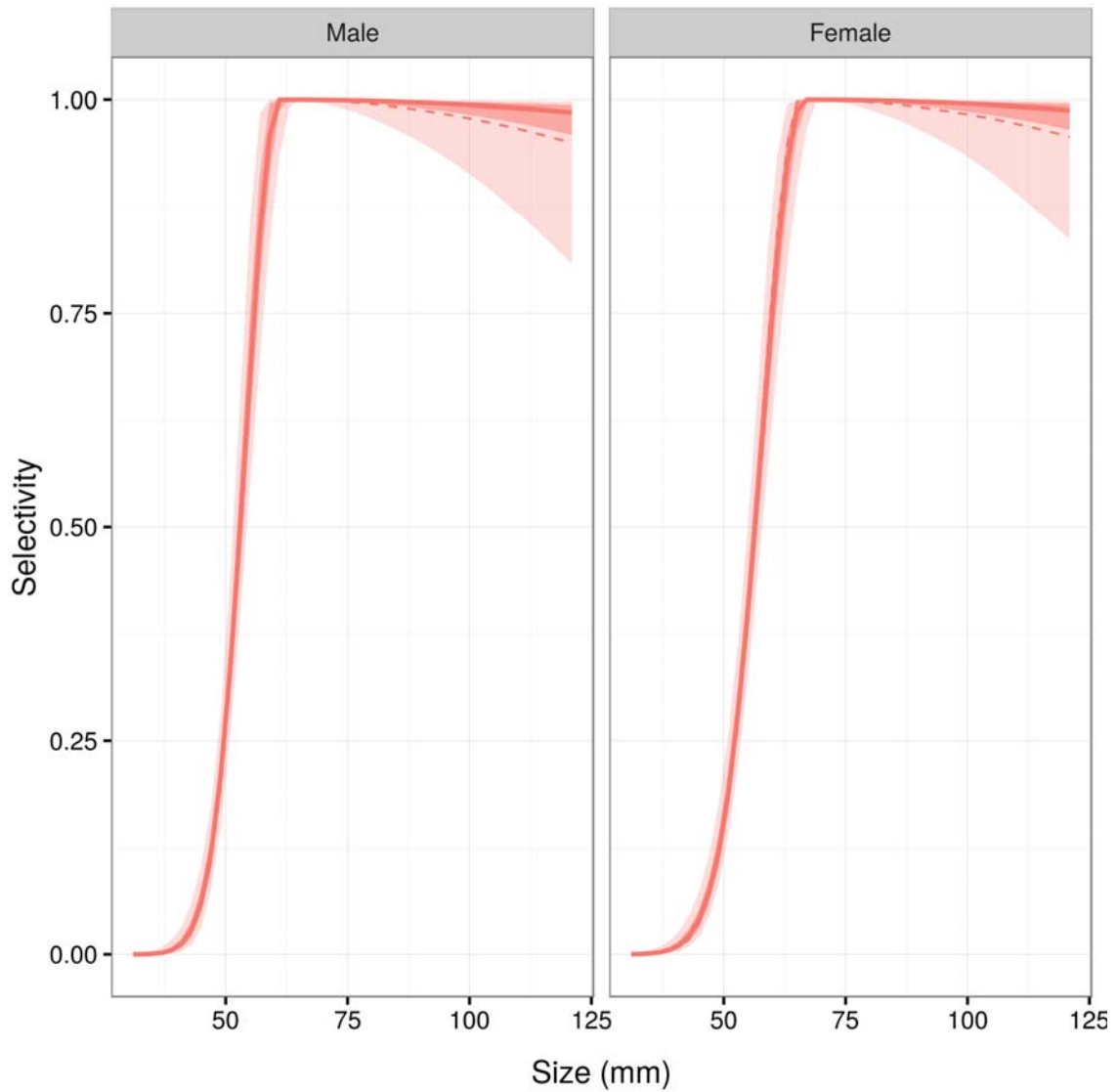


**Figure 70: CRA 6 base case selectivity by sex, with the solid line indicating the posterior median and the variable intensity coloured bands showing the 50% and 90% credible intervals. Dashed lines indicate the corresponding MAP estimates.**

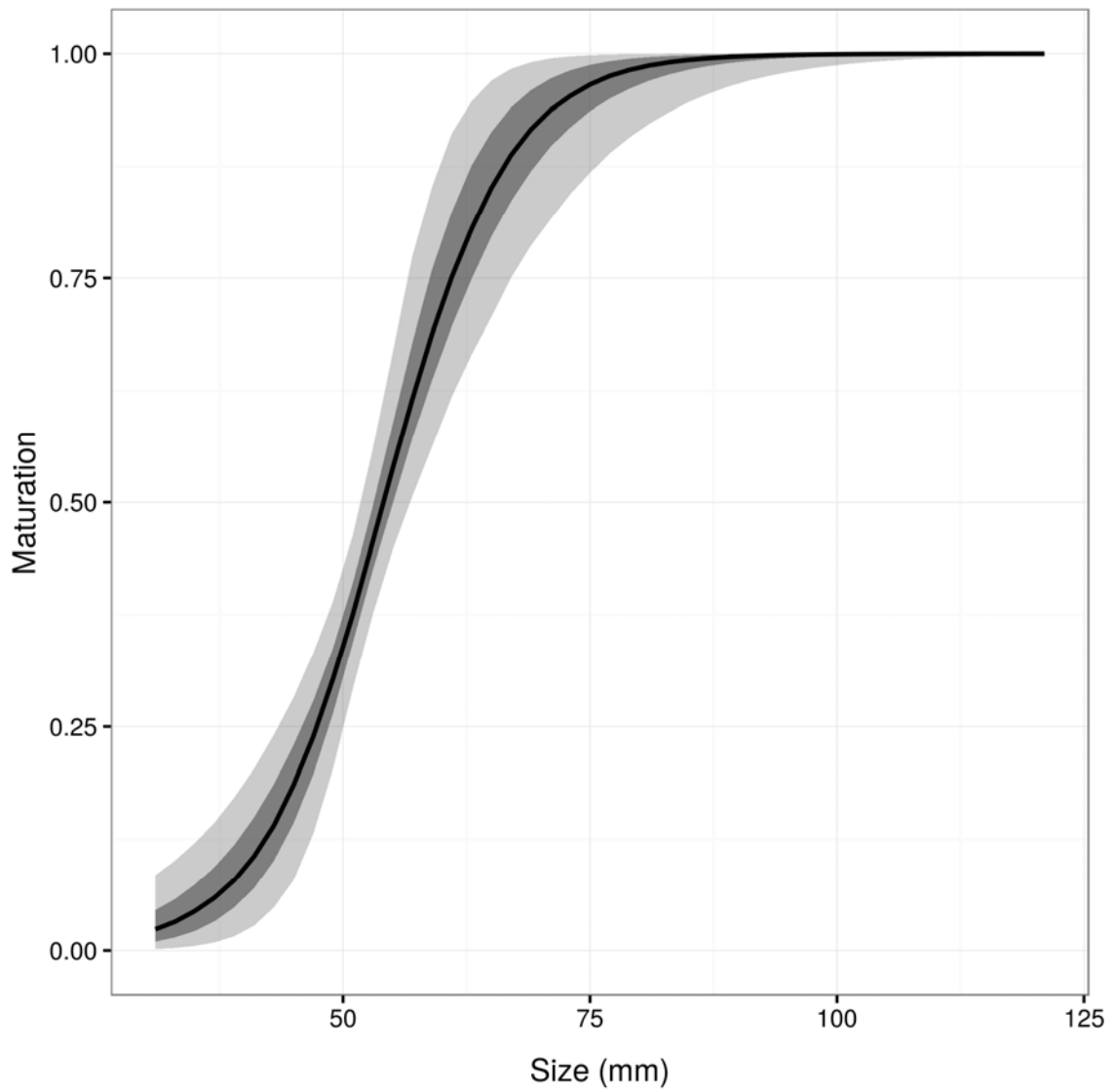


**Figure 71: CRA 6 base case female maturity, where the solid line indicates the posterior median and grey shading with variable intensity indicates the 50% and 90% credible intervals. A dashed line (not visible) indicates the corresponding MAP estimates.**

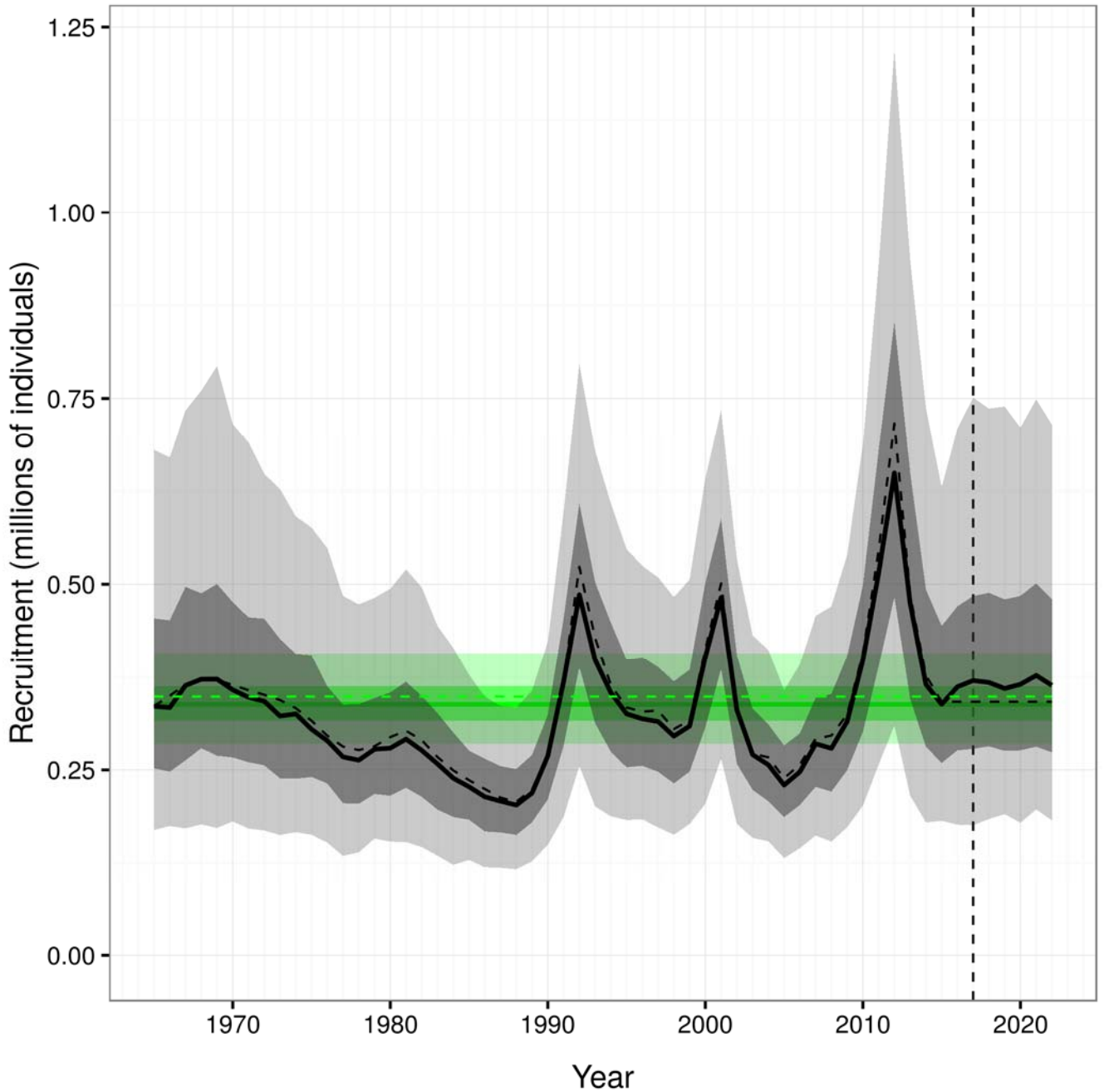


**Figure 72:** CRA 6 base case recruitment in 000 000's, where the dashed black line indicates the MAP, the solid black line indicates the median of the posterior and variable shading intensity indicates the 50% and 90% credible intervals. The horizontal solid green line is the median of the posterior for  $R_0$  with green shading indicating the 50% and 90% credible intervals for  $R_0$ . The vertical dashed line is the final year of the reconstruction period and the dashed green line is the MAP for  $R_0$ . Projection recruitments (plotted to the right of the vertical dashed line) are based on the mean and standard deviation of the 2006–2015 recruitment and the 1965–2015 estimated autocorrelation.

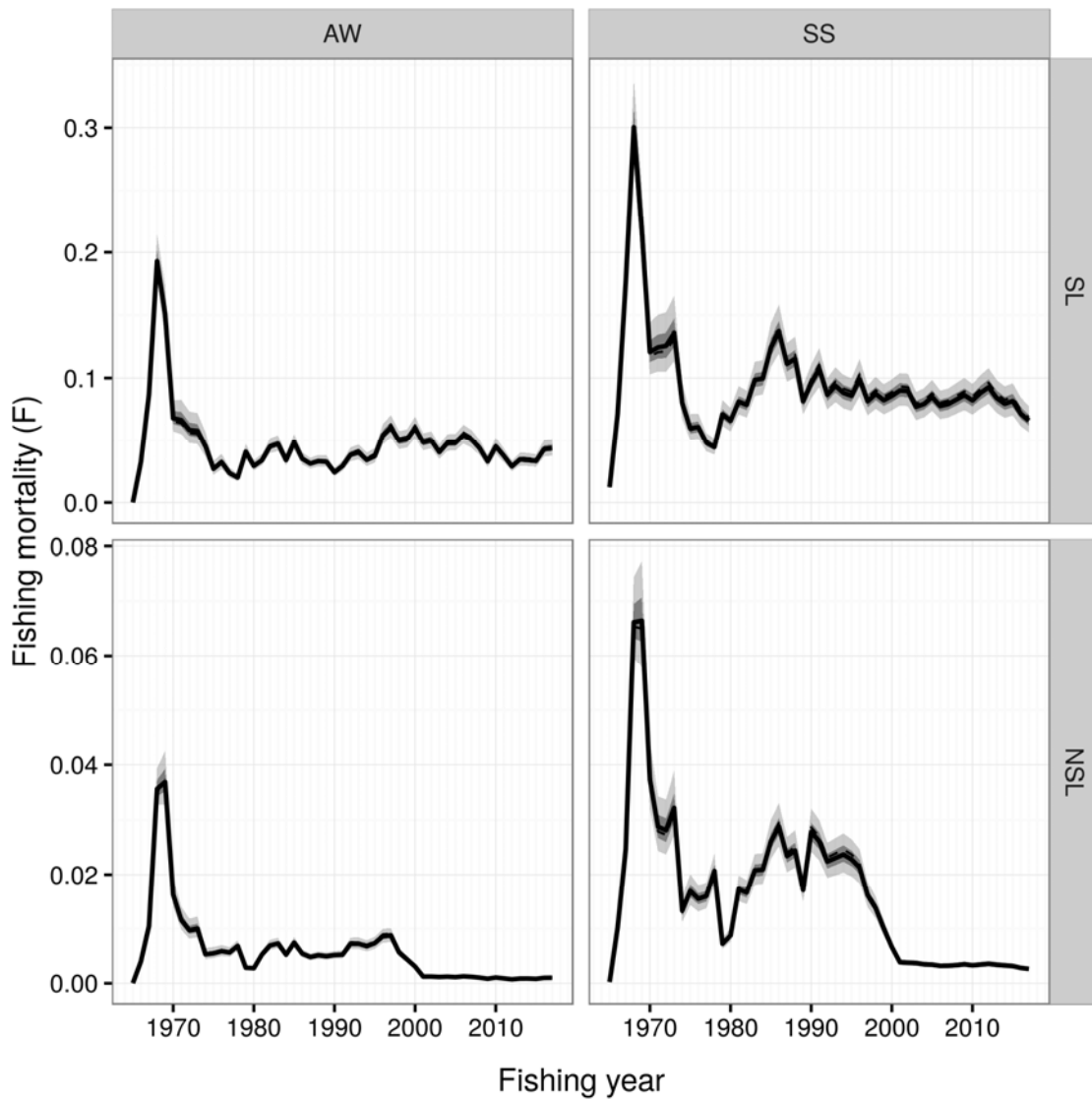


**Figure 73:** CRA 6 base case fishing mortality by year, season, and fishery (SL = size limited; NSL = non size limited), with the dashed black line (not visible) indicating the MAP, the solid black line indicating the median of the posterior and variable shading intensity indicating the 50% and 90% credible intervals.

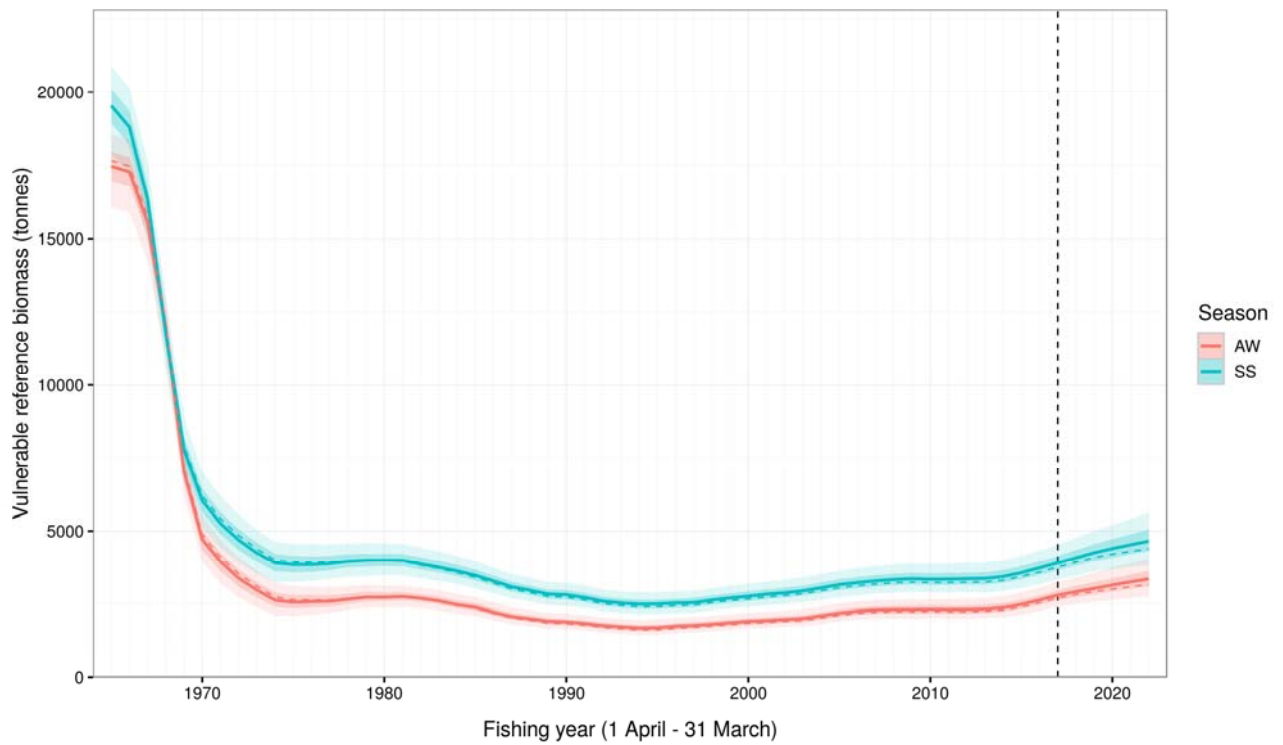


**Figure 74:** Posterior distribution of the CRA 6 base case vulnerable reference biomass by season, with dashed lines indicating the equivalent MAP estimates. Variable shading intensity indicates the 50% and 90% credible intervals. The vertical dashed line indicates the last year of the reconstruction period, after which the projected vulnerable reference biomass is shown. Projections use the recruitments described in Figure 72.

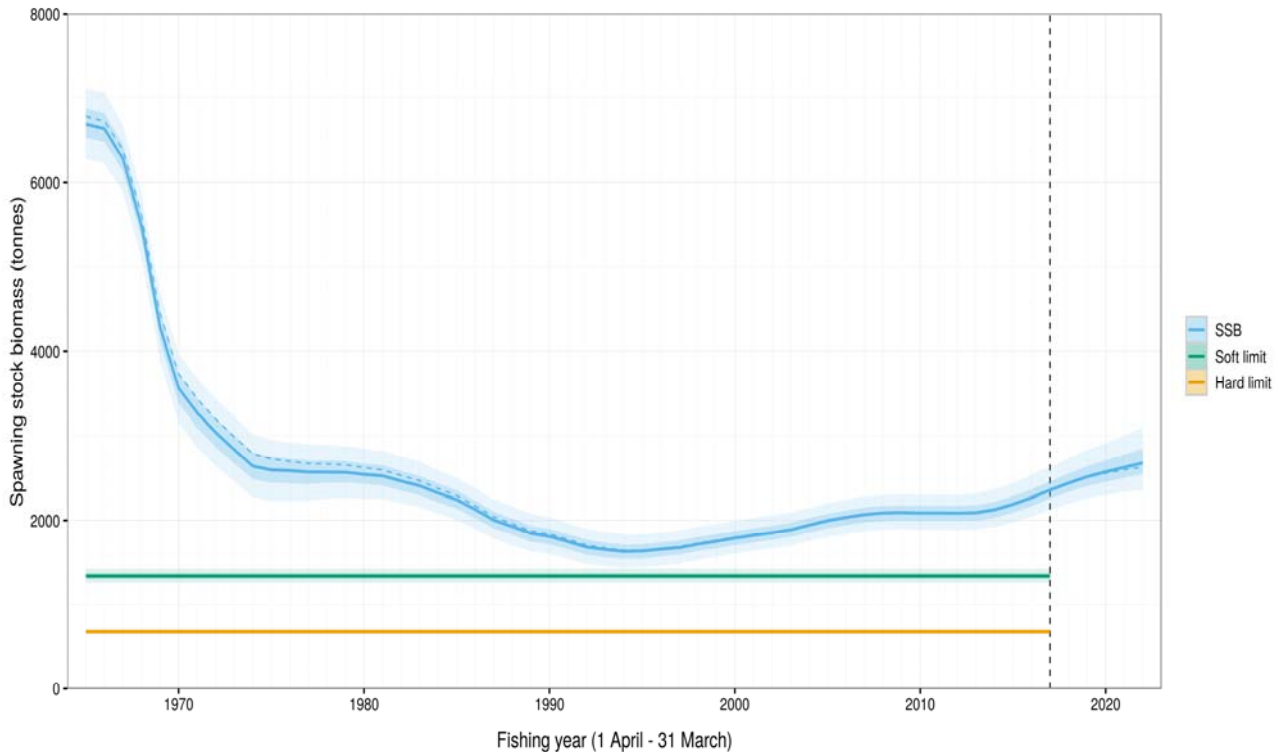


**Figure 75:** Posterior distribution of the CRA 6 base case spawning biomass, with dashed lines indicating the equivalent MAP estimates. Variable shading intensity indicates the 50% and 90% credible intervals. The vertical dashed line indicates the last year of the reconstruction period, after which the projected spawning biomass is shown. Projections use the recruitments described in Figure 72.

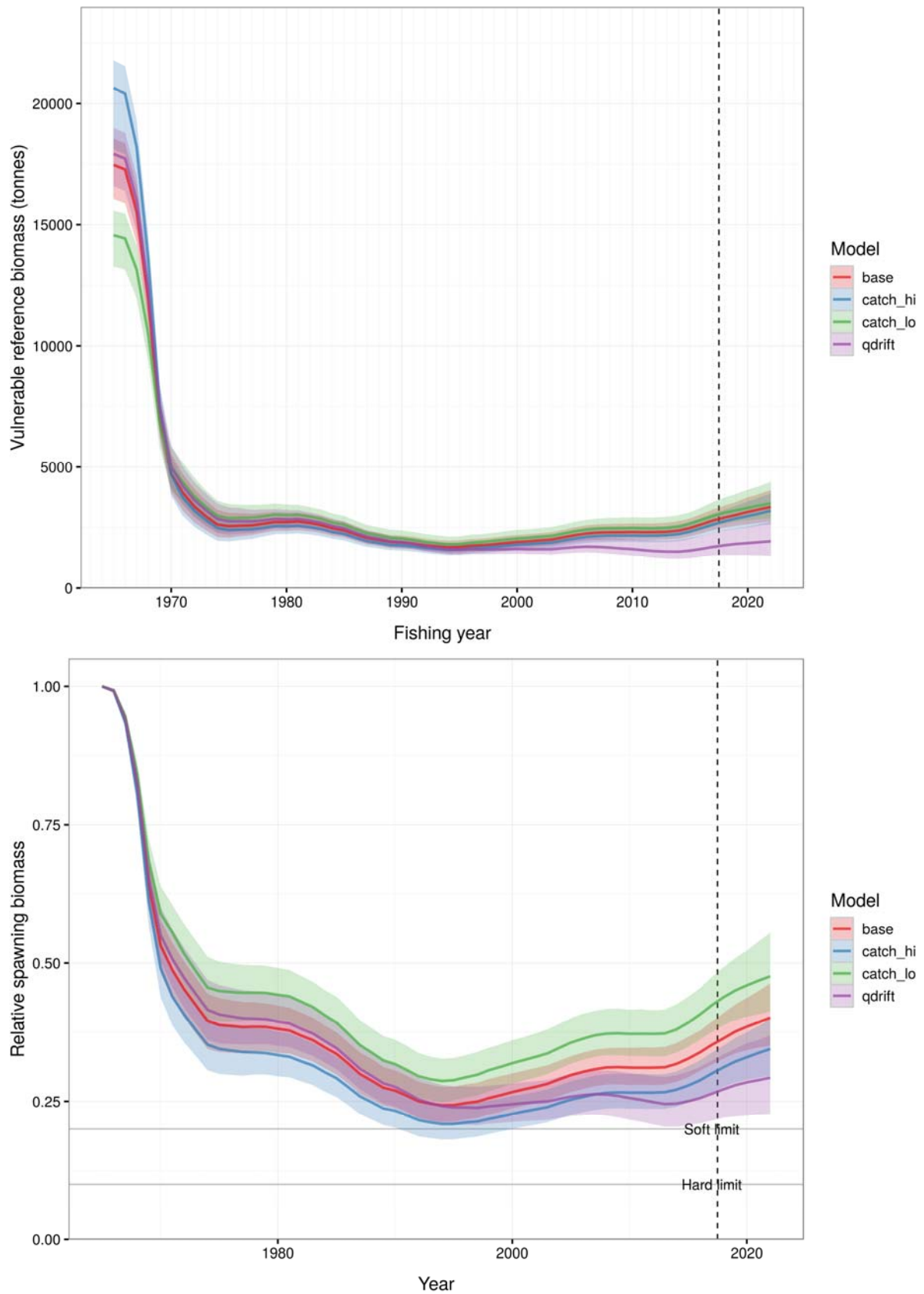


**Figure 76:** Comparison of the vulnerable reference biomass [upper panel] and relative spawning stock biomass [lower panel] trajectories between the base run and the three sensitivity runs (Table 6). The vertical dashed line indicates the last year of the reconstruction period, after which the projected biomass is shown. Projections use the recruitments described in Figure 72.

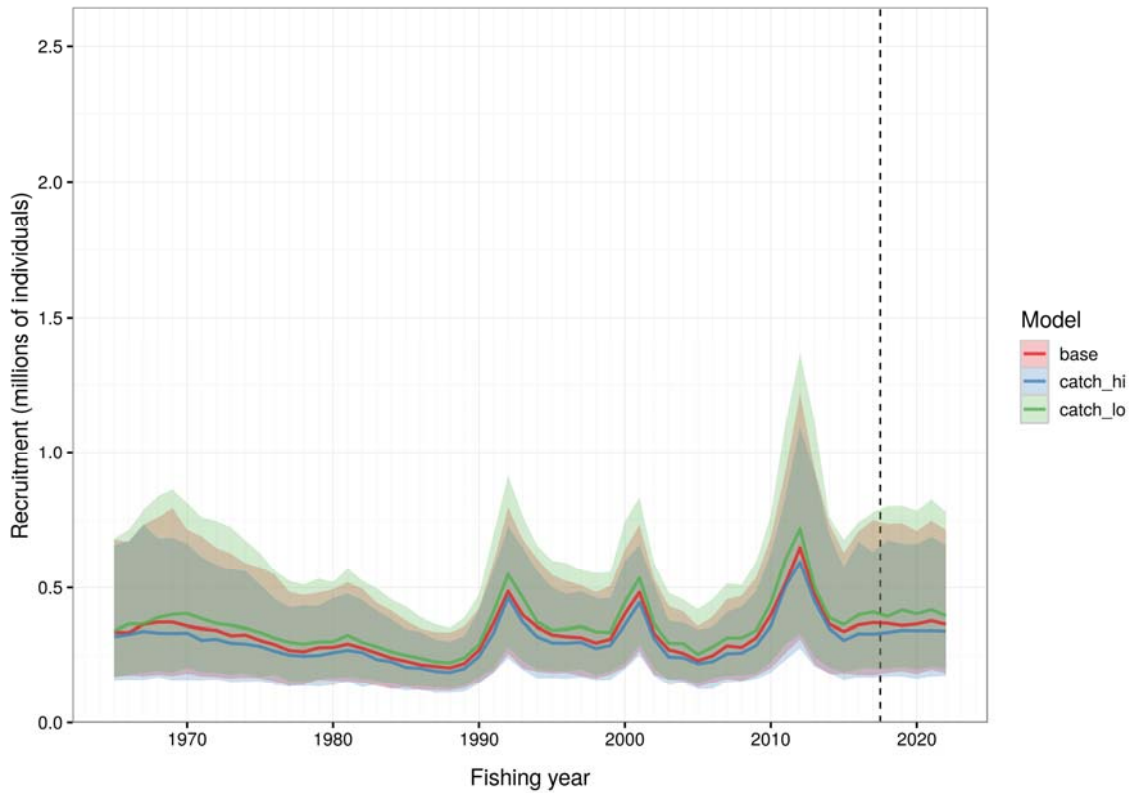


**Figure 77:** Comparison of recruitment trajectories between the base run and the two catch sensitivity runs (Table 6). Vertical dashed line placed at the last year of the reconstruction period followed by the projections (see Figure 72 for explanation of projection procedure).

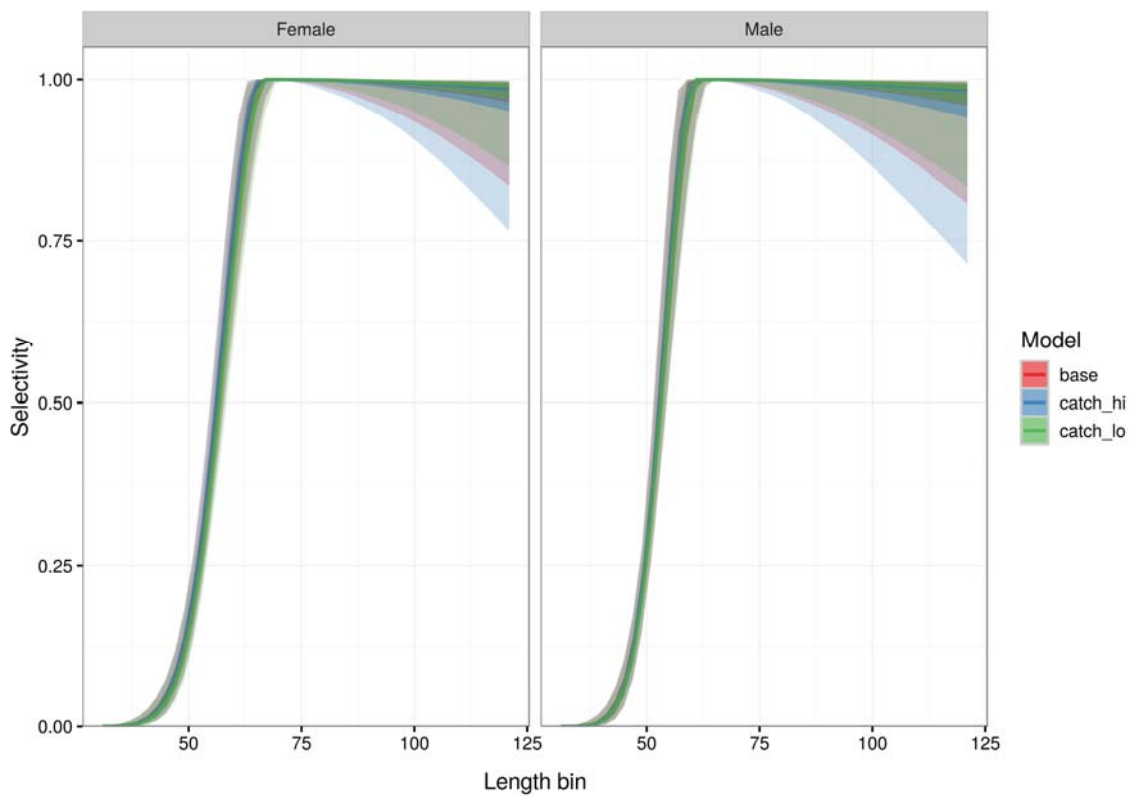


**Figure 78:** Comparison of selectivity curves between the base run and the two catch sensitivity runs (Table 6).

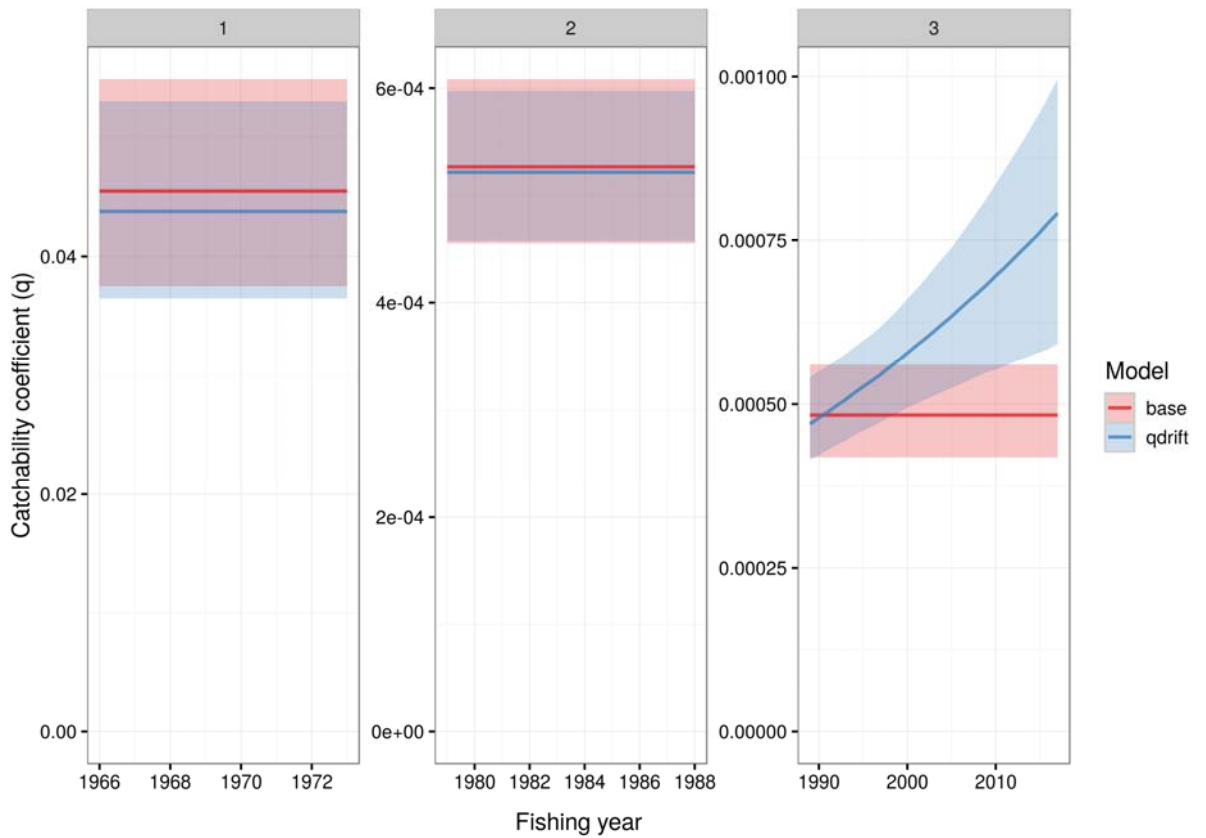


**Figure 79: Comparison of  $q$  estimates between the base run and the qdrift sensitivity run (Table 6): 1=CR CPUE  $q$ ; 2=FSU CPUE  $q$ ; 3=CELR CPUE  $q$ .**

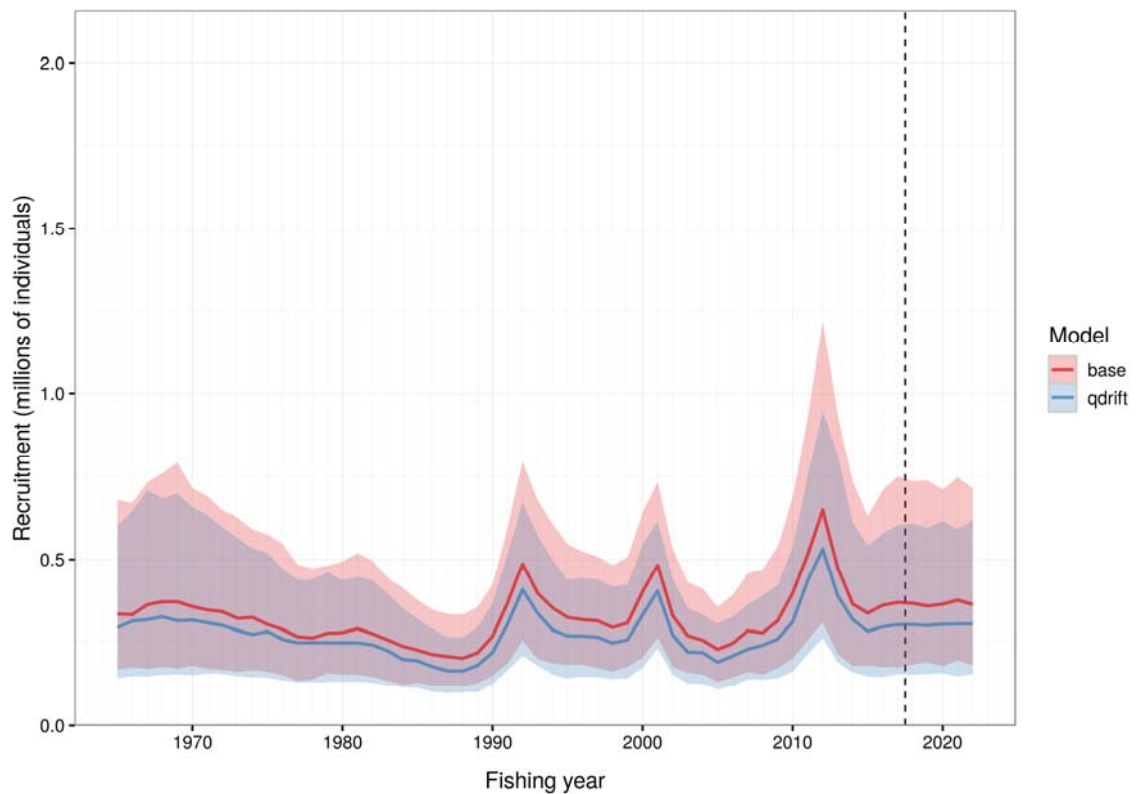


**Figure 80: Comparison of recruitment trajectories between the base run and the q-drift sensitivity run (Table 6). Vertical dashed line placed at the last year of the reconstruction period followed by the projections (see Figure 72 for explanation of projection procedure).**

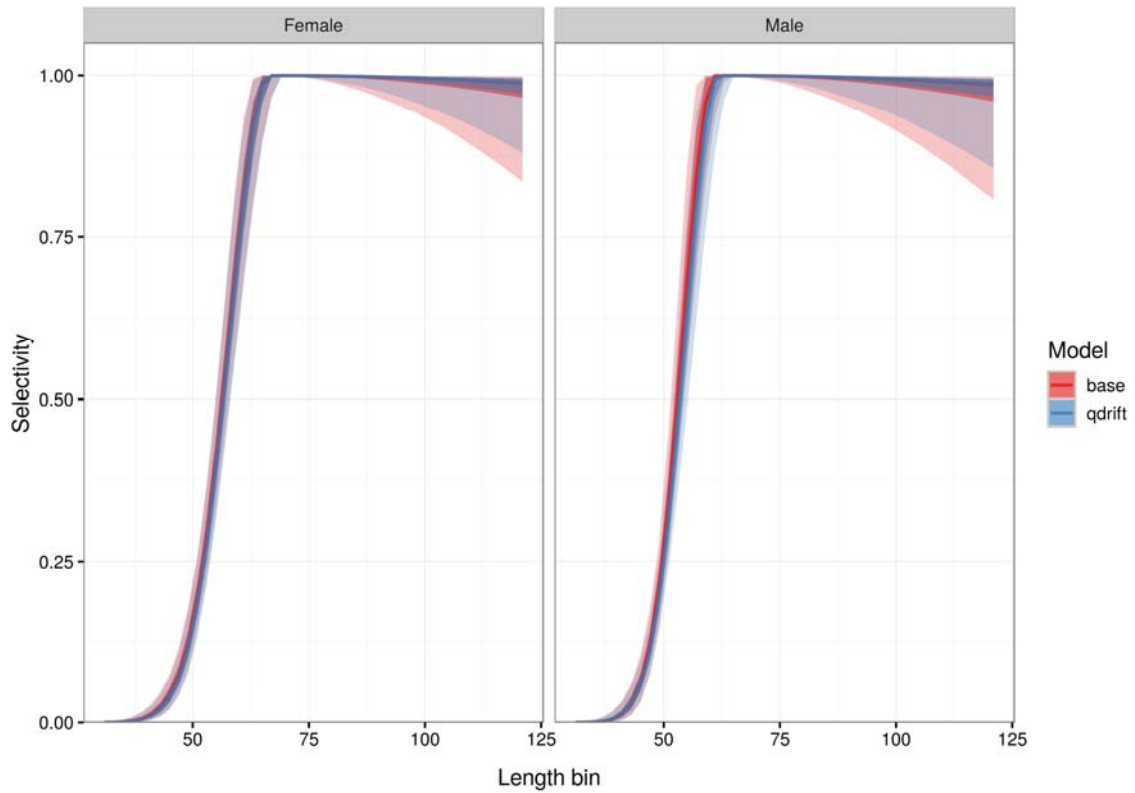


**Figure 81: Comparison of selectivity curves between the base run and the q-drift sensitivity run (Table 6).**

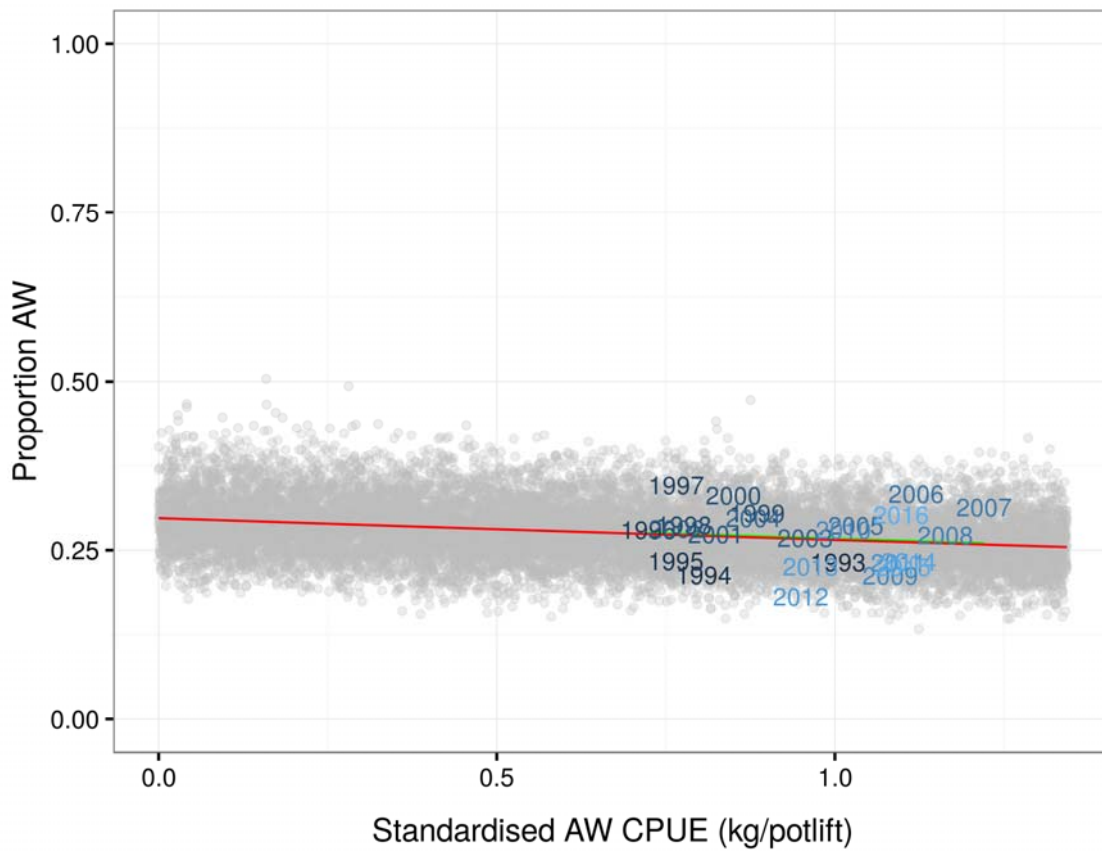


**Figure 82: Observed proportion of catch taken in AW vs. the standardised AW CPUE. The red line shows a predictive logistic regression, the grey points are simulations from the logistic regression, and the green line shows the predictive linear regression.**

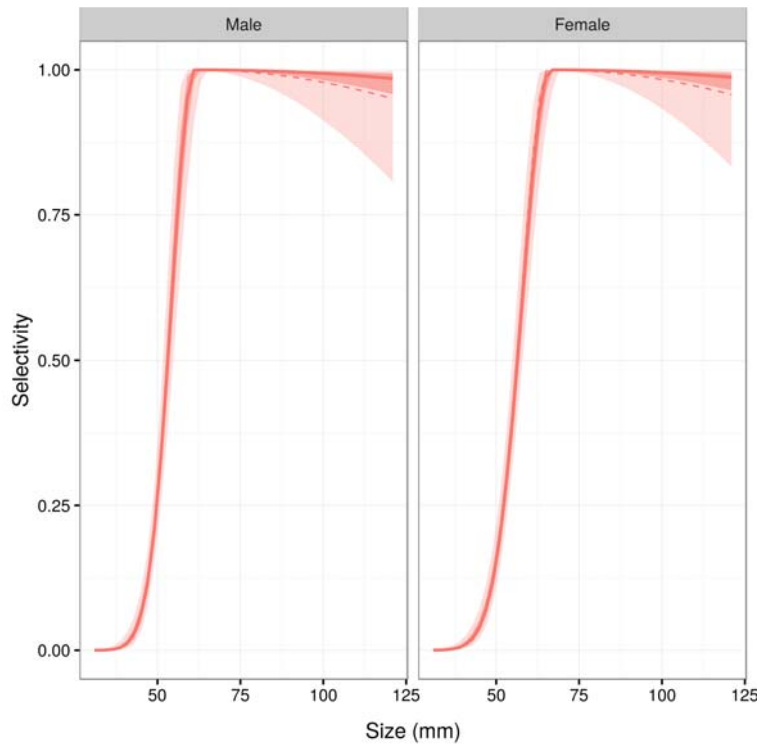


Figure 83: CRA 6 *combined* model average selectivity by sex, with the solid line indicating the posterior median and the variable intensity coloured bands showing the 50% and 90% credible intervals. Dashed lines indicate the corresponding MAP estimates from the *base* run.

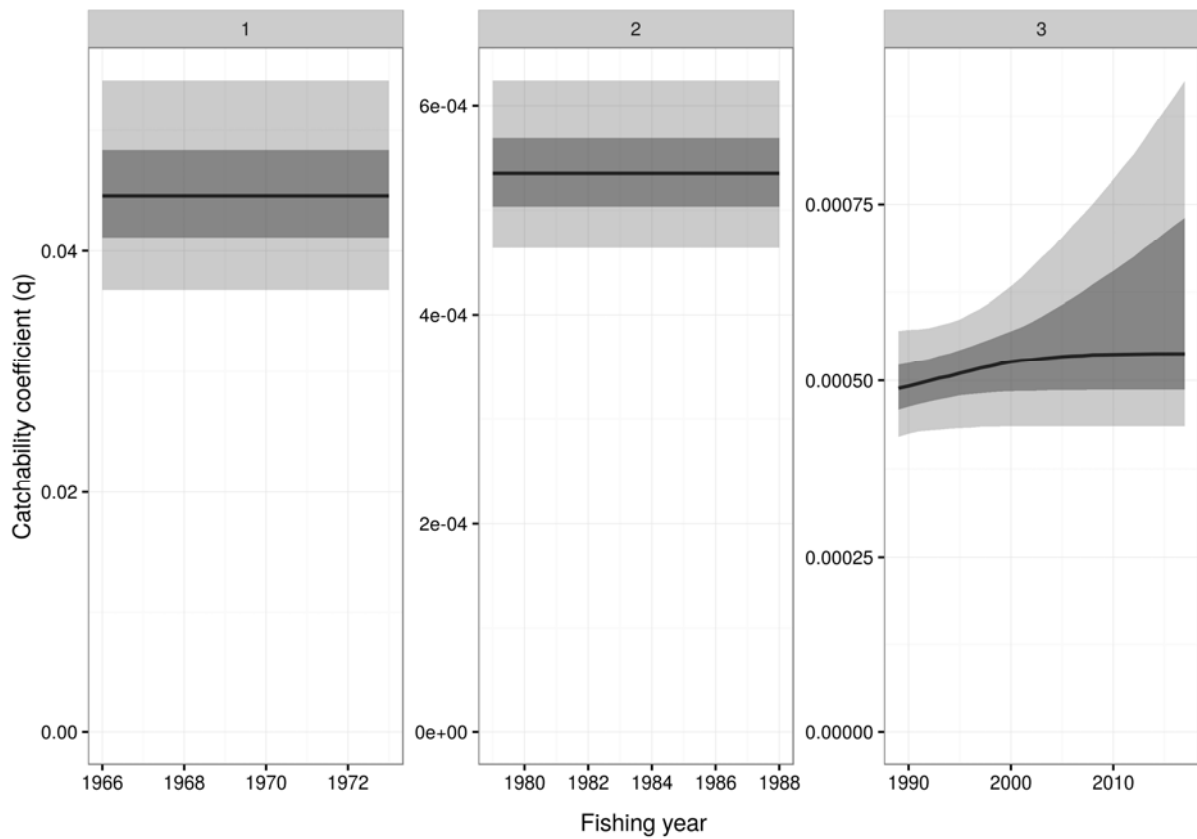
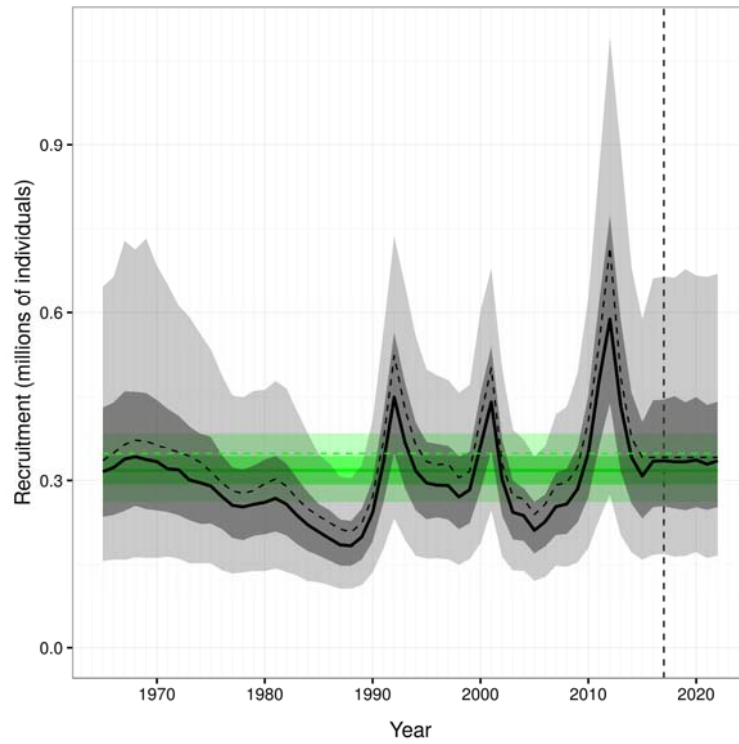
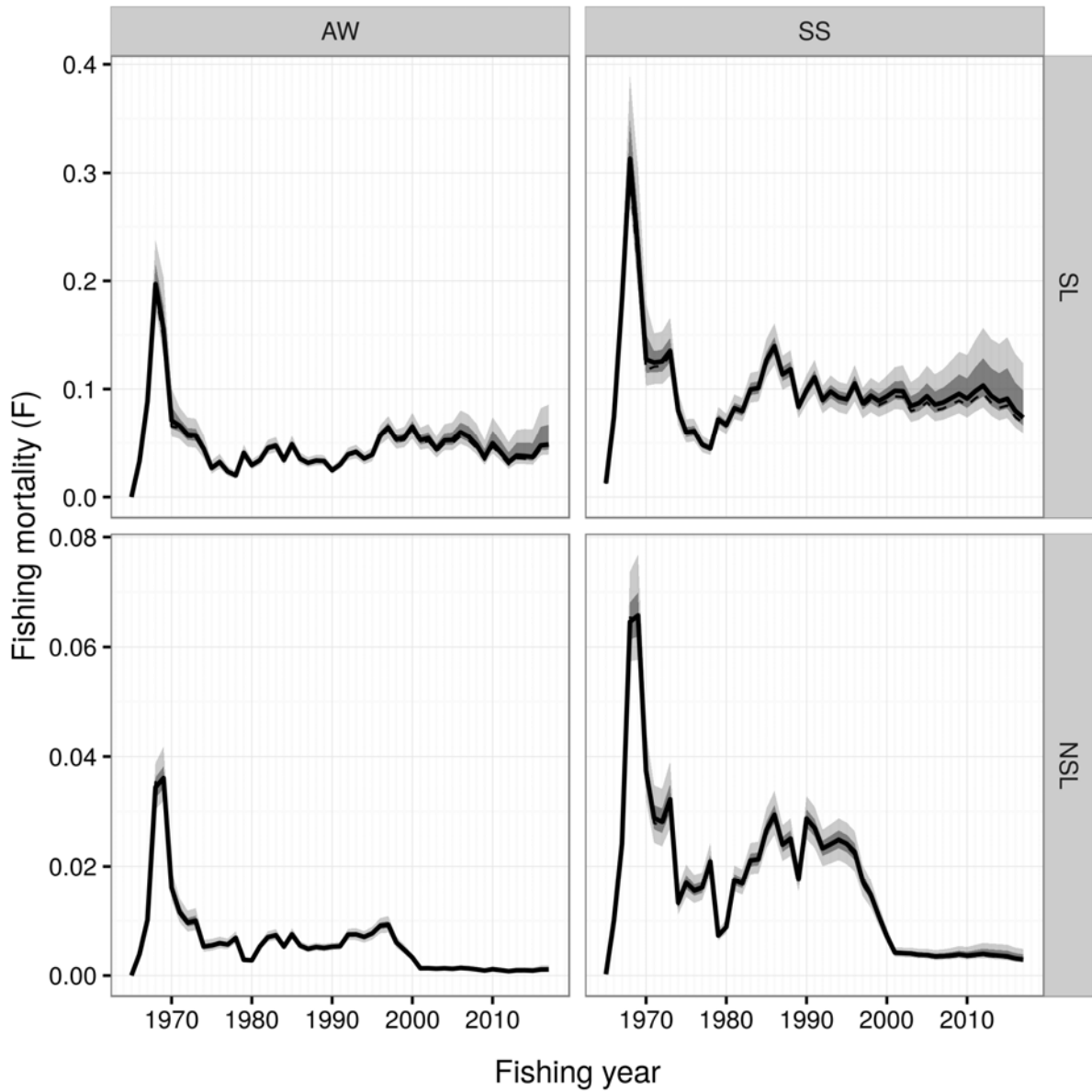


Figure 84: Posterior distribution of  $q$  for the *combined* model average run (Table 6): 1=CR CPUE  $q$ ; 2=FSU CPUE  $q$ ; 3=CELR CPUE  $q$ .



**Figure 85:** CRA 6 *combined* model average recruitment in 000 000's, where the dashed black line indicates the MAP, the solid black line indicates the median of the posterior, and variable shading intensity indicates the 50% and 90% credible intervals. The horizontal solid green line is the median of the posterior for  $R_0$  with green shading indicating the 50% and 90% credible intervals for  $R_0$ . The dashed green line is the MAP for  $R_0$  from the *base* run. The vertical dashed line is the final year of the reconstruction period. Projection recruitments (plotted to the right of the vertical dashed line) are based on the mean and standard deviation of the 2006–2015 recruitment and the 1965–2015 estimated autocorrelation. Projection recruitment for the MAP is fixed at the 2015 estimate.



**Figure 86:** CRA 6 combined model average fishing mortality by year, season, and fishery (SL = size limited; NSL = non size limited), with the dashed black line (not visible) indicating the MAP, the solid black line indicating the median of the posterior and variable shading intensity indicating the 50% and 90% credible intervals.

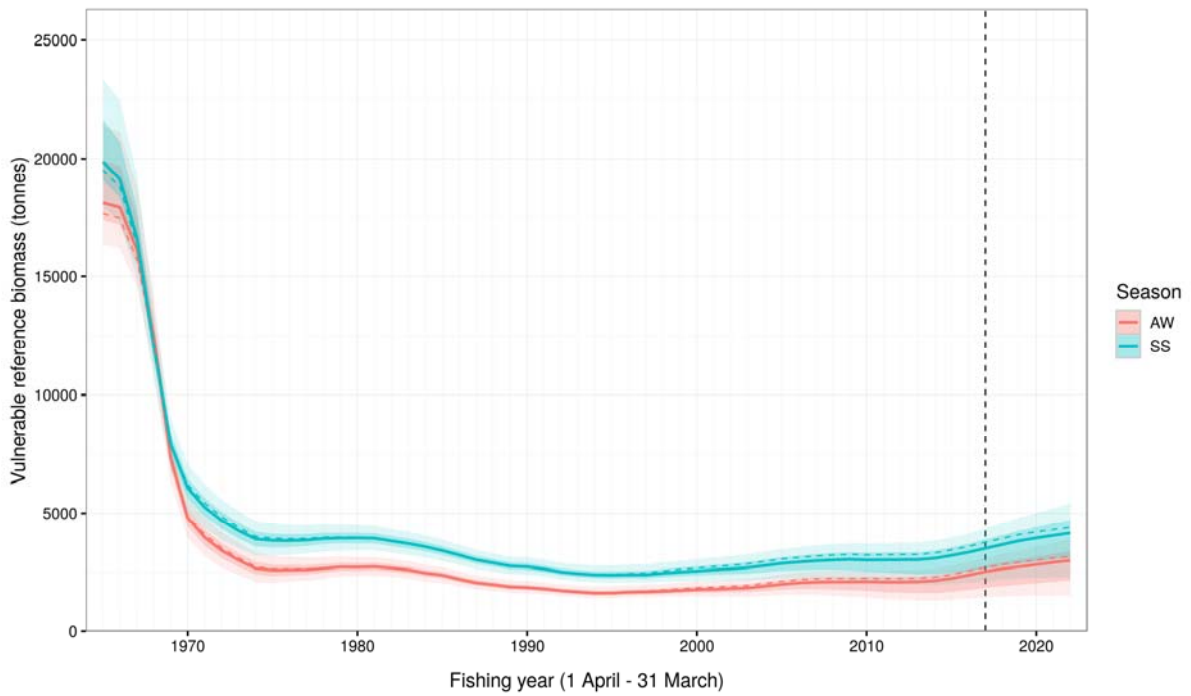


**Figure 87:** CRA 6 *combined* model average vulnerable reference biomass over the model reconstruction period. Solid lines indicate the median vulnerable biomass by season, shading indicates the 50% and 90% credible intervals for each series, and dashed lines indicate the MAP from the *base* run. The biomass in each year uses the final reconstruction year's selectivity and MLS.

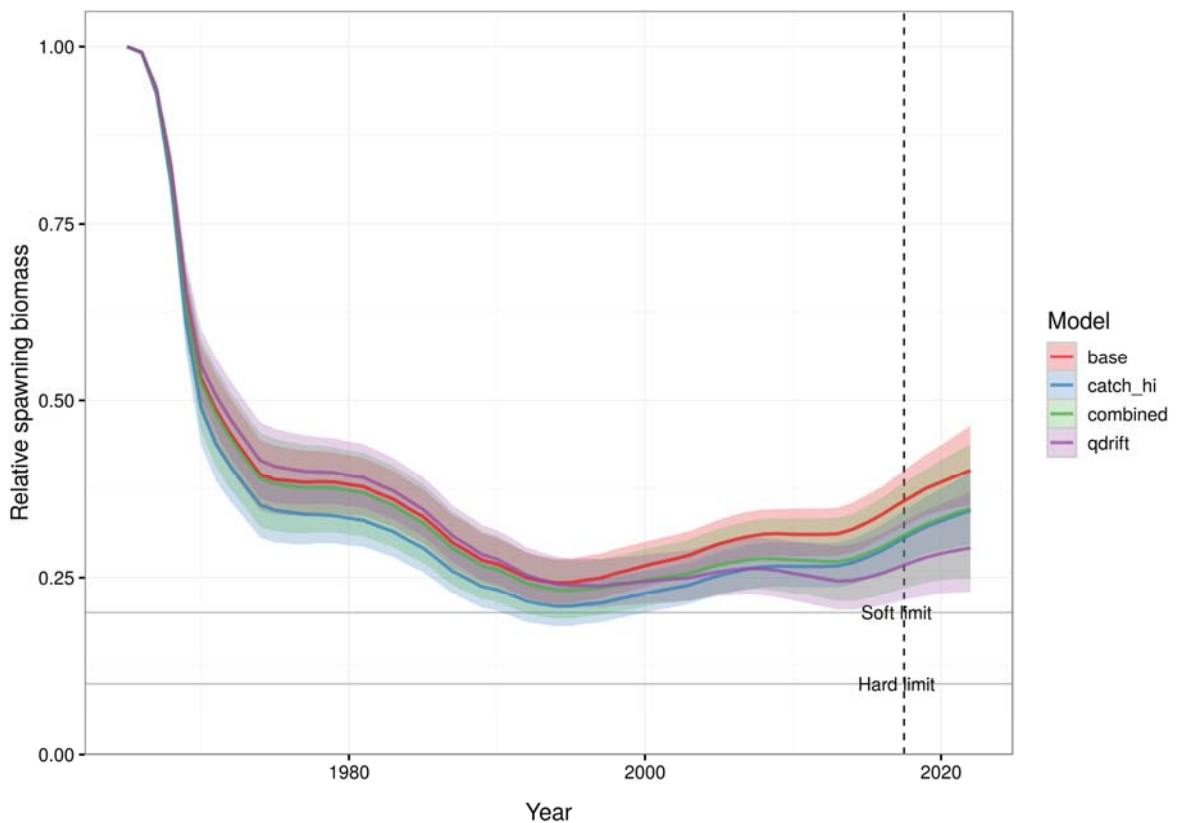


**Figure 88:** Comparison of the relative spawning stock biomass trajectories between the *base*, *catch\_hi* and *q\_drift* runs with the *combined* model. The vertical dashed line indicates the last year of the reconstruction period, after which the projected biomass is shown.

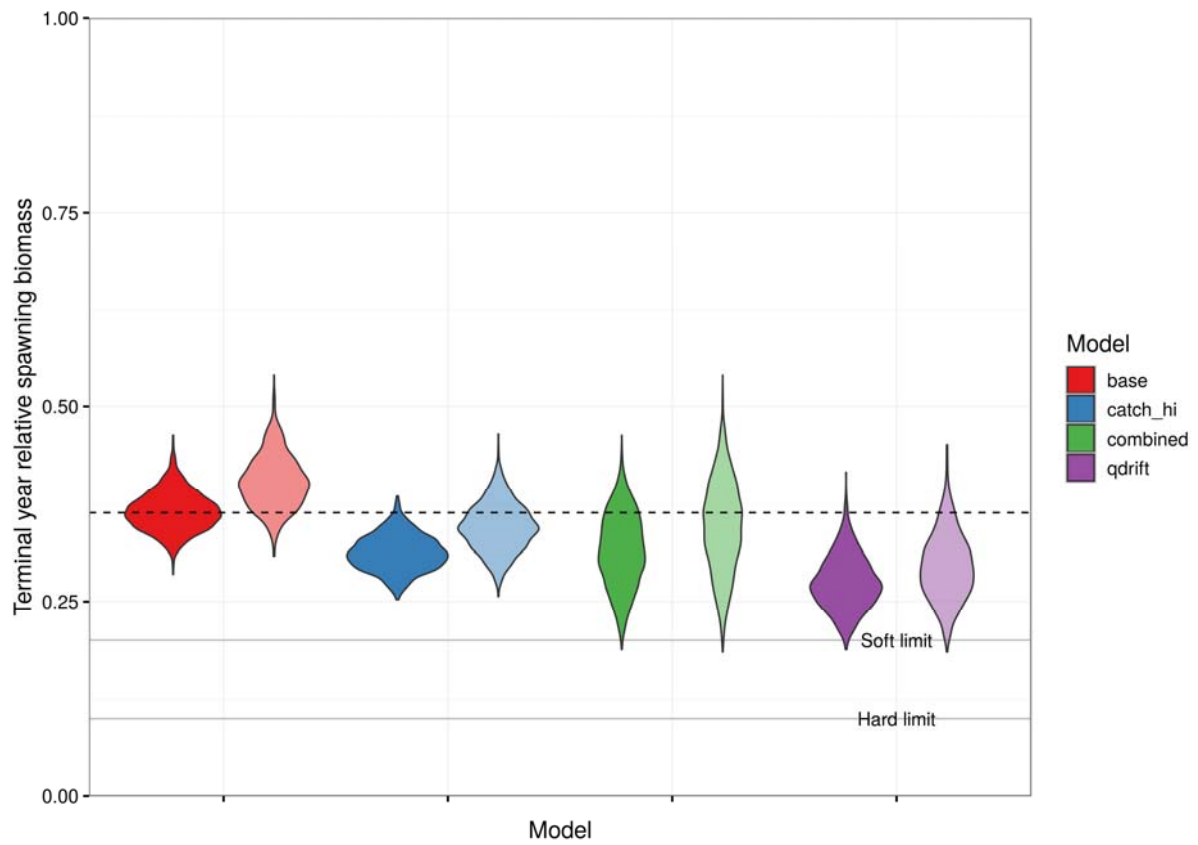


**Figure 89:** Comparison of the relative spawning stock biomass as a proportion of  $SSB_0$  in the terminal reconstruction year (dark shading, 2018) and the terminal projection year (light shading, 2022) between the *base*, *catch\_hi* and *q\_drift* runs with the *combined* model. The horizontal dashed line shows the mean  $SSB_y / SSB_0$  for all eight distributions.